SACCADES TO DOUBLY-FLASHED TARGETS

by

Li Wing Lau

A thesis submitted in conformity with the requirements
for the degree of Master of Science
Graduate Department of Physiology
University of Toronto

Abstract

The effect of a second pulse on saccadic performance was examined by asking the subject to track a stimulus, and measuring the resulting saccade. The latency data was examined with a bootstrapping method to determine objectively the modality of the population; the results were that the majority of them were unimodal; however, because a sizeable portion of the histograms also showed "shoulders" at similar latencies, the possibility of sub-populations could not be eliminated. The effect of the second pulse was also examined by comparing the cumulative histograms of each of the two-pulse conditions with the one of the single pulse configurations (SP) and with a model which gave the latency distribution expected from a two-pulse stimulus if the two pulses were processed independently by the saccadic system. The results showed the effect of the second pulse differed greatly depending on which yardstick was used.

TABLE OF CONTENTS

LIST OF FIGURES

LIST OF TABLES

Introduction

The saccadic system has been the subject of many studies, by virtue of the fact that saccades are an important and highly-stereotypical kind of eye movement. Because they are highly optimized for foveation, they are used extensively in everyday tasks such as reading and driving.

In addition to electrophysiological and behavioural method of study, models have been designed in an attempt to further understand the neural processes that underlie them. One modeling approach had been to apply linear system theory and view the eye as a system composed of linear elements (such as transducers and filters), and non-linear elements. An example was the "waiting time" model (Doma & Hallett, 1988a; Barnes, 1995), based on Fuortes & Hodgkins (1964), which later modeled the process as a series of six low-pass resistance-capacitance (RC) filters followed by a nonlinear threshold. In such a model, the linear elements provided the delay and integration caused by the neural circuitry in the retina, while the thresholding element determined whether the signal coming out of the filter was sufficient to cause a saccade. The remaining computation (ie. extracting the position of the stimulus, determining the torques needed to foveate the eye on the stimulus, etc.) were treated as an additional fixed delay that was added on top of time needed the signal to pass through the RC filters and cross the threshold. The motivation for using a delay constant as a quick-and-dirty substitute for the remaining computation could be seen from Pieron's law which has been shown to fit the manual reaction time data (Vaughan et al, 1966; Mansfield, 1973) as well as saccadic latencies to small lit targets (Doma & Hallett, 1988b). Pieron's law is a power function of the form:

$$R - R_{\infty} = kI^{\beta} \quad \text{.....(1.1)}$$

where R_{∞} is the irreducible minimum reaction time, I, the luminance, and k and ß are constants.

A logical development from such an approach was to determine the impulse response function of linear system in question. The impulse response is the response of the system to an impulse input (ie. a pulse of infinite height and infinitesimal width, and whose integral is one), and its importance stems from the fact that once the impulse response is known, the system's response to any input can be calculated.

Estimating the impulse response functions of photoreceptors was conceptually straight-forward--stimulate a photoreceptor with a brief pulse of light and measure the resulting membrane

current. Such experiments have been done on rods and cones of the *Macaca Fascicularis* monkey (Baylor D.A.et al., 1984; Schnapf J.L. et al., 1990), and more recently, on human rods (Kraft T.W. et al., 1993). For rods, the impulse response function was found to be unimodal, and resembled the impulse function for a series of low-pass filters: for the monkey rods examined, it was to a series of six low-pass filters, and for human rods, a series of four to five low-pass filters. The time to peak for both impulse functions was to the order of 200ms. For cones, the impulse function was bimodal and resembled the output of a bandpass filter whose peak frequency was around 5 Hz. The time to peak, which varied from cone to cone, varied from a low of 30ms to a high of 80ms; the mean time to peak was 54ms. For both types of photoreceptor, it was found that the response-stimulus relation could be described relatively well with the function, 1 - exp(-x), where x is some function of stimulus strength.

For something more abstract like the perceptual system, determining the impulse function was more problematic as direct measurement was no longer possible. Most of the early experiments that made the attempt did so by trying to infer it from psychophysical experiments that measured how performance, such as sensitivity or latency, varied with different stimulus configurations (see Table 1.1). The problem with such an approach was that, as witnessed in the earlier experiments, while the amplitude information of the impulse response function could be readily extracted from the data, its phase component was not. Stork and Falk (1987) tried to circumvent the problem by applying the Kramers-Krönig relationship to the amplitude component to reconstruct the phase information. The result obtained was a biphasic impulse function, which was in agreement with prior studies. However, as was pointed out (Victor, 1989), in order for the Kramers-Krönig relationship to be applicable, the system had to be a minimum-phase transducer, an assumption which was not necessarily true. Later approaches, such as Roufs and Blommaert's perturbation technique (1981) and Tyler's temporal deblurring (1992), suggested that the perceptual impulse function was triphasic--a large positive lobe preceded and succeeded by smaller negative lobes.

In light of the confusion, the initial aim of this thesis is to revisit the problem and try to approximate the shape of the impulse response function by approaching the question with a straightforward psychophysical experiment. It was thought that this could be done by examining the effects of stimulus configuration on traditional measures of oculomotor performance, such as

Author	Method	Conclusions	Assumptions / Models
Rashbass (1970)	the relative intensities of a pair of pulses at threshold were shown to be related to the autocorrelation of the i.r.f		
Kelly (1971)	flicker thresholds were measured and were used to compute the parameters of a model whose i.r.f. could be derived.	biphasic i.r.f.	model consists of a diffusion stage followed by a nonlinear inhibition stage
Watson & Nachmias (1977)	a biphasic i.r.f was assumed and then shown to be compatible with the results of Rashbass' (1970) experiment	biphasic i.r.f.	the model used was a probability summation model based on Tolhurst (1975) and Quick (1974)
Roufs & Blommaert (1981)	perturbation method--the effects of varying the relative position of 2 pulses at threshold were used to derive the i.r.f.	triphasic i.r.f	the system is a linear peak-detector
Georgeson (1987)	a biphasic i.r.f. was assumed and shown to be compatible with contrast sensitivity measurements	biphasic i.r.f.	a series of linear filters followed by a non-linear decision rule
Stork & Falk (1987)	the Kramers-Krönig relations were used to reconstruct the phase spectrum (and hence the i.r.f.) from flicker sensitivity data	biphasic i.r.f.	minimum-phase assumption
Tyler (1992)	temporal deblurring--phase information was extracted by observing the system's performance to a stimulus composed of a number of sine waves at various harmonics	triphasic i.r.f.	
Manahilov (1995)	the apparent brightness of a bar was measured and the results were used to fit a model	triphasic i.r.f.	the model treats the process as a signal propagating through a multilayered network with a certain spatiotemporal impulse function

Table 1.1: Summary of various estimates of the perceptual impulse response function (i.r.f.)

frequency of response, mean latencies and cumulative histograms, to obtain an estimate for the shape of the impulse function. However, this was later abandoned because of the realization that any latency function would be a rather insensitive measure of the rising phase of the impulse response function, and that a model by Hallett showed that a photoreceptor model of latency was inadequate because it could not account for the large variance in saccadic latency. As a result, it seemed better to undertake a qualitative exploration of two-pulse effects, particularly as little has been done to examine its effects on saccades and its latencies.

Method

2.1 Apparatus

The experiment employed the following apparatus to produce the stimulus and track the ensuing eye movements: a non-contacting eye-tracker (EMMA) which was made up of an optical head and a signal processor box, a data acquisition card (National Instruments' PC-DIO-96), an personal computer based on an Intel's 80486 microprocessor, some light-emitting diodes (LEDs), a custom-made expansion card designed and built by the Computing Support Division of the Faculty of Medicine to control the LEDs, a digital signal processing (DSP) board built around a Texas Instruments' TMS320C30 DSP chip, and two analogue-to-digital (A/D) converters. The original EMMA system (ie. optical head plus signal processing box) was used for the yellow-green experiments; the later experiments with the red LEDs used the DSP board and the A/D converters to replace the signal processing box.

2.1.1 EMMA Eye Tracker

Tracking eye movement was accomplished with the non-contacting Eye Movement Monitoring Apparatus (EMMA). It was built by University of Toronto's Institute of Biomedical Engineering and has a temporal resolution of 1 msec and a spatial resolution of 3 min arc. Other working and design details of the apparatus could be found in Eizenman et al. (1984).

The apparatus was composed of two parts: an optical head and a signal processing box which was used only in the main yellow-green experiments. The optical head was a contraption of lens, mirrors, infrared sensing phototransistors and uses a gallium arsenide diode as its infrared source. With the use of its lens and a dichroic mirror, the infrared beam was directed at the subject's eye. Some of the beam, being reflected back by the cornea, was then redirected with the use of other mirrors and imaged on an array of 22 phototransistors (Figure 2.1). Because of the difference in the centre of curvature of the cornea and the centre of rotation of the eyeball, the position of the reflected beam on the sensor array would change correspondingly as the eye moved.

The signal of the 22 phototransistors was sent to the processing box, which would then

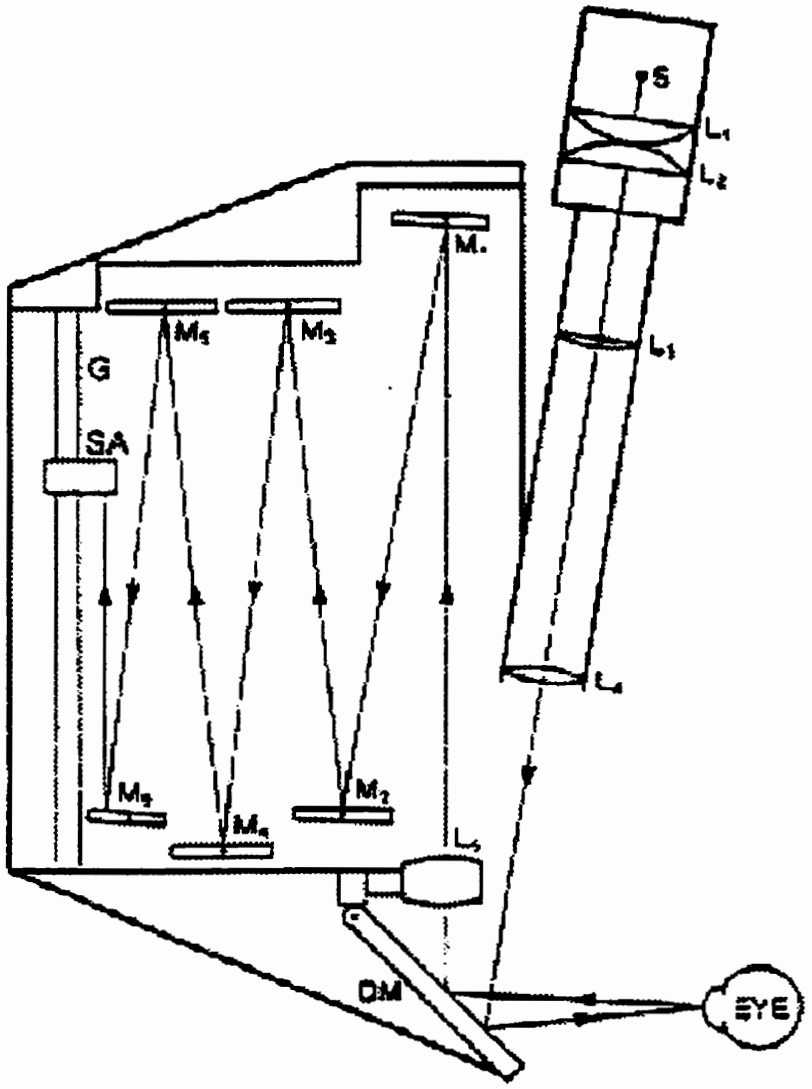

Figure 2.1: Schematic of EMMA's optical system.

convert them into a 15-bit integer indicative of the eye position. (In reality, EMMA produced a 16-bit integer; however, the sixteenth bit does not count because the least significant bit has been commandeered to indicate whether the current value was a vertical or horizontal reading of the eye position.) The first step in processing the phototransistor signal was to compare it against a fixed threshold to eliminate system noise. Then, making use of the fact that the signal should be in the shape of a bell, the location of the signal peak, which corresponded to the eye position, was calculated. This was accomplished by quickly sweeping the spatial signal to produce a temporal waveform and convolving it with a temporal interpolating weighting function to produce a "zero-crossing" waveform. The location where this zero-crossing waveform crossed zero would correspond to the location where the original spatial signal had a peak. As a zero crossing could be located very accurately in time, the position of the original spatial peaks could be determined to within about 1/256 of the phototransistor spacing.

2.1.2 Data Acquisition Card, PC-DIO-96

The data acquisition card (DAC)--a PC-DIO-96, made by National Instrument, was an off-the-shelf 96-bit, parallel, digital, I/O interface card for Intel x86-based computers with an ISA bus. In addition to this card, a small TTL circuit (Figure 2.2) consisting of two NAND gates was required by the computer to read the stream of numbers from EMMA. The circuit, designed and built by James MacLean, provided the data acquisition card with the "handshake" it needed to operate in a strobed input mode. Reading in data with a handshake was superior to simply polling the output lines of EMMA because a handshake ensured that the DAC would not attempt to read EMMA's output lines while it was in the process of loading a new output value.

When EMMA has a new piece of datum, it would signal the fact by switching on one of its output lines (DR) temporarily. If the DAC was ready to read it in, as indicated by an off logic state on its line IBFA, the 2 NAND gates would drive the two strobe lines (STBA* & STBB*) off. This, in turn, would cause the DAC to raise an interrupt to the computer to transfer control over to the DAC and allow it load the 16-bit datum (EMMA-0 - EMMA-15) into its memory. The act of loading the datum would then clear the IBFA line and set the DAC for a new piece of datum.

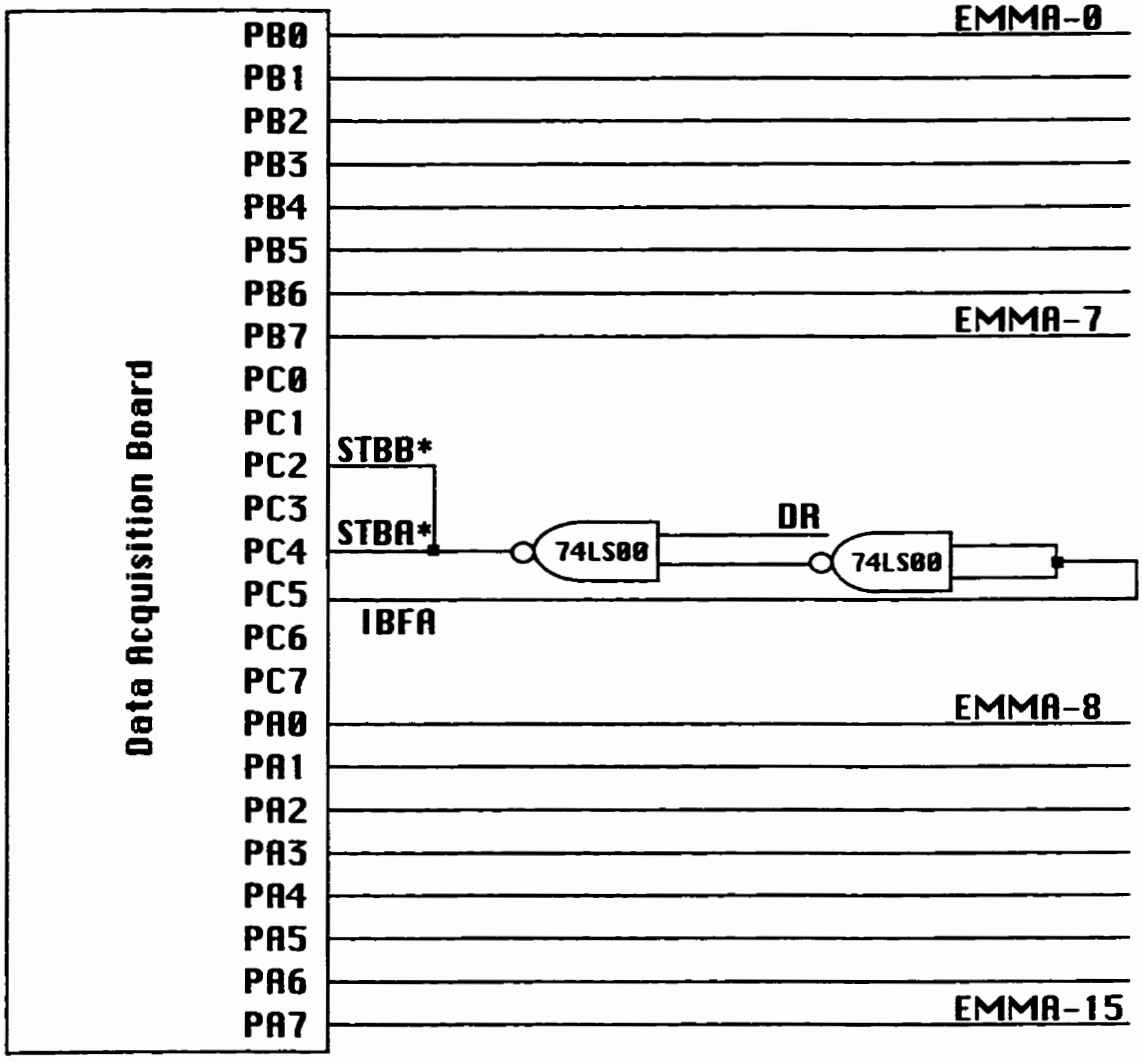

Fig. 2.2: A schematic diagram of the connections between EMMA, the data acquisition board, and the TTL circuit. Port A and port B (labeled PA* and PB*) of the data acquisition card (DAC) were used to read in data from EMMA's 16 bit port (labeled EMMA-0 through EMMA-15). Port C was used for the handshake. The signal indicating that EMMA has a piece of data ready to be read in was carried by the line labeled DR.

2.1.3 Computer

The computer was an Intel-486 based personal computer running Microsoft DOS 3.3 as its operating system. The program was specially written in C by the author for the purpose of the experiment. It was based on FORTRAN programs that ran similar experiments on a PDP-11-23 minicomputer, and on a program written in C by James MacLean that demonstrated the ability of the data acquisition card, PC-DIO-96, to act as an interface between the computer and EMMA's signal processing box.

Many versions of the program exists--some were predecessors of the program that used a different apparatus to control the target array, and some were variants of the program because it was easier to modify the program to run certain experiments than to write a description of them in the syntax required by the program. Only two versions are of importance. One, `newdisp3.exe`, was the version that was used to run the main yellow-green experiments and it is kept in the `c:\lilau\newdisp3` directory. The other, `dspexp.exe`, was used to run the red experiment and is kept in the `c:\lilau\dsp` directory. These two versions differ only in the manner in which it connected with EMMA--`newdisp3.exe` relied on EMMA's circuitry to compute the eye position, while `dspexp.exe` used a digital signal processing board to translate the activities of the phototransistors on EMMA's optical head into the eye's position (see section 2.1.6).

The program has been divided into twelve modules, most of which were of little consequence because they contained the routines that manage I/O and the user-interface. The most important files were `main.h`, which contained the definitions of the data structures used in the program, `expermnt.c`, which contained the subroutine that oversaw the control flow of the experiment, `emmatrac.c`, which contained the subroutines that controlled the DSP board, and `emma.c`, which contained the subroutines that read in EMMA's output via the data acquisition card.

When stripped of its supporting and user-interface functions, the program that ran the experiments performed two tasks. The first task was to control and co-ordinate the various pieces of hardware. This involved lighting and extinguishing the right LEDs at the appropriate times, reading in data from EMMA's digital output at a rate of 30 bits/ms and polling a push button used by the subject to start and to pause the experiment. The second task was to calculate the important parameters such as saccadic latency, peak velocity, saccade amplitude and duration from the stream

of eye positions coming from EMMA. (Latency was measured as the period between the onset of the stimulus and the beginning of a saccade, which was defined as the first moment at which the eye is moving at a speed in excess of 20 °/s.) Once these values were computed, they were saved onto the computer's hard disk for later off-line analysis.

2.1.4 Display and Diode Card

The stimulus array was made of 15 "super-bright" light-emitting diodes (LEDs) whose front has been grounded down and polished to eliminate blur. The grounding and polishing resulted in small square targets of 4 arc mins subtense. The LEDs, laid down in a horizontal arc, were positioned 114 cm from the subject. The central LED was red (peak wavelength was, according to the vendor, 670 nm) and it was used as the fixation point (FP) during the experiments. The remaining 14 LEDs were yellow-green (peak wavelength of 565 nm) and were placed in the periphery to serve as targets. A later experiment used a set of 14 red LEDs as targets; according to the catalogue, their peak wavelength was 635 nm. These LEDs, positioned on both sides of the centre red LED and spaced 0.5 degree apart, began at 2.5 degrees from the centre and ended at 5.5 degrees (Figure 2.3). The range of the targets was chosen to be within EMMA's linear range--in the calibration process, a linear regression of EMMA's output and eye positions often gave coefficient of correlation of around 0.99--and within a range of eccentricities that would produce saccades with stable and minimal latencies (Kalesnykas & Hallett, 1994). Fourteen target positions were used to reduce the possibility that the subject would be able to anticipate the target position, and also the chance that the subject would learn the stimulus target positions and use the information to guide the saccades.

The 15 LEDs were controlled with a custom-made ISA expansion card built by the Computing Support Division of the Faculty of Medicine at the University of Toronto. It was designed with the capacity of driving 48 diodes simultaneously at different intensities. Intensity of each diode was represented with an 8-bit integer; however, because the card is a voltage source (as opposed to current source) and drives the LEDs by applying a voltage across them, it is not capable of producing 256 different intensity settings as implied by the use of an 8-bit integer to represent intensity. The reason is that some of the voltages are not large enough to overcome the PN-

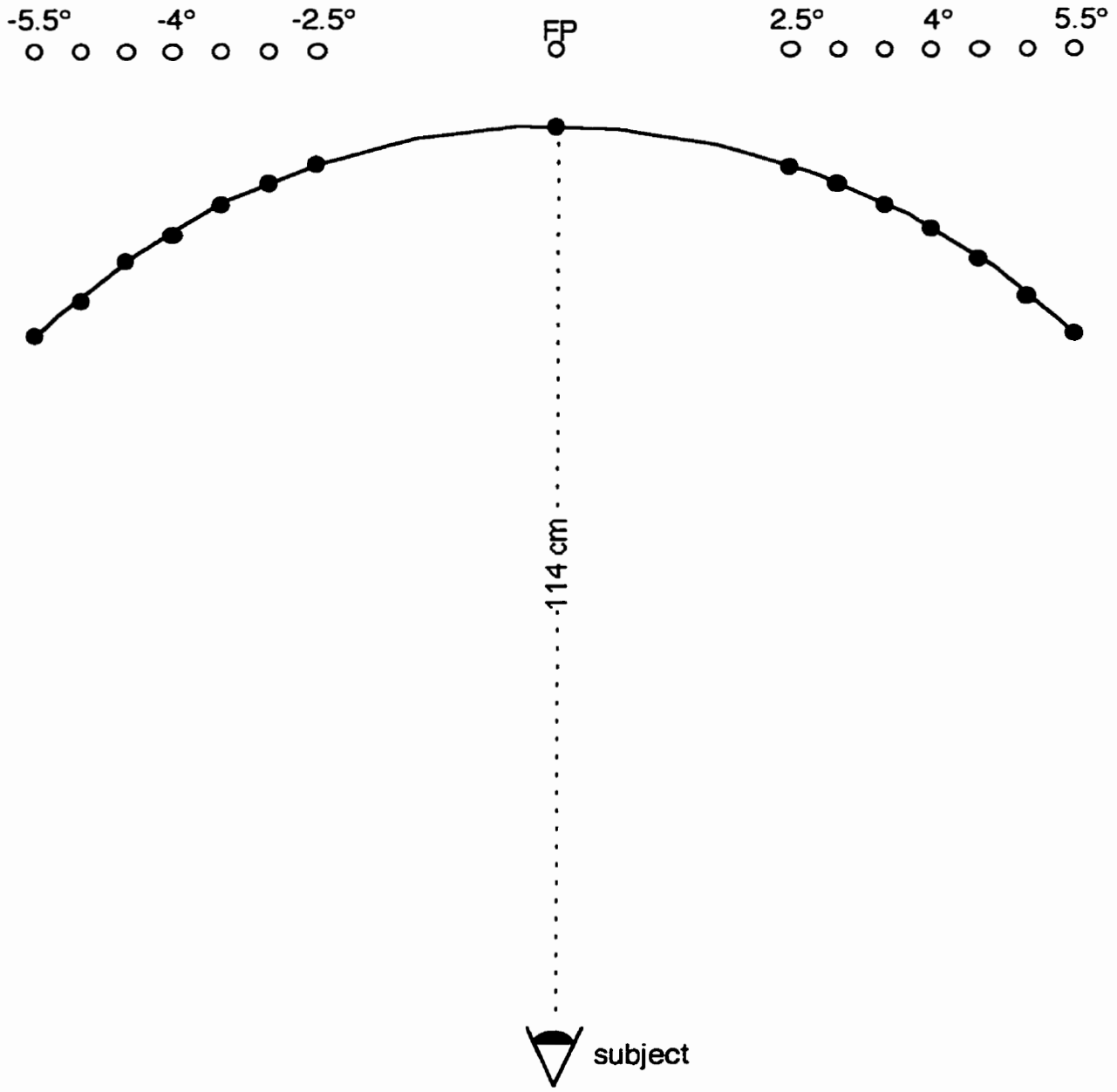

Figure 2.3: Schematic showing the arrangement of diodes in the target array. The LEDs were laid along an arc of a circle with a radius of 57cm, and were viewed from a distance of 114cm. FP is the fixation point. The diagram is not to scale.

junction of the LED. Thus, because the card was only capable of relatively small changes in diode intensities, larger changes, such as those of one or two orders of magnitude, were accomplished with Kodak gelatin neutral density filters. In addition to that, because each LED had its own lighting properties, matched output was accomplished by preparing beforehand a look-up table that cross-referenced card setting with output intensity for each LED.

2.1.5 Diode Temporal Calibration

While there was little doubt as to the precision of the computer's timing, the response of the LEDs may not be as sharp as that of the computer, and there was a need to verify that the computer's control of the LED onset and offset time was precise. To do this, an LED was programmed, using the same code fragments that were used in the experiment for controlling the LEDs, to repeat a cycle of being on for 5ms and off for 15ms. Its brightness was then profiled with a photomultiplier tube to examine how much lag there was between the application of a voltage and the LED reaching its target intensity. The results showed that the LED was on for a total duration of 5.4ms, and that it required about 0.2ms to switch from its off state to the target intensity or vice versa. Several other intensities were also tested in the same way and it was found that over the range of intensities employed in the experiments, no discernible differences in the lag time were observed. Once the target intensity was reached, deviation away from the target intensity was negligible. Therefore, the amount of energy in a 5ms pulse would be about the product of 5.2ms and the target intensity, if one made the approximation that the intensity profile of the LED was in the shape of a trapezoid.

Finally, for the sake of convenience, flash duration would continue to be reported as 5ms in this report even though the actual time for which the LED was on was longer.

2.1.6 Diode Energy

The experiment expressed intensities in terms of a subject-dependent logarithmic unit, FT, based on the subject's foveal threshold. The advantage of using such a unit was that it would tend to reduce inter-subject variability in performance (such as saccadic latency) that would arise from

subject-dependent parameters such as pupil diameter, efficiency in utilising photons and other factors that effect the amount of light energy available for the visual system.

Conversion from the FT unit to more conventional units could by taking into account the following set of relationship between intensity, luminance, and the viewing conditions under which the foveal threshold was determined. The first of these relationship is between the target intensity *I* and its luminance *L* reflected off a nearby magnesite ($MgCO_3$) surface. The equation for this calibration arrangement is

$$L = I\ R / (\pi \times d^2) \quad \text{.....(2.1)}$$

where

L = luminance of the $MgCO_3$ block in candela / m^2 as measured by a photometer
I = intensity of the target in candela
R = reflectance of the surface (for a $MgCO_3$ block, $R_{565nm} = 0.975$)
d = distance between the target and the $MgCO_3$ surface in cm

A factor of π is required by Lambert's law for a perfect diffuser.

Next, FT units, in photopic lumens, could be related to the target intensity I by the following equation.

$$FT = (1/F) \times \pi \times (p^2 / 4) \times (1 / D^2) \quad \times \quad I \quad \text{..... (2.2)}$$

where

F = attenuation factor of the neutral density filter used to bring I to foveal threshold
p = pupil diameter in m
D = distance between the light source and eye in m
I = intensity of the light source in candela

A factor of π is in the equation for pupillary area. The factor, *F*, was required because neutral density filters were used to compensate for the limited range of intensities that the diode card was capable of producing. When setting foveal threshold, the subject was asked to adjust the intensity of the diode positioned behind a neutral density 3 filter until the light of the diode was barely visible. Instead of using the nominal value given by the manufacturer, the value of *F* was obtained by measurement. The value of *L* in equation (2.1) was obtained by placing an LED *d* cm in front of a $MgCO_3$ block, and then measuring its luminance with a Spectra Pritchard photometer.

Once the FT units have been converted into photopic lumens, they can be converted into other units such as ergs/sec or quanta/sec.

To convert to ergs/sec, one applies the equation

$$W_\lambda = P / V_\lambda \times 6.797 \times 10^{-5} \quad \text{.....(2.3)}$$

where

P = FT in units of photopic lumens
V_λ = relative spectral luminous efficiency function

The constant in the equation is the "mechanical equivalents of light".

To convert into photons/sec, one would divide the equation (2.3) by the energy (measured in ergs) of each photon. The energy of a photon with a wavelength of λ is

$$E = h \times c / \lambda \quad \text{..... (2.4)}$$

where

h = Planck's constant, 6.624940×10^{-26} ergs·sec
c = speed of light, 2.997925×10^{10} cm/sec
λ = wavelength of the photon in cm.

Thus, a photon with a wavelength of 565 nm has 3.51×10^{-12} ergs of energy. The energy in a flash could then be found by multiplying FT units in quanta/sec by the target duration.

According to the set of calculations prescribed above, the energy in one yellow-green FT unit was between of 10913 and 16255 quanta/sec (Table 2.1). These values compared favourably with another estimate of one yellow-green FT by Claire Barnes (1995) who reported a value of 8563 quanta/sec. The same calculations were done for the red diodes (Table 2.1, column LL(red)), and a value of 68657 quanta/sec was obtained for red FT units, which compared favourably with Barnes' value of 64263 quanta/sec. As the last two columns of Table 2.1 has shown, the values are rough estimates only, and the reason why they were written with four or five digits is for the sake of traceability and quality control.

2.1.7 Analogue-to-digital converters and DSP board

For the experiments using red LEDs as targets, a slightly different apparatus was used to track eye movement. The processing box was replaced with two analogue-to-digital converters (A/D converters) and a digital signal processing (DSP) board. The A/D converter was manufactured by SPECTRUM Signal Processing Inc., and was designed to connect to the PC via its ISA expansion slots. Each card had 32 analogue input channels, multiplexed to a 3-μsec 12-bit A/D converter and can sample data at a rate of up to 100 kHz. Each channel had its own input buffering and a first order low-pass filter to reduce unwanted high frequency noise. The DSP

	PH	RC	LL	LL (red)	PH (min)	PH (max)
R of $MgCO_3$	0.975	0.975	0.975	0.975	0.975	0.975
d (m)	0.08	0.08	0.08	0.082	0.079	0.081
L (cd/m^2)	0.00613	0.00896	0.00778	0.0062	0.0053	0.00695
I (cd)	0.000126411	0.000184771	0.000160437	0.000134327	0.00010658	0.000146926
pupil diameter (m)	0.006	0.006	0.0065	0.0065	0.0055	0.0065
F	1084	1084	1084	1084	1084	1084
D (m)	1.14	1.14	1.14	1.14	1.14	1.14
F (lumen)	2.53711E-12	3.7084E-12	3.77905E-12	3.16404E-12	1.79743E-12	3.46081E-12
V_λ	0.974	0.974	0.974	0.217	0.974	0.974
W (ergs/s)	3.83628E-08	5.60735E-08	5.71418E-08	2.1474E-07	2.71783E-08	5.23298E-08
lambda (cm)	0.0000565	0.0000565	0.0000565	0.0000635	0.0000565	0.0000565
E (ergs)	3.51523E-12	3.51523E-12	3.51523E-12	3.12773E-12	3.51523E-12	3.51523E-12
FT (quanta/s)	10913	15952	16255	68657	7732	14887

Table 2.1: Converting an FT-unit into units of quanta/sec. The last two columns shows an attempt to estimate the range in which the real value may lie by using measured values that are within the tolerances of measurement error to maximize and minimize the final quanta/sec calculation.

board, built around Texas Instrument's TMS320C30 DSP chip, was also designed and built by SPECTRUM Signal Processing Inc and connects to a PC via its ISA expansion slots. The board had a clock speed of 33.3 MHz and can perform 16.7 million instructions per second.

The DSP board filled the identical role as the processing box. The code for the DSP, `emmatrac.c` in the `c:\lilau\trac30` directory, was written by James MacLean and was optimized by the author. Because the DSP board did not have dedicated hardware to perform the calculations, it was slower that the processing box and shortcuts in the calculations had to be taken to give the same tracking rate. Like the processing box, the first step in the processing was to compare the signal against a threshold to eliminate system noise. Zero-crossings were then estimated by evaluating an approximation of the zero-crossing function at a number of points. Instead of convolving the signal on the phototransistors with the temporal interpolating weighting function, it was convolved with a smaller version of the weighting function. The real zero crossing was located by evaluating the zero-crossing function around the estimate.

In addition to conferring greater flexibility and ease to experimenting with the tracking algorithm, the largest benefit of switching to this system lay in that it permitted the implementation of a better algorithm for tracking zero crossings. In the original processing box, the eye position was deemed to be the leftmost zero crossing; in this new system, once the program has locked onto an appropriate zero crossing (which has been set to be the leftmost zero crossing between two lobes of at least a certain minimum amplitude), the system would track it until the amplitudes of the surrounding lobes were below a pre-set threshold.

2.2 Procedures:

2.2.1 Preparing the subject for EMMA

Some preparations were required before EMMA could be used to track a person's eye movement. The first step was to prepare a bite bar so that the subject's head could be stabilized when EMMA was in operation. Stability was important because by tracking eye movement via the corneal reflection, the machine was unable to distinguish head movement from eye movement. In addition to the bite bar, a forehead rest was also employed to help the subject maintain a still head. The second step was to position EMMA's optical head such that its infrared beam would land on

the left corneal and give a clean reflection that would be imaged on the phototransistor array. EMMA tracked only the movement of the left eye; in order to prevent the image in the right eye from affecting the left eye's movement, the right eye's view of the target array was occluded with a piece of black cloth. This setup was accomplished by first using the alignment lights on EMMA to get the approximate location of the infrared beam on the subject's eye, and then fine-tuning the position of the optical head so that the zero-crossing function, which could be monitored with an oscilloscope or with the computer itself if the DSP board was in operation, was clean and of sufficient amplitude over the range of eccentricities required by the experiment. The final step in preparing the subject for EMMA was to correlate its' 15-bit output with eye position. By asking the subject to fixate on a set of targets with known eccentricities, a linear regression could be performed on the EMMA's output and the target positions to obtain a scale factor that convert between the two; the resulting coefficient of correlation was usually on the order of 0.99.

2.2.2 The Basic Experiment

Because a large number of datapoints (~300 per each interstimulus interval) were needed for some of the data analysis, the experiment was broken into a number of sessions and done over a period of several days.

Before a session of the experiment began, the subject was given a drop of mydriatic and was allowed to dark adapt for a period of twenty minute. Initially, a 1% solution of cyclogyl was used, but later experiments switched to a 0.5% or 1.0% solution of the weaker mydriatic, mydriacyl. Once the dark adaptation period has elapsed, the experiment began.

In the centre of the subject's field of view, a red fixation LED was lit at an intensity 10 times that of the targets, and it was on for a random period that lasted anywhere between 1.5 seconds and 2.5 seconds. The subject was instructed to fixate it. The purpose of having a fixation period whose duration varied was to prevent the subject from anticipating the offset of the fixation LED and the onset of the peripheral target. At the end of the fixation period, the fixation LED was extinguished and a target was presented at one of the fourteen possible eccentricities on the diode display array. Its position was random, as was the stimulus configuration. Eight stimulus configurations were used: a single flash at one unit of intensity, a single flash at two units of

intensity, or two flashes at one unit of intensity with a delay of either 17ms, 30ms, 55ms, 80ms, 105ms, or 130ms (See Figure 2.4). Delay was defined to be the interval between the start of the first flash and the start of the second flash. The subject was instructed to make a saccade to the target if he saw the target; otherwise, he was to keep his eyes stationary. The subject was given a window of 1 second to respond to the stimulus; considering that most saccades occur within 600ms of target onset under such stimulus conditions (ie. Figure 3.3) and that a lack of a response by such a time usually means that the stimulus has not been not detected, the allotted time was deemed ample for the slowest saccade. At the end of the trial, the computer produced a soft click to notify the subject of a bad trial if the record of the saccade seemed strange (ie. overly short latencies, spurious saccades that were too fast or too short). Usually, this meant that EMMA was having trouble tracking the subject's eye position because he blinked or has moved his head away from the position for which EMMA was calibrated. When this happened, the subject was urged to take a short break and put his head back into the position it was in when the calibration was done. Smooth progress was signified by silence.

A session consisted of 800 such trials and took about one hour to complete.

2.3 Subjects:

Four subjects participated in the experiments. Of them, only one, PH, had any prior experience with this type of experiment. PH is a male subject in his late fifties. Subject RC is a male subject in his twenties whose left eye is myopic (-6.5 dioptre). During the various sessions of the experiment, neither PH nor RC wore any corrective lens. The remaining two male subjects, LL and SH, were myopic in their left eye (-5.5 dioptre and -4.25 respectively) and wore contact lens during the experiment. The data of SH were not used because the variation between the sessions of data was large and hence could not be pooled and treated as if they were of the same population.

Test runs were done with LL to see whether the contact lens would interfere with eye tracking process (ie. slippage) and the results showed that they did not.

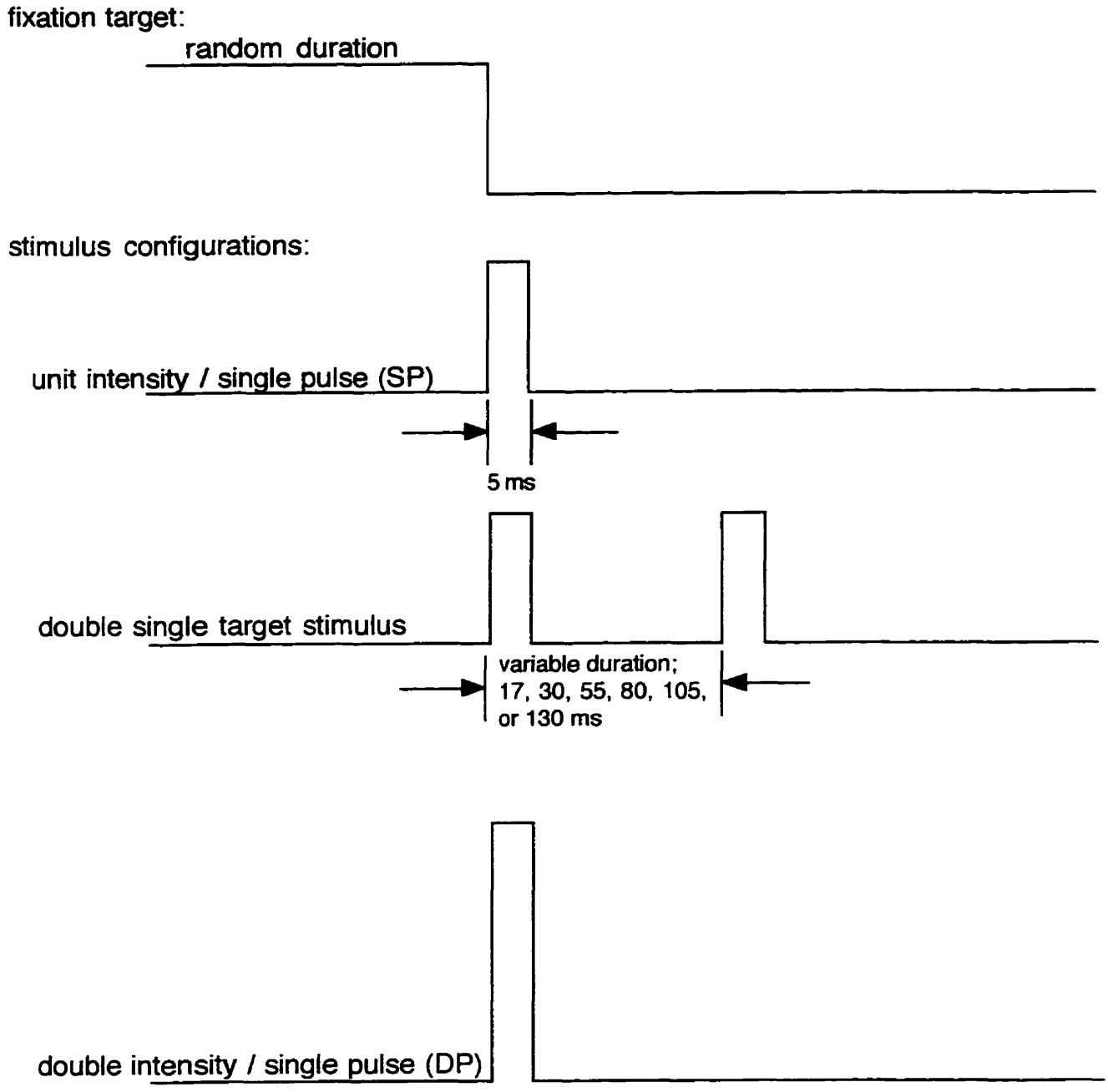

Figure 2.4: Schematic of a trial. After a fixation period of random duration, one of the 8 stimulus configurations shown above was presented to the subject.

2.4 Data Analysis and Data Trimming:

The stream of data from EMMA was processed in two steps. The first step, done as the data was coming in from EMMA, was where the descriptive characteristics of the saccade, namely saccadic latency, amplitude, peak velocity and duration, were calculated. These values were saved at the end of each trial onto the computer's hard drive for an offline analysis.

The first step of the offline analysis was to filter out the bad data from the raw data. Tracking eye movement via the corneal reflections has its shortcomings and one of them was that head movements were registered incorrectly as eye movements. Small head movements, which would occur occasionally, would result in the infrared beam moving out of focus or off the cornea and disrupt the tracking, resulting in nonsensical records of saccadic eye movement. These, in addition to anticipatory saccades, needed to be filtered out and was accomplished by rejecting saccades according the following criteria:

a) saccades with latencies less than 100 ms as they are deemed to be anticipatory (Kalesnykas & Hallett, 1987 & 1994)

b) spurious saccades with peak velocities in excess of 800°/s as these are blinks(Carpenter, 1977; Eizenman et al, 1984)

c) saccades with short duration (ie. less than 5 ms) and low speed (ie. around 20°/s) as they are most likely small eye lids or head movements

Finally, as a way to screen out inadvertent eye movement from reasons such as loss of attention to the task at hand, and to ensure that the saccade was truly directed at the target, saccadic amplitude had to be at least half of target amplitude. Such a cutoff may sound arbitrary and it is. However, an examination of some preliminary data showed that only a few data points per session were affected by this criterion and therefore the effect of this screen to the analyses that follow is minimal. This criterion was applied only to the bright data; for the dim data, this criterion was relaxed to allow for larger data sets.

The number of trials left after this pruning process varied from subject to subject and from session to session; on average, about one quarter of the raw data was eliminated, mostly because the subject has shifted his head and caused EMMA to fail to track the eye. What remained were then used listed by day, and subjected to an ANOVA test, taking a p-value of 5% as the cutoff, to

ensure that the data could be treated as if they were drawn from the same population. If the p-value was less than 5%, the day whose mean was the farthest from the grand mean was dropped until the p-value was acceptable. In total, 36,999 datapoints were recorded from the three subjects for main yellow-green experiment; 8,757 datapoints (23.67%) were rejected on the three criteria aforementioned, and 213 datapoints (0.58%) were removed because they were direction errors. Finally, an additional 3,428 (9.27%) datapoints were rejected by the ANOVA test. The remaining 24,601 datapoints were then used in the analyses detailed in the results section.

Results

3.1 Mean Latency and Frequency of Response

3.1.1 Frequency of Saccadic Response

In most previous experiments, conditions were such that saccades were elicited at each trial; on the rare occasions that there was no saccadic response, the absence was usually attributed to subject inattentiveness (eg. G.R. Barnes & Gresty, 1973; van Asten et al, 1988). However, the absence of a response could be caused by other reasons as well: when the energy of the stimulus was low, it was observed that the saccadic response became probabilistic (Barnes, 1995), and furthermore, when plotted against target energy, the resulting curve resembled the sigmoidal probabilistic curves found in psychophysical experiments like Hecht and Pirenne's classic 1942 study on visual threshold.

Before proceeding with the data, two things needed to be pointed out. One, in order to facilitate comparison with Barnes' results, it should be pointed out that a 5 millisecond flash at the FT+3 intensity (corresponding to having about 5 FT x sec of energy per pulse) would fall into the suprathreshold region in her experiments, while the same flash at the FT+1 and FT+0.5 intensity (corresponding to about 0.05 and 0.02 FT x sec of energy per pulse respectively) would fall in her probabilistic range for detection by the rods. The second point that needed to be made was that, although FT settings have been hereto successful in normalizing this laboratory's data by allowing for intersubject and intersession variations in optical factors such as pupillary diameter, the FT approach was less than ideal for the current experiment as the FT unit would only normalize for stimuli falling on the fovea rather than the periphery. Nevertheless, target intensity was still denominated in units of FT for the sake of continuity with experiments conducted previously in the laboratory. As will be made apparent later, a possible consequence was that subject LL's stimulus intensities seemed anomalous as judged by the latency and frequency of saccadic response results. Because of this aberration, the various subject-stimulus combinations were divided into three groups: a "bright target" group consisting of the subject-target combinations of LL's FT+3, RC's FT+3, and PH's FT+3, an "intermediate target" group consisting of LL's FT+1 data, and a "dim target" group made up of the remaining data (ie. LL's FT+0.5, RC's FT+1 and PH's FT+1). Because the results of the intermediate targets were very similar to those of the bright targets, the

two will be discussed together in the following sections.

As expected, the frequency of saccadic response did not change significantly with the length of the delay between the pulses for bright and intermediate targets; while it varied from subject to subject, the variations within subjects were small. The frequency of responses of the two of the subjects, RC and PH, for this stimulus intensity was around 99%. Since there were many trials, the fact that the subjects would miss a number of stimulus is to be expected and as a result, few frequencies in Figure 3.1 reached exactly 100%. The number for the third subject LL was lower, and it fluctuated around 95%. (The 89% frequency of saccadic response observed at the FT+3, single pulse/double intensity stimulus configuration might be an anomaly, considering that LL's intermediate data did not show a similar drop for the same stimulus configuration.)

In the case of the dim targets, the frequency of saccadic response for all three subjects (ie. PH at FT+1, RC at FT+1 and LL at FT+0.5) was flat initially, but dropped as the time interval between the two pulses was increased. As illustrated in Figure 3.1, the extent of the plateau and the decline varied from subject to subject.

From this perspective, the presence of a second pulse was (unsurprisingly) facilitatory for the dim targets for all delays that were tested, when compared against the single pulse/unit intensity stimulus. In addition, for short delays, the variation in the frequency of response was small, agreeing with the observations in Barnes' study, where it was observed that for a single pulse stimulus with intensity and duration within the range that was examined, duration could be traded off against intensity without affecting the frequency of response; all that mattered was that the stimulus energy remained constant. The measured extent of this constancy varied from subject to subject (30ms to 105ms). As expected, for the bright and intermediate targets, the second pulse was irrelevant for response frequency, as pulse response frequency was already high.

3.1.2 Mean Latency

Target intensity is one of many factors that can affect saccadic latencies. At dim intensities, saccadic latencies were long and variable, but as the intensity increased, they were observed to shorten sharply initially, only to level off and arrive at a minimum latency at high intensities (Wheeless et al, 1967; Doma & Hallett, 1988a, b); furthermore, when latencies were graphed

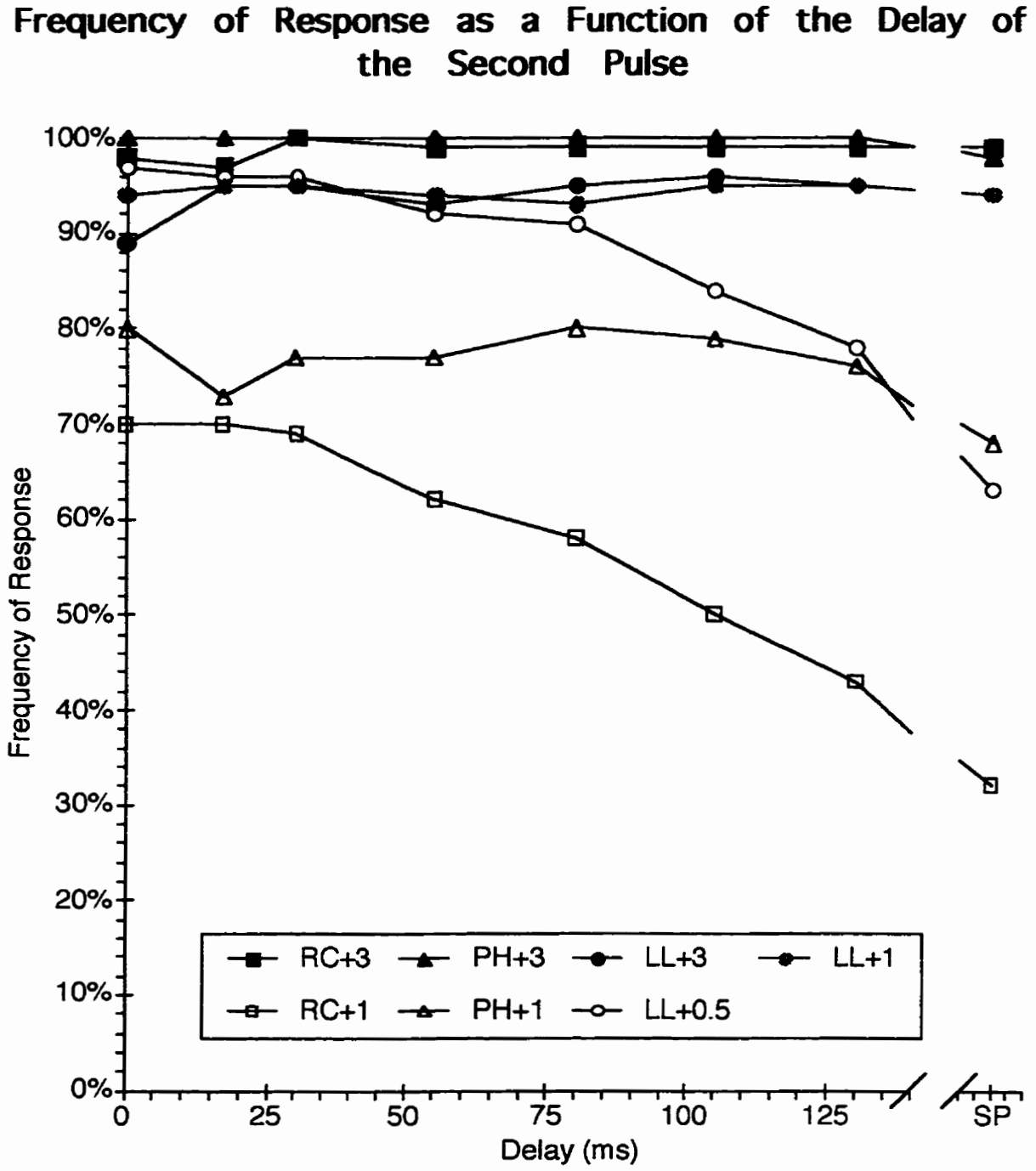

Figure 3.1: Frequency of saccadic response as a function of delay of the second pulse. A time delay of zero corresponds to a single pulse with twice the unit intensity, while the SP condition can be thought of as a 2-pulse stimulus with the second pulse delayed indefinitely. Note that the LL+1 line lies amongst the FT+3 data.

against intensity, it was found that the graph could be fitted to a function known as Pieron's law (Doma & Hallett, 1988a):

$$L(I) = L_{\infty} + kI^{\beta} \quad \text{.....(3.1)}$$

where

L(I) = saccadic latency,
L_{∞} = the minimum latency for the task,
I = the intensity,
k and β are constants with $\beta < 0$.

Since intensity is a factor that affects latencies, it is natural to expect that target energy can also affect latencies. It does, but the relationship between the two is not as well studied, nor is it as straightforward. When Barnes (1995) plotted saccadic latencies against energy from experiments in which target intensities were held constant, the graphs showed a region of overlap, where latency was a function of energy, and regions where latency was intensity-dependent.

For the bright and intermediate targets, the variation in average latency for all the subjects, as the delay in the presentation of the second pulse was increased from 17ms to 130ms, was small and on the order of the standard error of the mean (SEM); it was, therefore, difficult to draw statistically meaningful statements on how when the second pulse was presented would affect average latency. However, the difference between the average latencies to double-flash targets and those to single flash/double intensity targets was large enough to be statistically meaningful (See Figure 3.2, bottom). In view of a "waiting time" model, these two observations pointed to a system whose effective integration time at these intensities was shorter than 17ms.

In the case of the dim targets, the overall trend was that as the presentation of the second pulse was delayed, the mean latency increased. The small deviation from this trend occurred for two of the subjects (RC and LL) when the mean latency to targets consisting of one pulse at unit intensity (SP) became shorter than those in response to double pulses with long delays. In an experiment measuring the reaction time of subjects to doubly-flashed targets, Grossberg (1970) reported a similar effect for a late second pulse, thereby raising the possibility that a second pulse falling 100 or so milliseconds after an initial pulse was inhibitory. Such a statement, namely that the mean latency and the frequency of response exhibited divergent behaviours, needs not be contradictory because if mean latency was the more sensitive criterion, a change in the input could affect with it, without appreciably affecting the other.

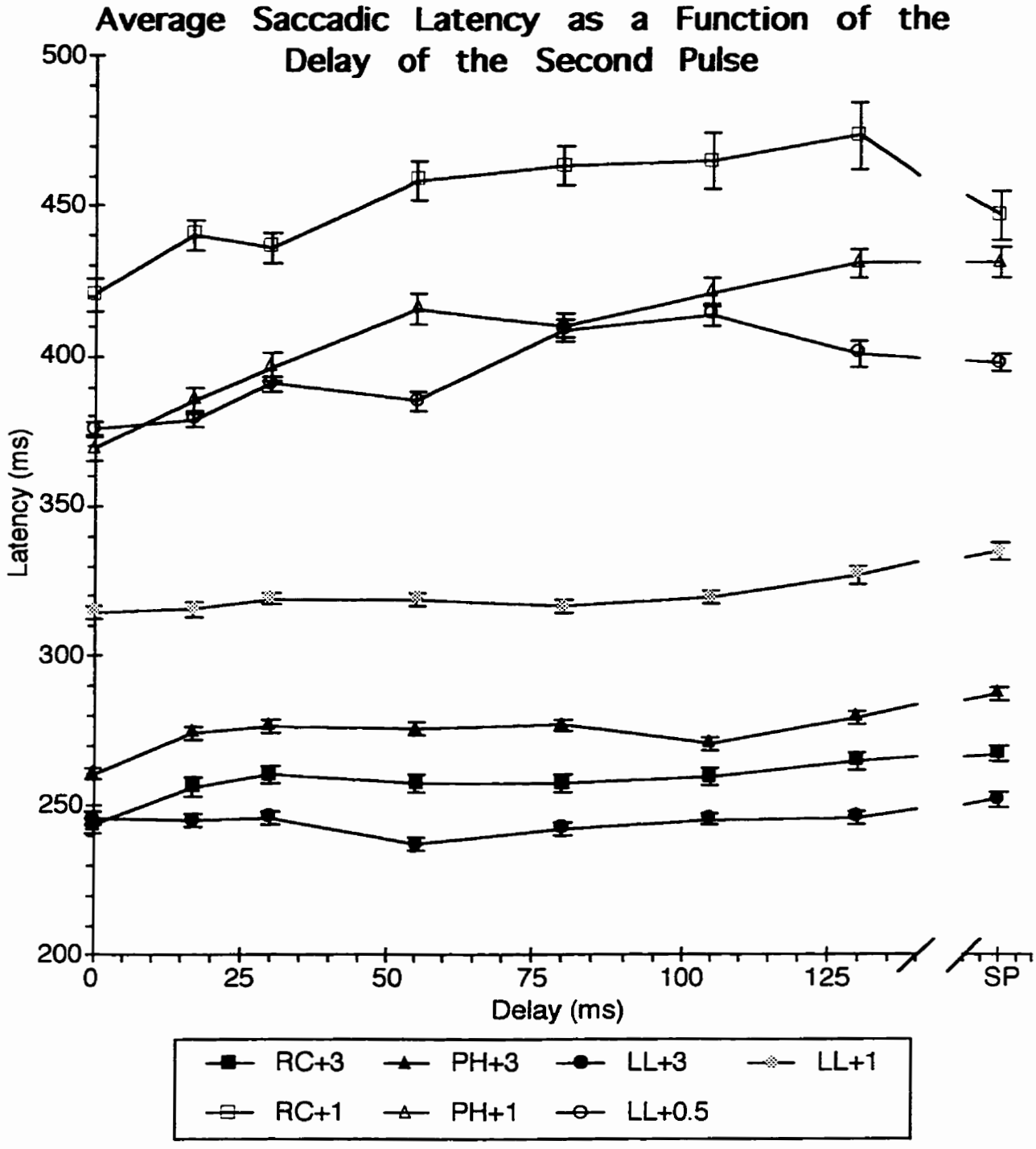

Figure 3.2: Average latency as a function of the time delay of the second pulse. Errors bars are set to 1 standard error of the mean. The graphs roughly divides into 3 groups: the bright data (ie. XX+3), the dim data (ie. RC+1, PH+1, LL+0.5), and an intermediate group (ie. LL+1).

In addition to mean latencies, median latencies were also examined in the same way and they yielded similar observations.

3.2 Modalities of the Latency Histograms

It has been suggested in the literature that there are more than one kind of saccades. When latency data were collected from a number of subjects using the gap and the overlap condition, it was argued by Fischer (Fischer et al., 1993) that the data supported a trimodal distribution. Taking the position that each mode corresponded to one type of saccade, he named them, in order of increasing latencies, the express saccades, fast regular and slow regular. However, while such a division is highly attractive (Fischer and Boch, 1993; Fischer et al., 1993; Hallett, 1993) because it could be taken as further evidence that saccadic programming could be broken into a number of "subroutines" that could be executed independently (Abrams & Jonides, 1988), the correctness of such a division is far from conclusive, because the argument in the aforementioned paper seemed to hinge on a earlier paper (Fischer & Ramsperger, 1984) that showed the existence of a separate population of saccades with very short latencies, and the goodness of fit of a trimodal model with free parameters as a posterior support for the hypothesis. The problem with fitting data to a trimodal distribution without first establishing that it is trimodal is that it is possible for one to obtain a seemingly multimodal sample from a unimodal distribution if the sample size is small; since speaking strictly, from a numerical analysis viewpoint, all that is required for a mode is to have a bin whose frequency is higher than its two flanking bins. For example, since there were only a few saccades for each latency bin in the panel in Figure 3.6 corresponding to a delay of 55ms, the period around 375ms, by virtue of having one or two saccades fewer than expected, created the appearance of a bimodal distribution. However, before one can claim that it is bimodal, one needs to ascertain that, given the scatter of the data, the perceived dip in distribution is significant, and not an artefact of too few samples. Others have raised similar questions. There have been experiments, using the same gap paradigm as was employed in Fischer's experiments, which questioned whether the short latency saccades that were observed constituted a separate population (Wenban-Smith & Findlay, 1991; Reuter-Lorenz et al., 1991; Cameron & Albano, 1994).

Out of this context then comes the question of how many modes do the histograms obtained from the current experiment have? A priori, one could argue that any number up to six is conceivable, if one allows the assumption that each of a pulse pair may generate an express saccade, a fast regular and a slow regular mode.

A model-free statistical method employing bootstrapping (Silverman, 1981; Izenman and Sommer, 1988; Efron and Tibshirani, 1993) was used as an objective way of determining the data's modality. The first step of the test was to convolve a bootstrapped sample of the data with a Gaussian to obtain a Gaussian kernel density estimate. The standard deviation of the smoothing Gaussian kernel, h_k, was chosen such that it was the smallest possible value that would make the Gaussian kernel density estimate of the original data to have k modes. The assigned significance level, ASL, was defined to be the frequency with which bootstrap resamplings of the smoothed data would generate more than k modes. The rationale behind the technique is that if k was chosen to be artificially low, then smoothing would be extreme (ie. h_k is large) and convolving a resampled data set with the Gaussian kernel would rarely increase the number of modes, and so ASL would be low. Once the ASLs for a number of modalities have been computed for a given experimental conditions, the lowest value of k at which ASL exceeds some predetermined cutoff such as 5% was taken to be the best estimate of modality. A stricter criterion corresponds to a higher ASL.

The latency data were examined with this algorithm, with each modality being tested with 1000 bootstrap samples to obtain an ASL value for that modality. The results are tabulated in Tables 3.1 and its supplements, and the figures 3.3 through 3.9 show the histograms and their corresponding kernel density estimates obtained from the algorithm. Window widths, h_k, corresponding to an ASL of at least 0.10 were used.

The majority, 72% (41/56), of the 56 conditions tested were unimodal, if the ASL cutoff value was taken to be 5%. Of the remaining, 23% (15/56) were bimodal and the rest, trimodal or higher. If a more stringent ASL of 10% was used, about 66% (37/56) were unimodal, 27% (15/56) were bimodal and the rest (4/56) had three or more modes (Tables 3.1 and 3.1 supplement A, B). However, if one were allowed to apply judgment and discard some outlying modes as spurious (ie. Figure 3.3, delay = 17ms panel at 600ms), then more histograms would have fewer

Subject RC:

Intensity = FT+3

modes	Δp=0	Δp=17	Δp=30	Δp=55	Δp=80	Δp=105	Δp=130	SP
1	0.52 (12)	0.00 (58)	0.00 (69)	0.35 (40)	0.31 (40)	0.05 (34)	0.17 (39)	0.03 (44)
2	0.56 (10)	0.15 (22)	0.60 (13)	0.01 (36)	0.16(28)	0.41 (22)	0.00 (34)	0.26 (18)
3	0.83 (7)	0.26 (12)	0.21 (13)	0.33 (17)	0.09 (22)	0.17 (17)	0.10 (22)	0.03 (17)

Intensity = FT+1

modes	Δp=0	Δp=17	Δp=30	Δp=55	Δp=80	Δp=105	Δp=130	SP
1	0.36 (37)	0.24 (37)	0.04 (75)	0.16 (41)	0.89 (22)	0.40 (38)	0.71 (37)	0.5 (28)
2	0.33 (25)	0.04 (29)	0.48 (27)	0.95 (16)	0.48 (22)	0.54 (28)	0.40 (33)	0.32 (24)
3	0.2 (21)	0.08 (24)	0.24 (22)	0.71 (16)	0.22 (20)	0.44 (24)	0.28 (29)	0.13 (23)

Subject PH:

Intensity = FT+3

modes	Δp=0	Δp=17	Δp=30	Δp=55	Δp=80	Δp=105	Δp=130	SP
1	0.30 (12)	0.41 (12)	0.66 (10)	0.66 (10)	0.19 (18)	0.54 (9)	0.27 (14)	0.02 (43)
2	0.07 (11)	0.14 (11)	0.24 (10)	0.28 (10)	0.36 (12)	0.18 (9)	0.06 (13)	0.07 (20)
3	0.13 (9)	0.20 (8)	0.06 (10)	0.06 (10)	0.90 (7)	0.02 (9)	0.72 (7)	0.03 (17)

Intensity = FT+1

modes	Δp=0	Δp=17	Δp=30	Δp=55	Δp=80	Δp=105	Δp=130	SP
1	0.01 (35)	0.00 (37)	0.13 (58)	0.10 (60)	0.53 (39)	0.55 (33)	0.34 (35)	0.02 (53)
2	0.38 (20)	0.14 (21)	0.17 (34)	0.06 (39)	0.03 (39)	0.62 (21)	0.66 (19)	0.24 (27)
3	0.60 (11)	0.29 (14)	0.05 (28)	0.01 (37)	0.25 (27)	0.50 (18)	0.52 (17)	0.07 (23)

Subject LL:

Intensity = FT+3

modes	Δp=0	Δp=17	Δp=30	Δp=55	Δp=80	Δp=105	Δp=130	SP
1	0.24 (19)	0.12 (17)	0.15 (15)	0.10 (19)	0.34 (18)	0.14 (21)	0.23 (16)	0.02 (35)
2	0.24 (15)	0.28 (11)	0.11 (11)	0.30 (11)	0.03 (16)	0.67 (11)	0.05 (15)	0.01 (23)
3	0.42 (11)	0.26 (9)	0.05 (10)	0.33 (8)	0.14 (12)	0.40 (9)	0.47 (8)	0.15 (11)

Intensity = FT+1

modes	Δp=0	Δp=17	Δp=30	Δp=55	Δp=80	Δp=105	Δp=130	SP
1	0.00 (70)	0.17 (21)	0.19 (17)	0.05 (42)	0.42 (15)	0.00 (52)	0.00 (84)	0.00 (44)
2	0.08 (19)	0.04 (18)	0.00 (17)	0.16 (20)	0.11 (13)	0.49 (20)	0.02 (45)	0.17 (19)
3	0.31 (12)	0.51 (10)	0.54 (8)	0.12 (13)	0.4 (9)	0.09 (18)	0.23 (21)	0.51 (12)

Intensity = FT+0.5

modes	Δp=0	Δp=17	Δp=30	Δp=55	Δp=80	Δp=105	Δp=130	SP
1	0.06 (35)	0.45 (22)	0.47 (27)	0.00 (81)	0.04 (59)	0.15 (45)	0.35 (31)	0.65 (24)
2	0.10 (19)	0.02 (22)	0.19 (19)	0.03 (32)	0.27 (26)	0.07 (31)	0.23 (27)	0.22 (20)
3	0.17 (14)	0.03 (18)	0.03 (18)	0.00 (28)	0.18 (21)	0.36 (17)	0.2 (22)	0.48 (14)

Table 3.1: The results of the bootstrap. The ASL-value of the first 3 modalities are shown with its window width, hk, rounded to the nearest millisecond, in parenthesis.

	Δp=0	Δp=17	Δp=30	Δp=55	Δp=80	Δp=105	Δp=130	SP
RC+3	U	M *	M *	U	U	U/M	U	M *
RC+1	U	U	M *	U	U	U	U	U/M
PH+3	U	U	U	U	U	U	U	M *
PH+1	M	M	U	U	U	U	U	M
LL+3	U	U	U	U	U	U	U	M
LL+1	M	U	U	U/M*	U	M *	M *	M *
LL+0.5	U/M*	U	U	M *	M *	U	U	U

Table 3.1 supplement A: Summary of the modality of the various latency distributions. An "U" represents a unimodal distribution, and an "M" represents a multimodal distribution. An "U/M" represents a condition which would be a unimodal distribution if a value of 0.05 was used as the ASL cutoff, and a multimodal distribution when a value of 0.10 was used. Entries marked with an asterisk (*) indicate that the number of modes in these distributions may be overstated because they each include a small mode, centred on only a few data points at long latencies.

	Δp=0	other values of Δp	SP	
Bright & Intermediate	3/1/0	20/3/1	0/3/1	23/7/2
Dim	2/1/0	14/4/0	2/1/0	18/6/0
	5/2/0	34/7/1	2/4/1	41/13/2

	Δp=0	other values of Δp	SP	
Bright & Intermediate	75/25/0	83/13/4	0/75/25	72/22/6
Dim	67/33/0	78/22/0	67/33/0	75/25/0
	71/29/0	81/17/2	29/57/14	73/23/4

Table 3.1 supplement B: Summary of the frequency of each modality. The numbers in each cell correspond to the frequency of a unimodal, bimodal, multimodal (ie. >2) distribution respectively. Top table contains the raw count and the bottom table contains the values of the top table normalized to 100% for each condition. An ASL-value of 0.05 was used as the cutoff.

modes: seven would be classified as bimodal, and the remaining, unimodal. While it may be tempting to discard them, one has to be certain that in doing so, one is not mistaking some property of the system that generates a few, but slow, saccades as noise. Since the initial motivation to use the bootstrapping technique was to avoid human judgment which may be skewered by prior expectations, the results obtained by the strict application of the statistical method were taken as correct.

When the results were divided by target intensities, an examination showed that for the

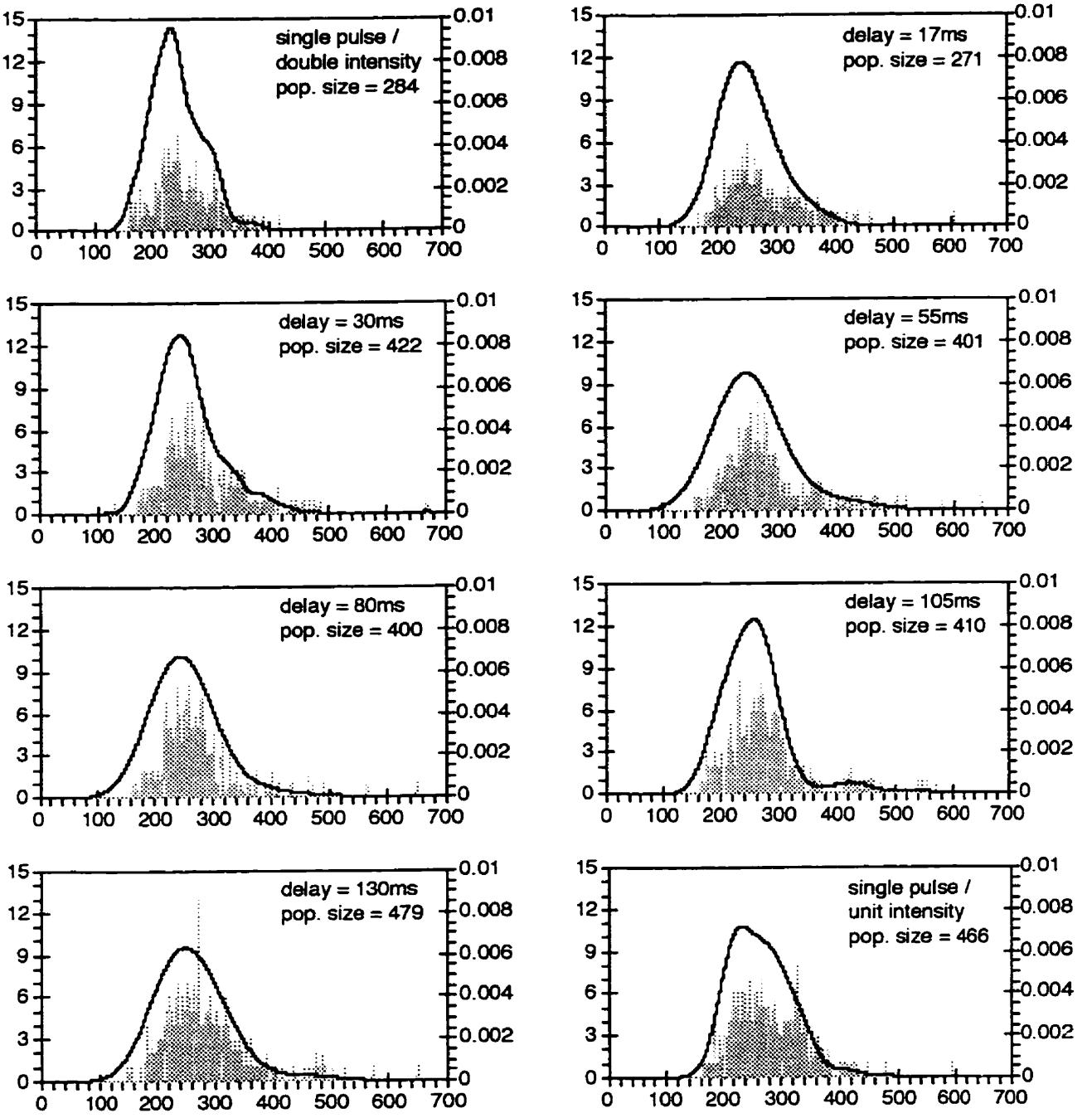

Figure 3.3: Latency histogram and their kernel density estimates. Notice that some of the modes are small and far from the main mode (ie. delay of 17ms at 600ms), and deciding whether these modes should be kept is a tricky issue since it is difficult to determine if they are noise or some property of the system. The data shown here is of subject RC at an intensity of FT+3, using h_k values in Table 3.1 with ASL of at least 0.1. The scale for the histogram is on the left; for the density estimate, the right.

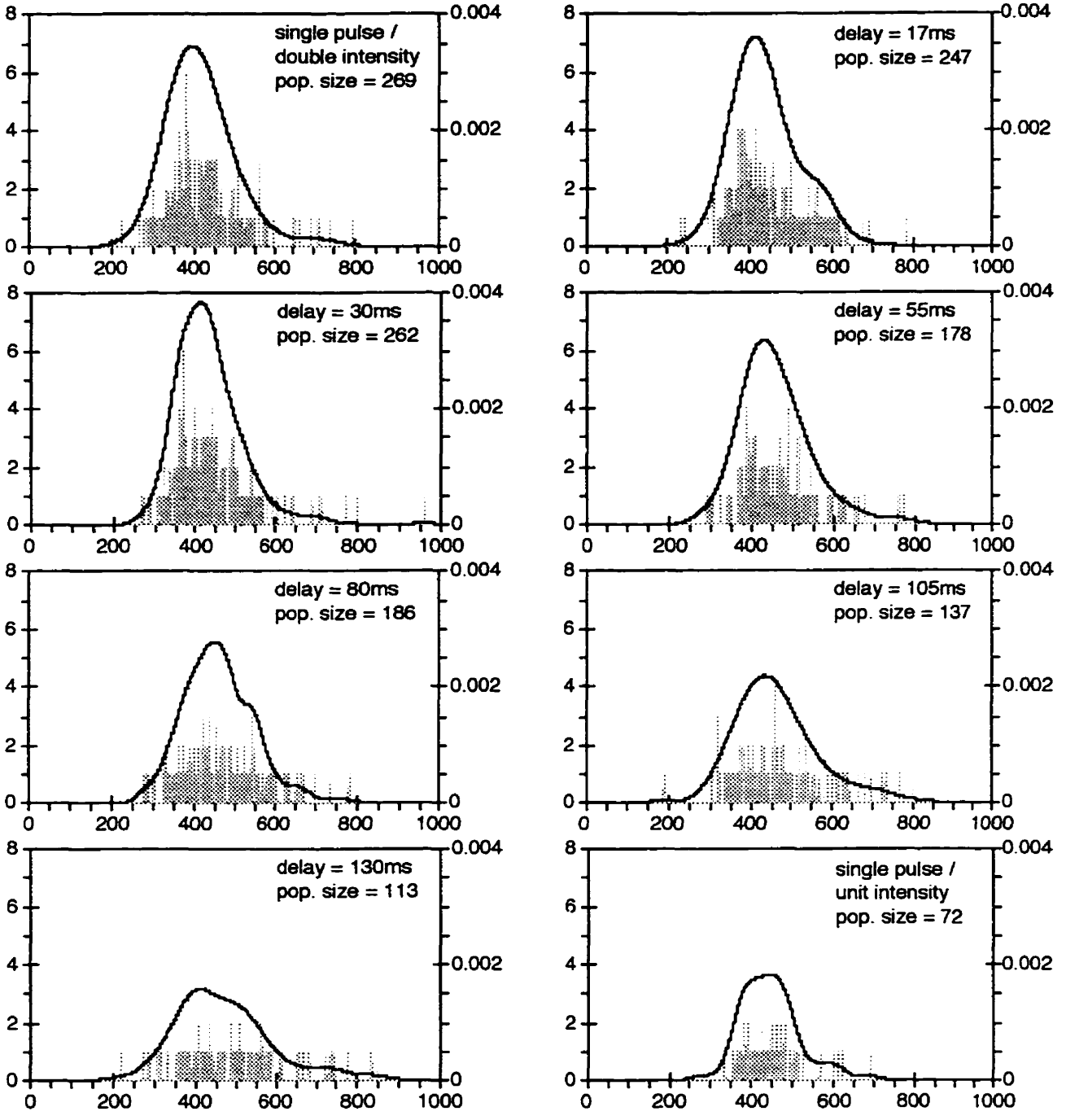

Figure 3.4: Latency histogram and their kernel density estimates. The kernel density estimates were obtained by convolving the histogram with a Gaussian using the values, taken from Table 3.1, which have an ASL-value of at least 0.1. The scale for the histogram is on the left; the one for the density estimate, the right. Subject RC at an intensity of FT+1.

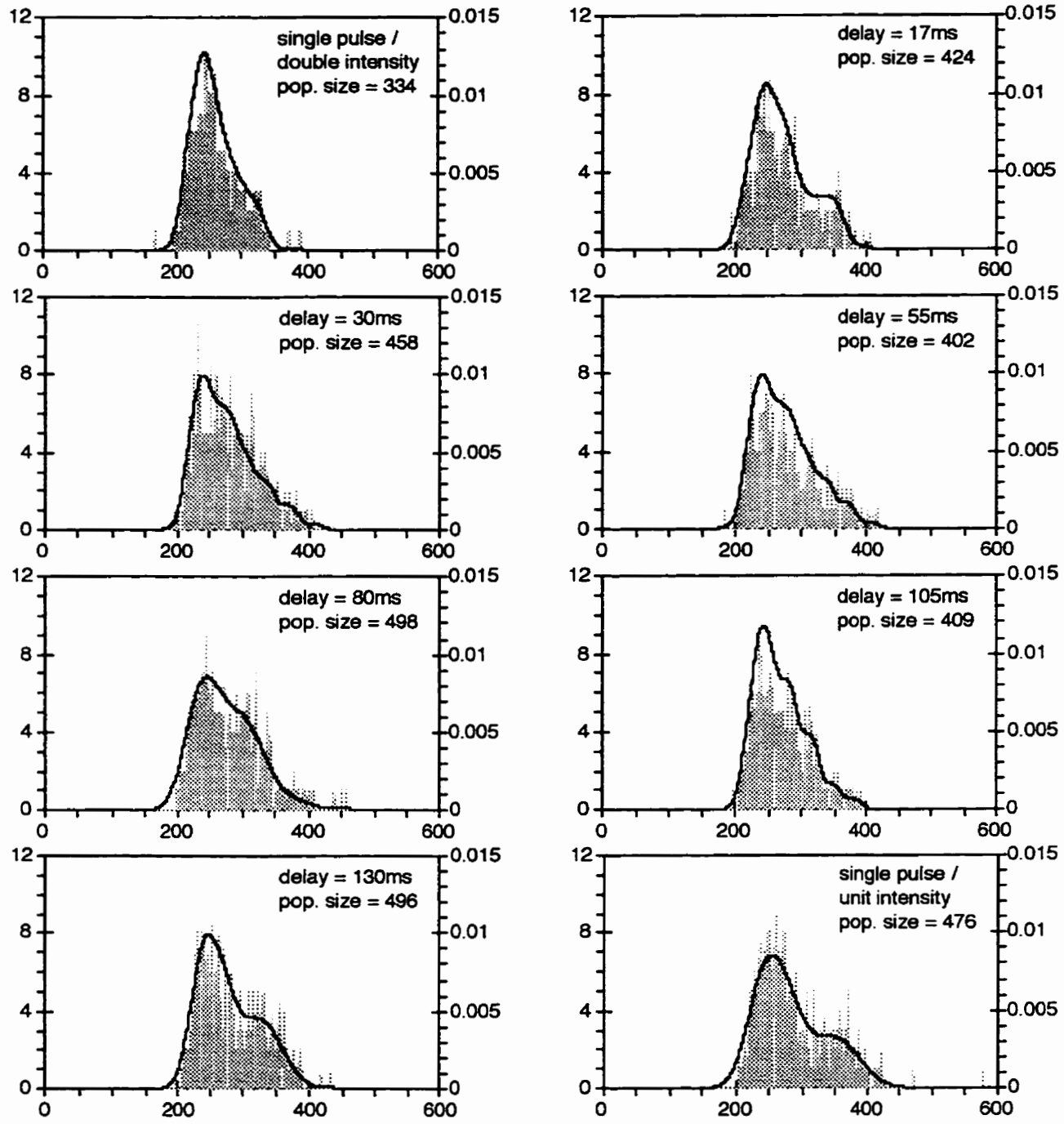

Figure 3.5: Latency histogram and their kernel density estimates. The kernel density estimates were obtained by convolving the histogram with a Gaussian using the values, taken from Table 3.1, which have an ASL-value of at least 0.1. The scale for the histogram is on the left; the one for the density estimate, the right. Subject PH at an intensity of FT+3.

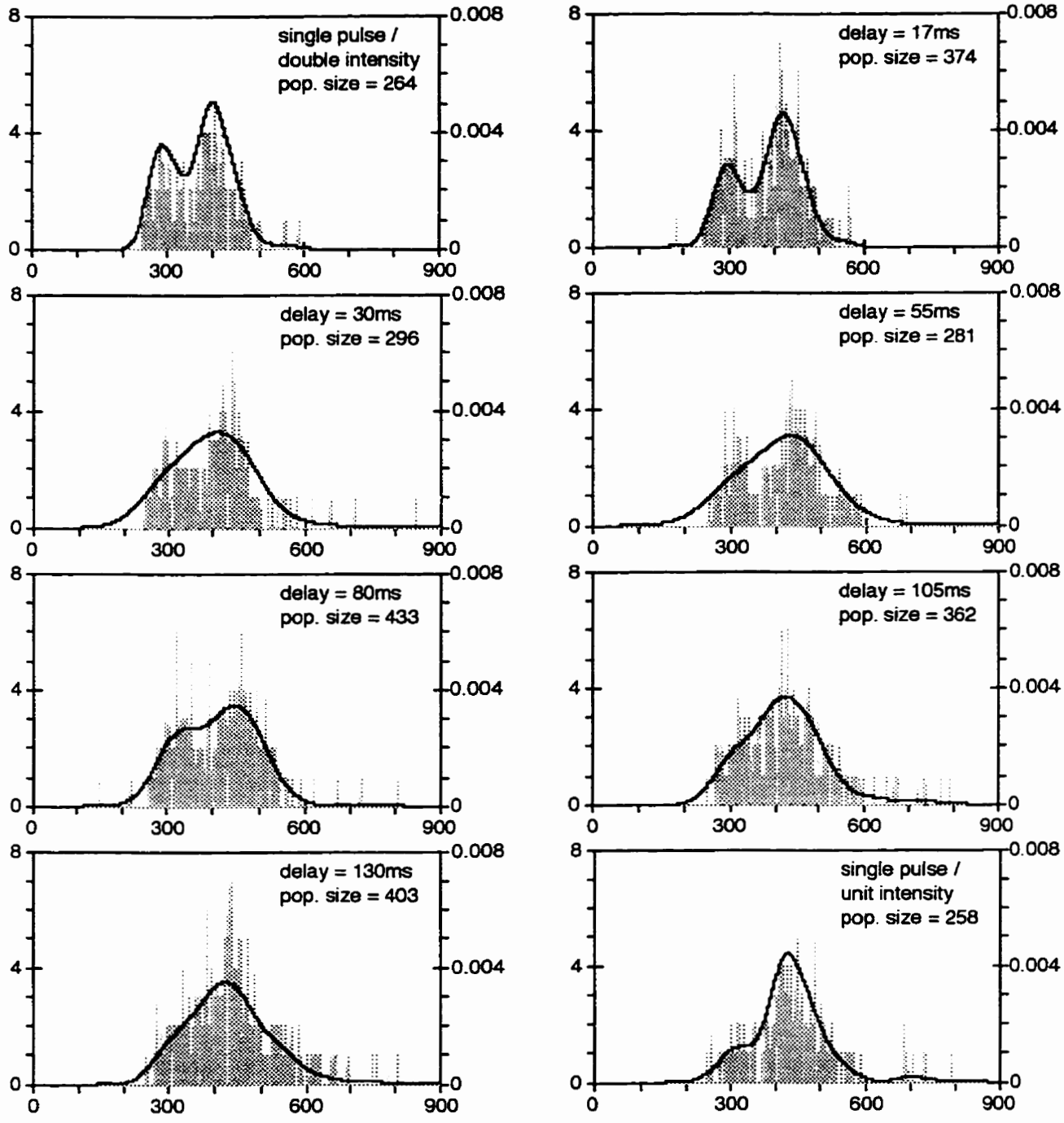

Figure 3.6: Latency histogram and their kernel density estimates. The kernel density estimates were obtained by convolving the histogram with a Gaussian using the values, taken from Table 3.1, which have an ASL-value of at least 0.1. The scale for the histogram is on the left; the one for the density estimate, the right. Subject PH at an intensity of FT+1.

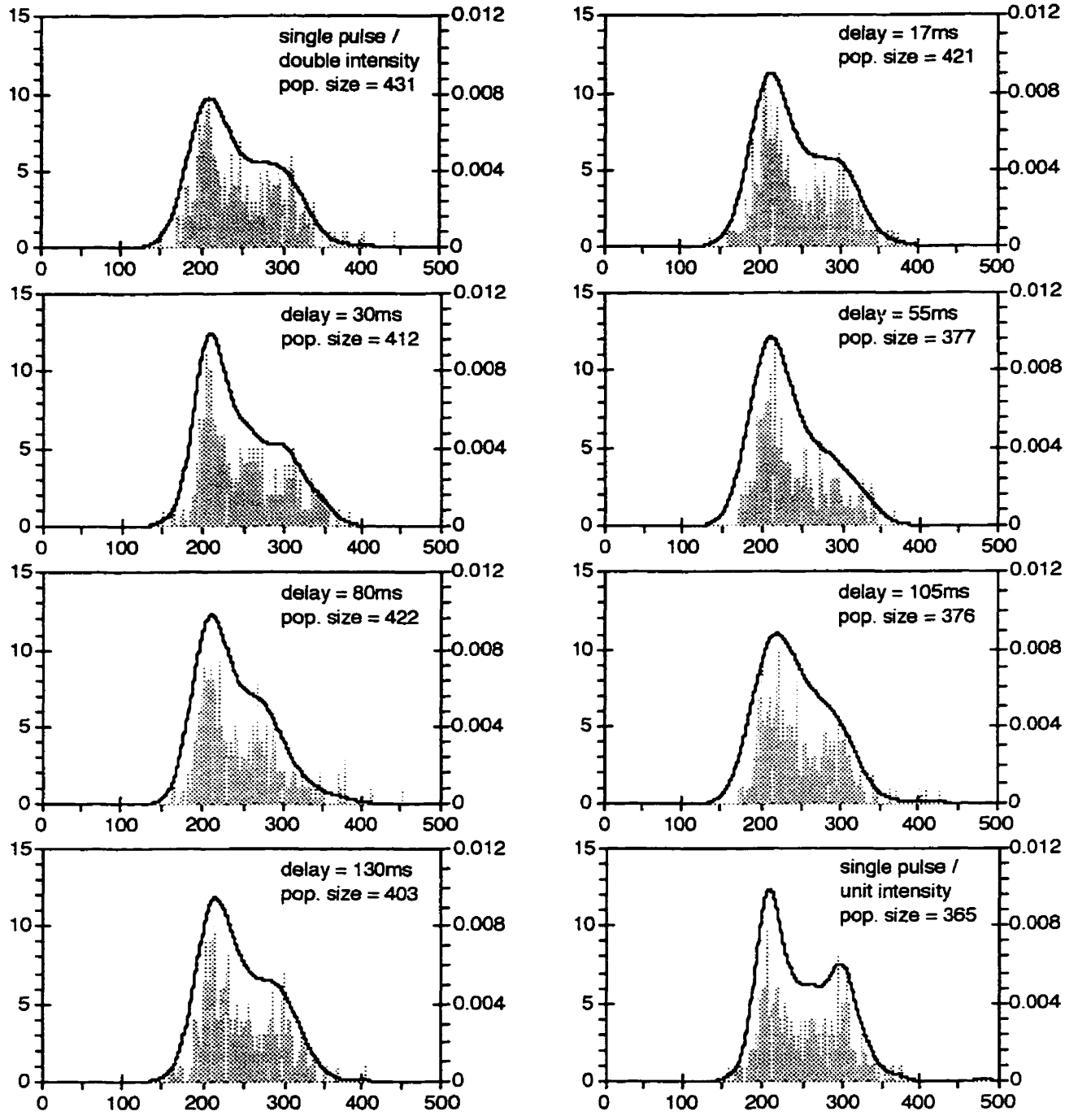

Figure 3.7: Latency histogram and their kernel density estimates. The kernel density estimates were obtained by convolving the histogram with a Gaussian using the values, taken from Table 3.1, which have an ASL-value of at least 0.1. The scale for the histogram is on the left; the one for the density estimate, the right. Subject LL at an intensity of FT+3.

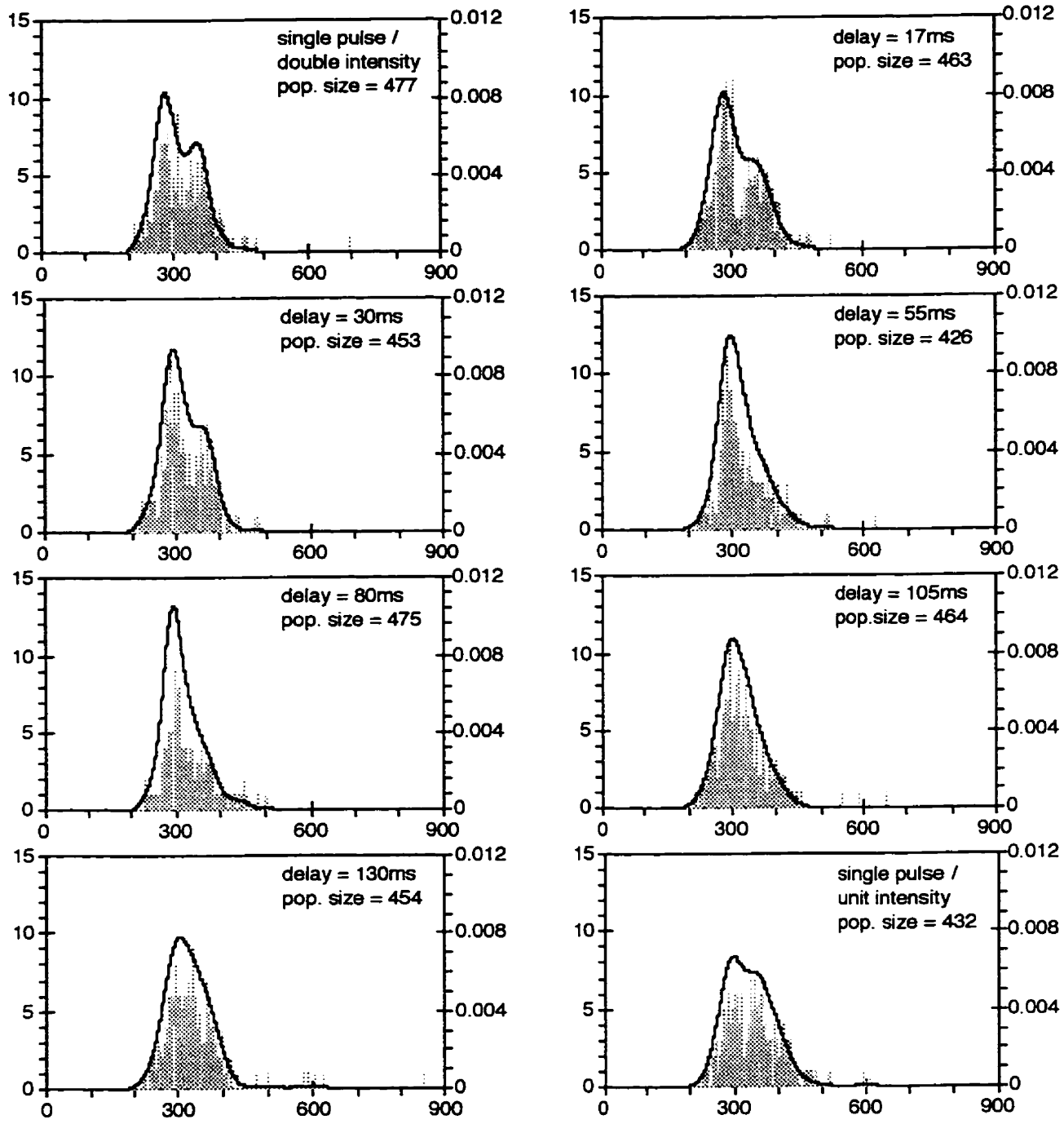

Figure 3.8: Latency histogram and their kernel density estimates. The kernel density estimates were obtained by convolving the histogram with a Gaussian using the values, taken from Table 3.1, which have an ASL-value of at least 0.1. The scale for the histogram is on the left; the one for the density estimate, the right. Subject LL at an intensity of FT+1.

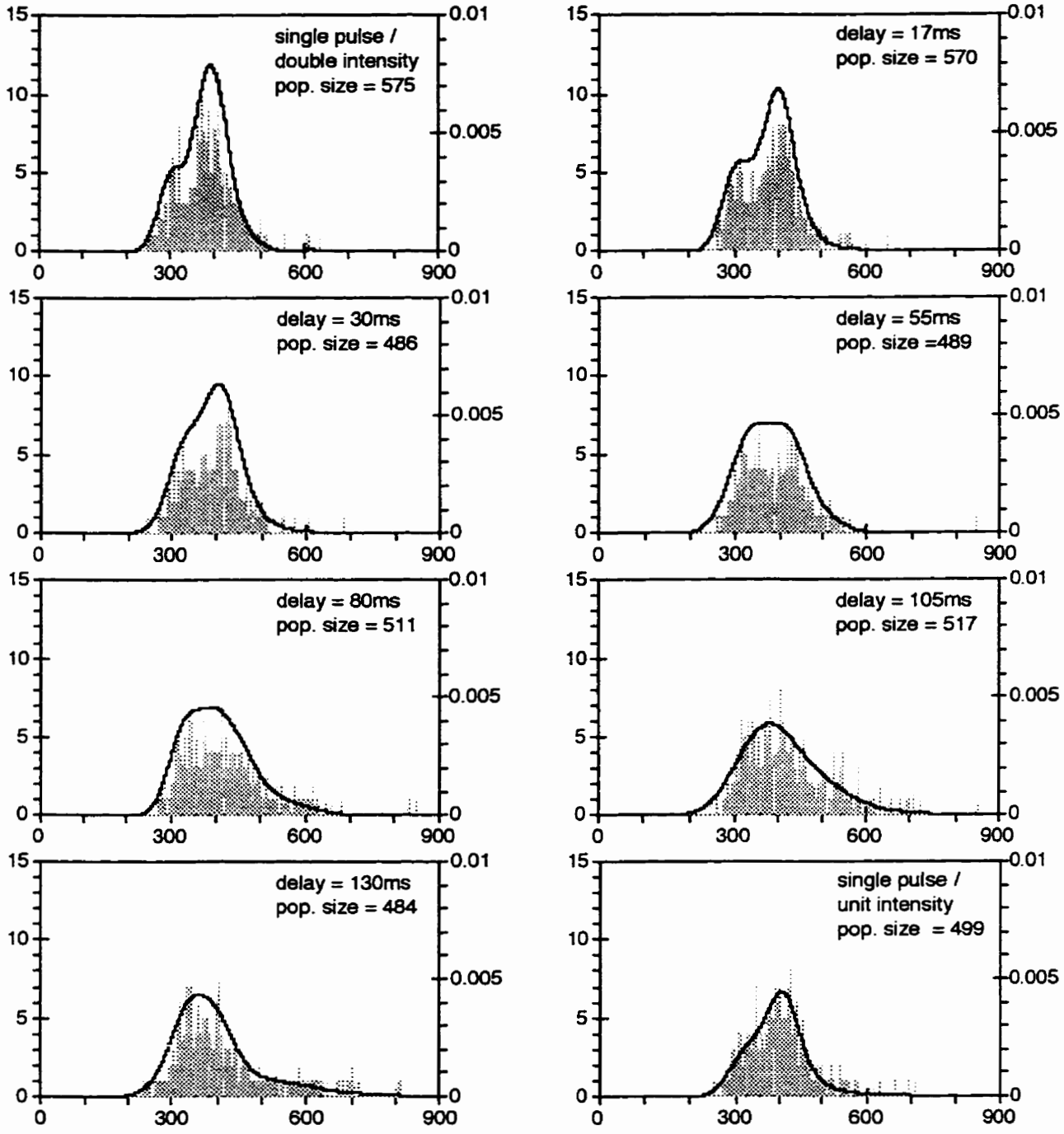

Figure 3.9: Latency histogram and their kernel density estimates. The kernel density estimates were obtained by convolving the histogram with a Gaussian using the values, taken from Table 3.1, which have an ASL-value of at least 0.1. The scale for the histogram is on the left; the one for the density estimate, the right. Subject LL at an intensity of FT+0.5.

single pulse/unit intensity conditions (SP), the data for the bright and intermediate intensities were multimodal. For other conditions at the same intensity, the situation was less clear, because even though the majority was unimodal, a sizable portion of the data from the subject RC and LL at the intensity of FT+1 was bimodal. This aberration may be due to a poorer quality of data as suggested by the larger window widths, h_k. Since RC had less experience in such experiments and LL was reacting to dimmer stimuli at the FT+1 intensity, data of lesser quality is certainly possible. As for the dim intensity, the instances of multimodality were scattered, and no useful observations could be drawn. Examination of the window width yielded only the expected observation that window widths tended to be larger than those at the brighter intensities, because saccadic latencies were more variable under such stimulus conditions.

In conclusion, the data, with the exception of the bright and intermediate SP condition, do not generally support a hypothesis of multiple peaks in the latency distribution for pooled sessions. However, it should be pointed out that the current experimental setup is not the ideal configuration for inducing express saccades (which is to say, a gap paradigm and few possible target eccentricities), even though it is conceptually possible that express saccades could still be elicited[1]. A more serious objection is that this bootstrapping technique has a bias to understate the number of modes (and hence, the number of populations), because it adopts the first modality whose ASL-value exceeds a predetermined threshold. In other words, while making the possibility of multimodal distribution of saccadic latency less likely, the test does not eliminate it altogether. This possibility is especially worth pursuing, considering that a close examination of the figures reveal all of the panels in Figures 3.5 and 3.7 exhibit a "shoulder" following the main peak at around 300ms for the bright intensities, and that many of the panels in Figures 3.6 and 3.9 exhibit also show a shoulder at around 300ms, but in this case, preceding the main peak. The shoulders found in RC's data did not conform to this pattern. At the FT+3 condition, most conditions did not

[1] Of the three common stimulus presentation paradigms--the gap, the standard displacement-step, and the overlap, the overlap paradigm results in the slowest saccades (Saslow, 1967). The additional delay is viewed usually as some additional cost incurred by the presence of the fixation point which is interfering somehow with saccadic programming. Considering that Fischer et al (1993) reported that express saccades were observed under the overlap paradigm, it is therefore not unreasonable to expect express saccades under the standard paradigm employed in the current experiment. More problematic was the use of seven target eccentricities versus the use of only one. In light of an experiment showing that subjects were able to initiate saccades faster if either amplitude or direction was known in advance (Abrams & Jonides, 1988), it is certainly possible that some of the latency reduction were attributable to the fact that only one target amplitude was used.

exhibit any shoulders (with the exception of the SP condition, single pulse/double intensity condition and a delay of 30ms at the FT+3 intensity), and its absence may be partially explained by the fact that his data at the FT+3 intensity were more scattered than the other two subjects, which resulted in larger values of h_k being used. At the FT+1 conditions, some of the panels did show shoulders, but they followed the main peak and were found in the 600ms region. The significance of these shoulders are unclear, but they may be signs that the latency distributions consist of a second and smaller population, whose presence is obscured by its proximity to the main population.

3.3 Cumulative Histograms and Difference of Such

Comparing the means and standard deviations of population of latencies gives only a limited picture of how latency was affected when the timing of the second pulse was manipulated; a more complete picture of what was happening could be obtained by reviewing all the data. This was done by examining the data as cumulative histograms and the differences between those curves and a baseline, one chosen to encapsulate the expectations of how a second pulse ought to effect latency distribution. By subtracting the baseline cumulative histogram from those observed for each condition, one could see how the second flash has either shortened (or lengthened) the latency of a population of saccades. But this begs the question: what is an appropriate baseline? What should the data be compared against to determine whether a second pulse with a delay of so many milliseconds is facilitatory or inhibitory?

3.3.1 The Single pulse/Unit intensity as a Baseline

One commonly-used baseline would be the single-pulse/unit intensity (SP) cumulative histogram plot; one could argue that if the object was to determine the effect of a second pulse of a certain time delay on latency distribution, one ought to do so by examining the cumulative histograms of double pulse stimuli against that of the SP condition. When this was done for RC's data, the results were unsurprising: the 2-pulse data were found to be producing more saccades with a shorter latency than the single-pulse data, as indicated by the fact that the difference obtained

by subtracting the cumulative histogram of the SP baseline from that for a 2-pulse data was mostly positive (Figure 3.10 and 3.11). The facilitatory effect of a second pulse was strongest at the short delay conditions, and is illustrated in the corresponding graphs as large areas under the solid curve (ie. Figure 3.10, top panel). The same was also true for the dimmer intensity. The other two subjects showed similar effects (Figure 3.12 through 3.16).

The shape of the curve (a rise, followed in some cases by a dip, and a plateau at a value greater than zero) reflects the relative distribution of the saccades in the test condition relative to that of the baseline. A bell shaped curve (ie. Figure 3.10, top panel) meant that the second pulse caused faster saccades to be produced, but did not produce more. A curve in the shape of a flattened "S" meant that (ie. Figure 3.11, top panel) not only did the second pulse produced a population of faster saccades, it also resulted in a higher total frequency of response. (Since the final value in a cumulative histogram is the total frequency of response, the height of the final plateau is the difference in the total frequency of response between the test condition and the baseline.) It would be nice if one was able to correlate the various bumps in these difference curves to the modes derived from the bootstrap method, but the fact is that the slope of these curves, and hence its shape, is the result of the relative magnitudes of the cumulative histograms of its two components, and hence, it does not necessarily follow that there is a meaningful relationship between these difference of cumulative histograms and the results of the bootstrap. Finally, the correspondence between these graphs and a graph of average latency is harder to discern, but it is there: plots with large areas under the curve tend to correspond to a shorter than SP latency.

3.3.2 Statistical Independence as a Baseline

Using the single-pulse/unit intensity cumulative histogram plot as the baseline may introduce a bias that overstates the facilitatory effect of the second pulse because it does not take into account that the double pulse stimuli have twice as much energy. Nor does it take into account that there are two pulses in the stimulus. As has been pointed out elsewhere, the inclusion or exclusion of such a fact may have a great impact on the final interpretation of the data (Watson, 1982). Since the object of the experiment was to examine how the two pulses in the stimulus

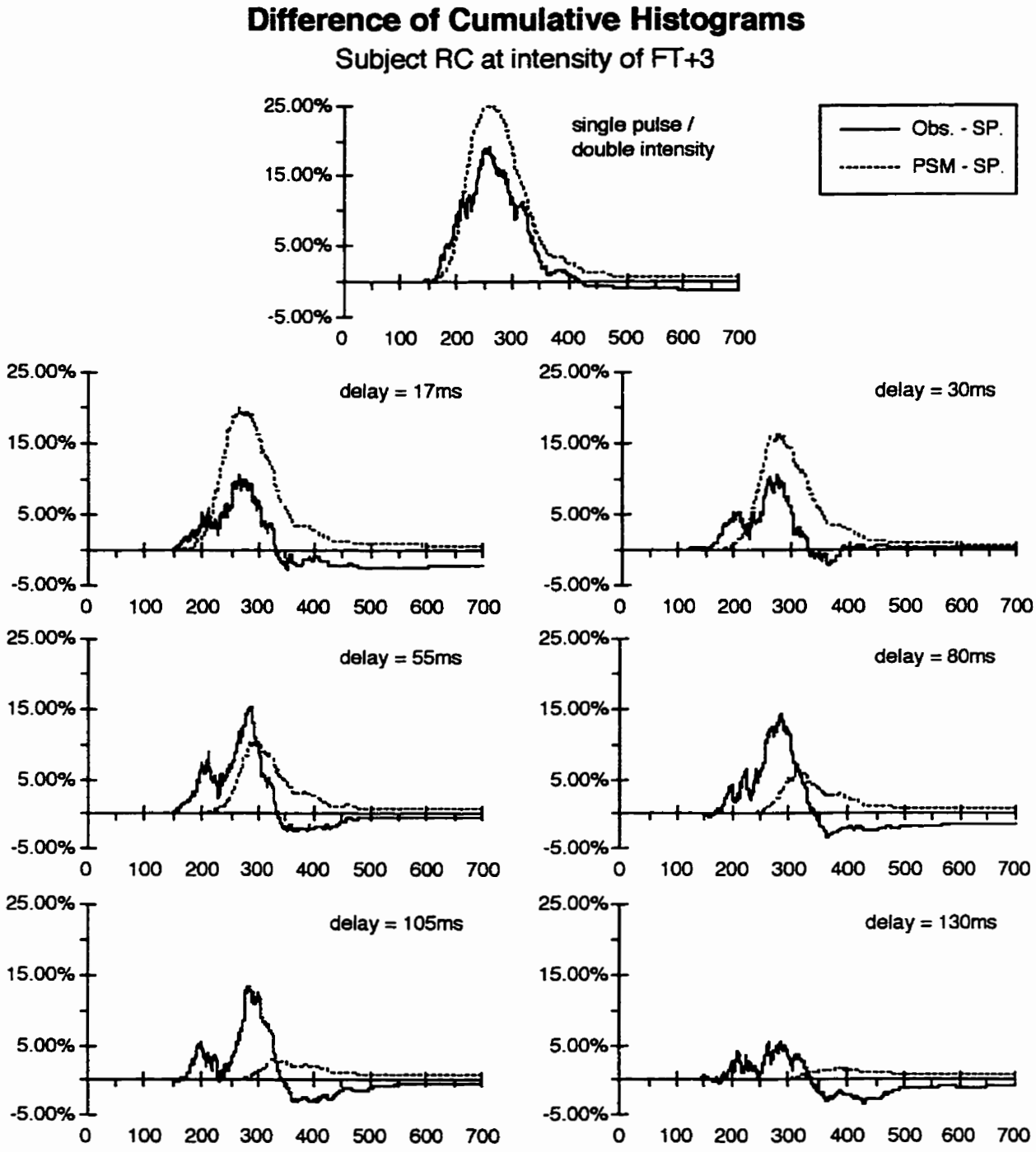

Figure 3.10: The effect of presenting a second pulse of light on latency distribution was determining by comparing the observed data (Obs.) with two baselines--the single pulse/unit intensity condition (SP) and the probability summation model (PSM). The extent of the effect when measured against the PSM baseline is shown by the difference of the two curves. Subject RC at an intensity of FT+3.

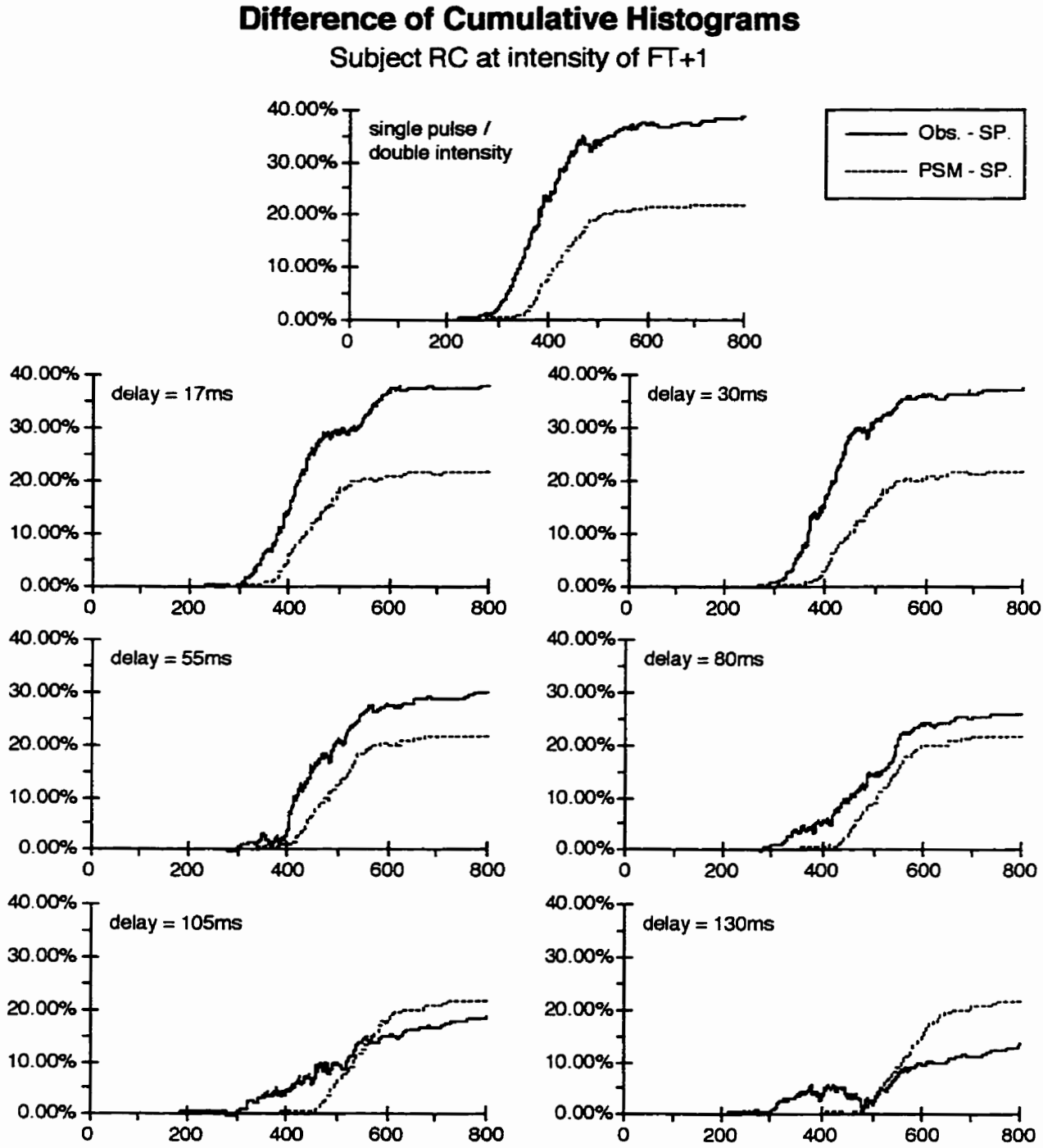

Figure 3.11: The effect of presenting a second pulse of light on latency distribution was determining by comparing the observed data (Obs.) with two baselines--the single pulse/unit intensity condition (SP) and the probability summation model (PSM). The extent of the effect when measured against the PSM baseline is shown by the difference of the two curves. Subject RC at an intensity of FT+1.

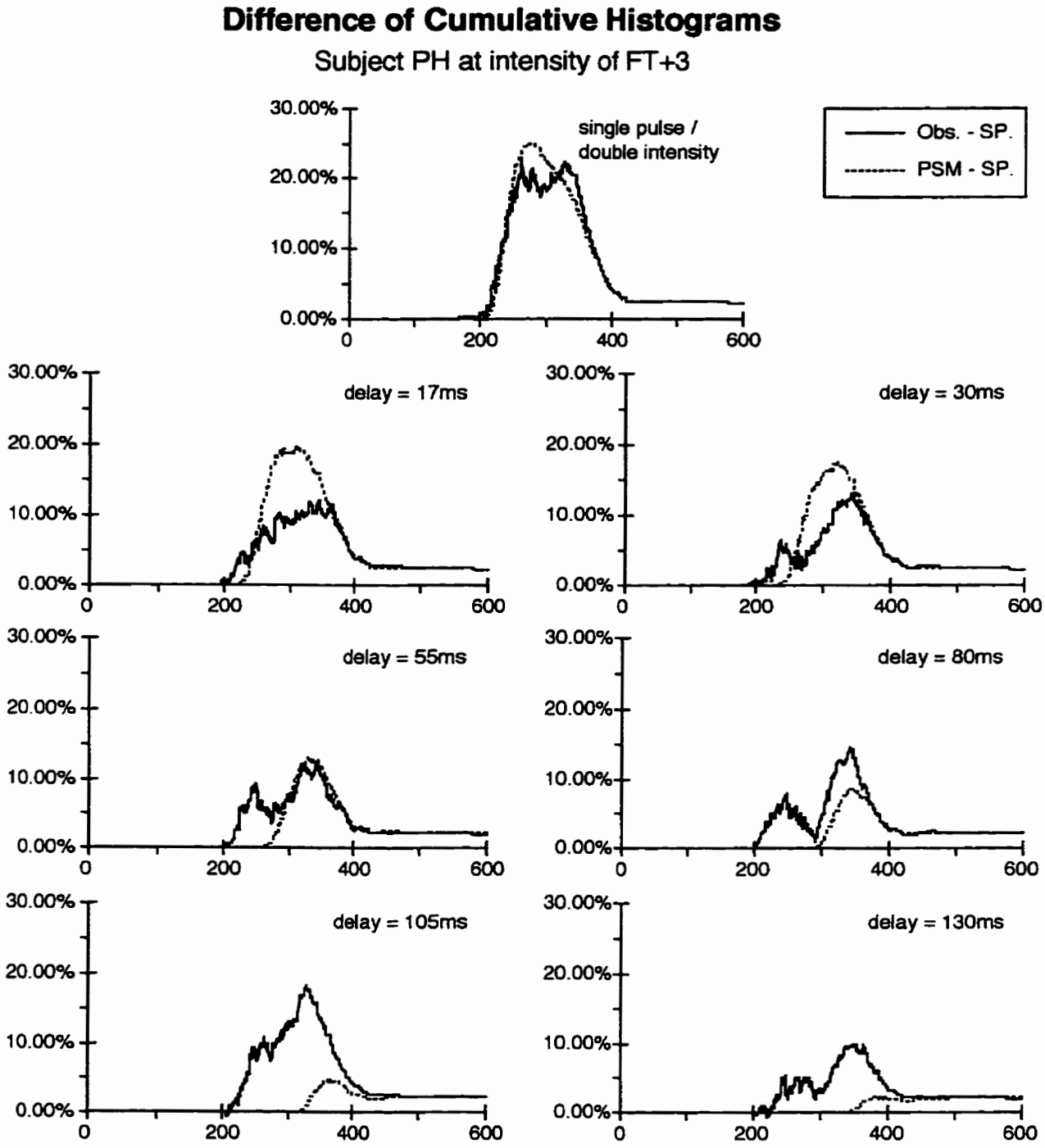

Figure 3.12: The effect of presenting a second pulse of light on latency distribution was determining by comparing the observed data (Obs.) with two baselines--the single pulse/unit intensity condition (SP) and the probability summation model (PSM). The extent of the effect when measured against the PSM baseline is shown by the difference of the two curves. Subject PH at an intensity of FT+3.

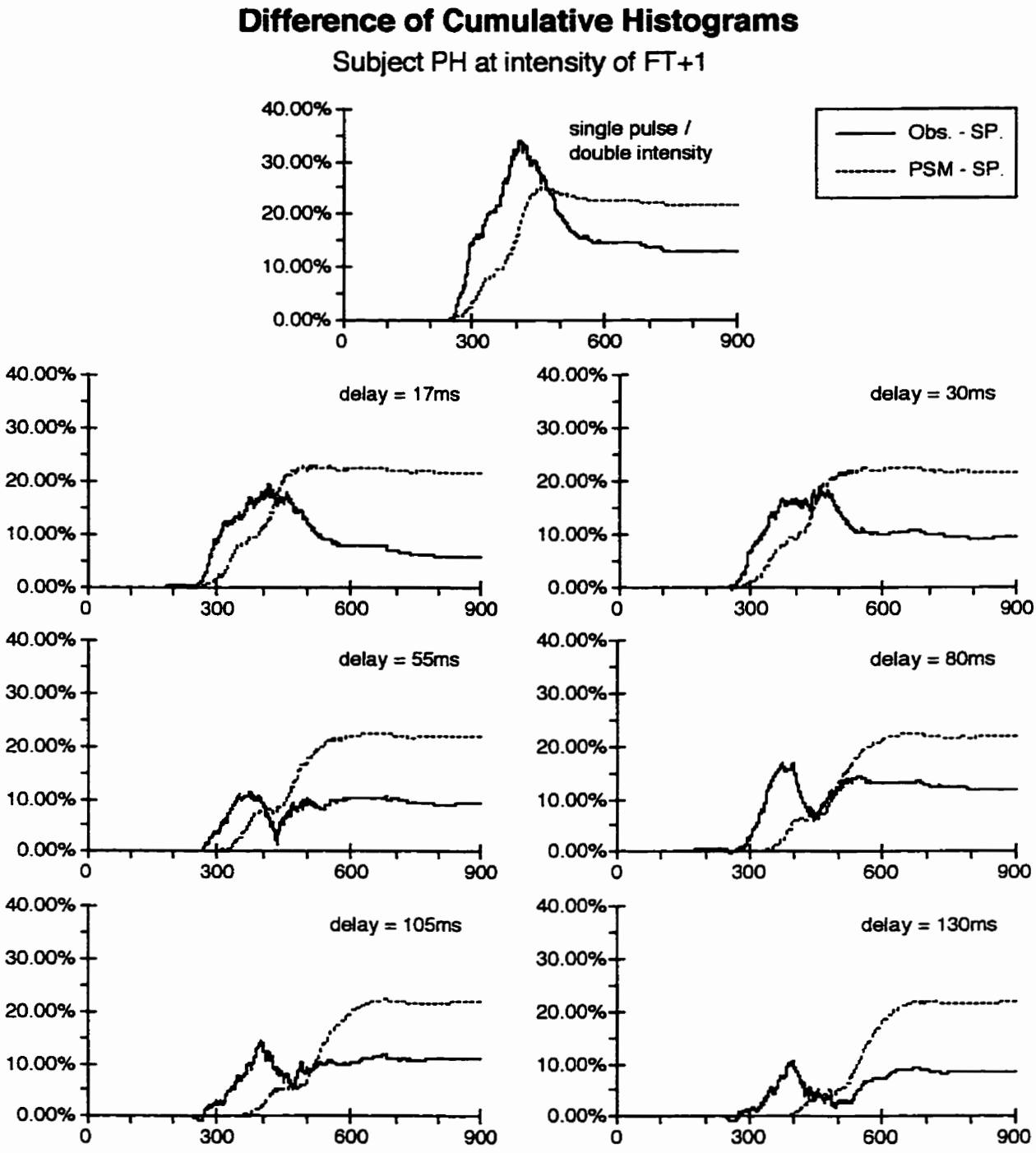

Figure 3.13: The effect of presenting a second pulse of light on latency distribution was determining by comparing the observed data (Obs.) with two baselines--the single pulse/unit intensity condition (SP) and the probability summation model (PSM). The extent of the effect when measured against the PSM baseline is shown by the difference of the two curves. Subject PH at an intensity of FT+1.

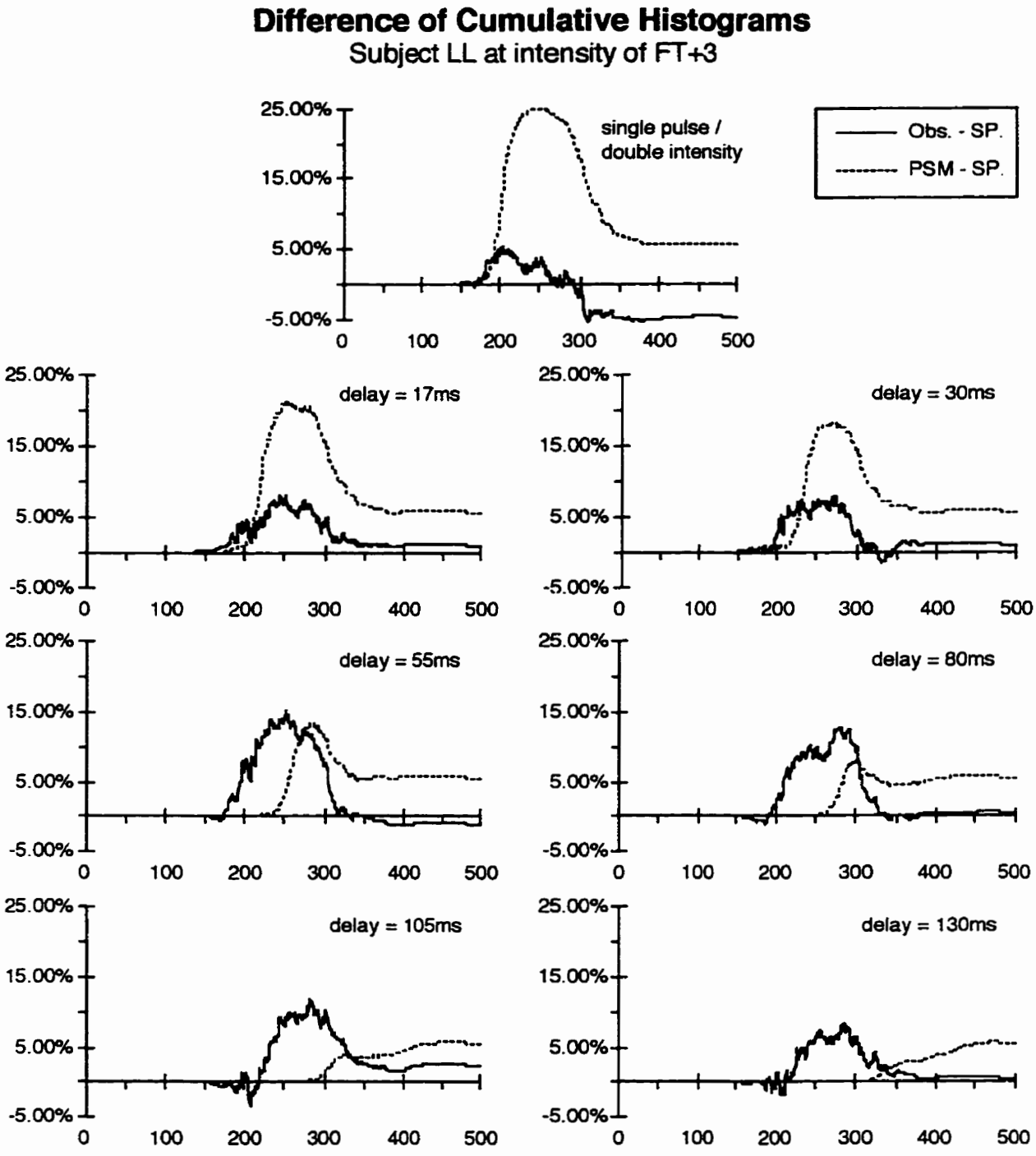

Figure 3.14: The effect of presenting a second pulse of light on latency distribution was determining by comparing the observed data (Obs.) with two baselines--the single pulse/unit intensity condition (SP) and the probability summation model (PSM). The extent of the effect when measured against the PSM baseline is shown by the difference of the two curves. Subject LL at an intensity of FT+3.

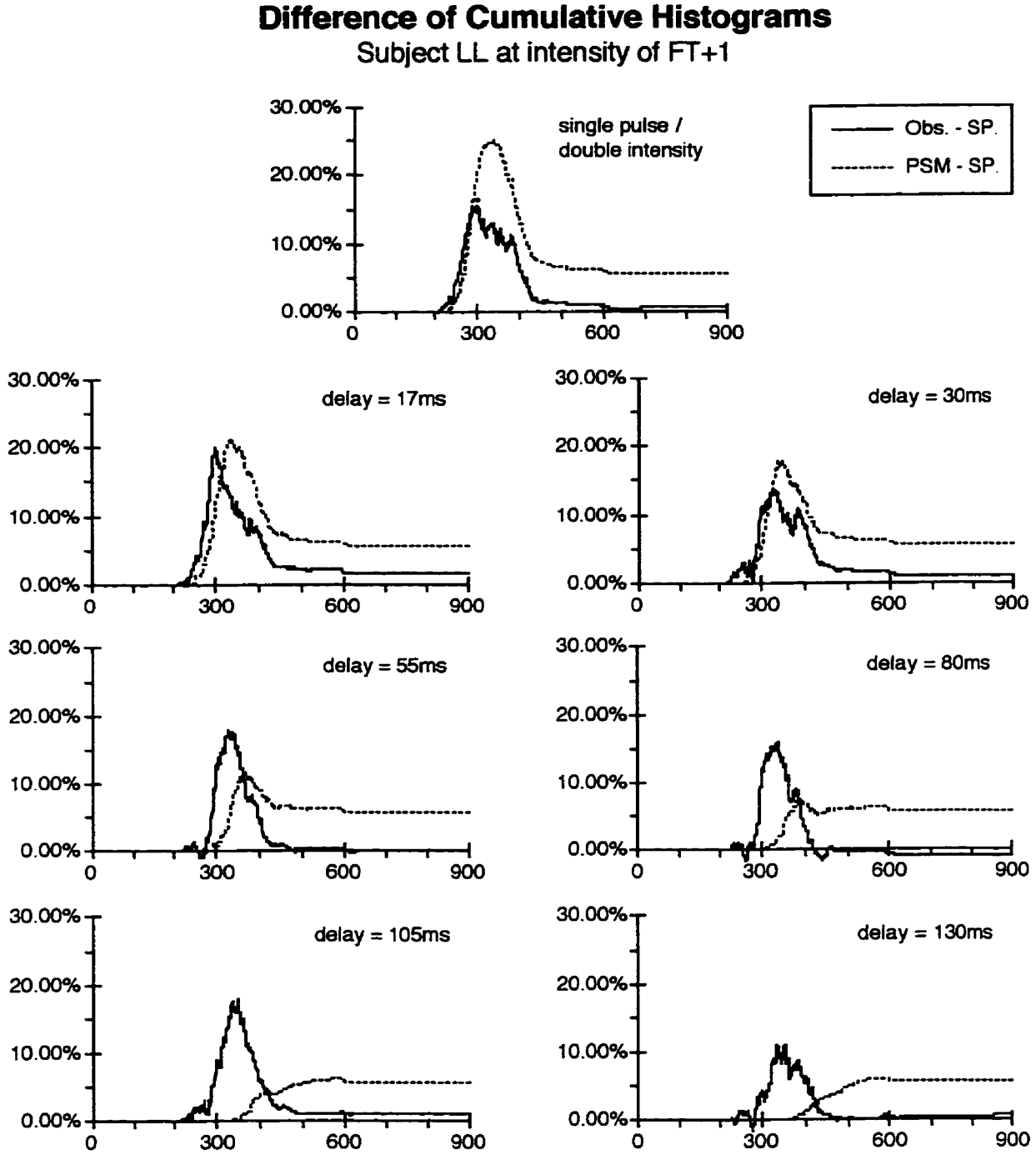

Figure 3.15: The effect of presenting a second pulse of light on latency distribution was determining by comparing the observed data (Obs.) with two baselines--the single pulse/unit intensity condition (SP) and the probability summation model (PSM). The extent of the effect when measured against the PSM baseline is shown by the difference of the two curves. Subject LL at an intensity of FT+1.

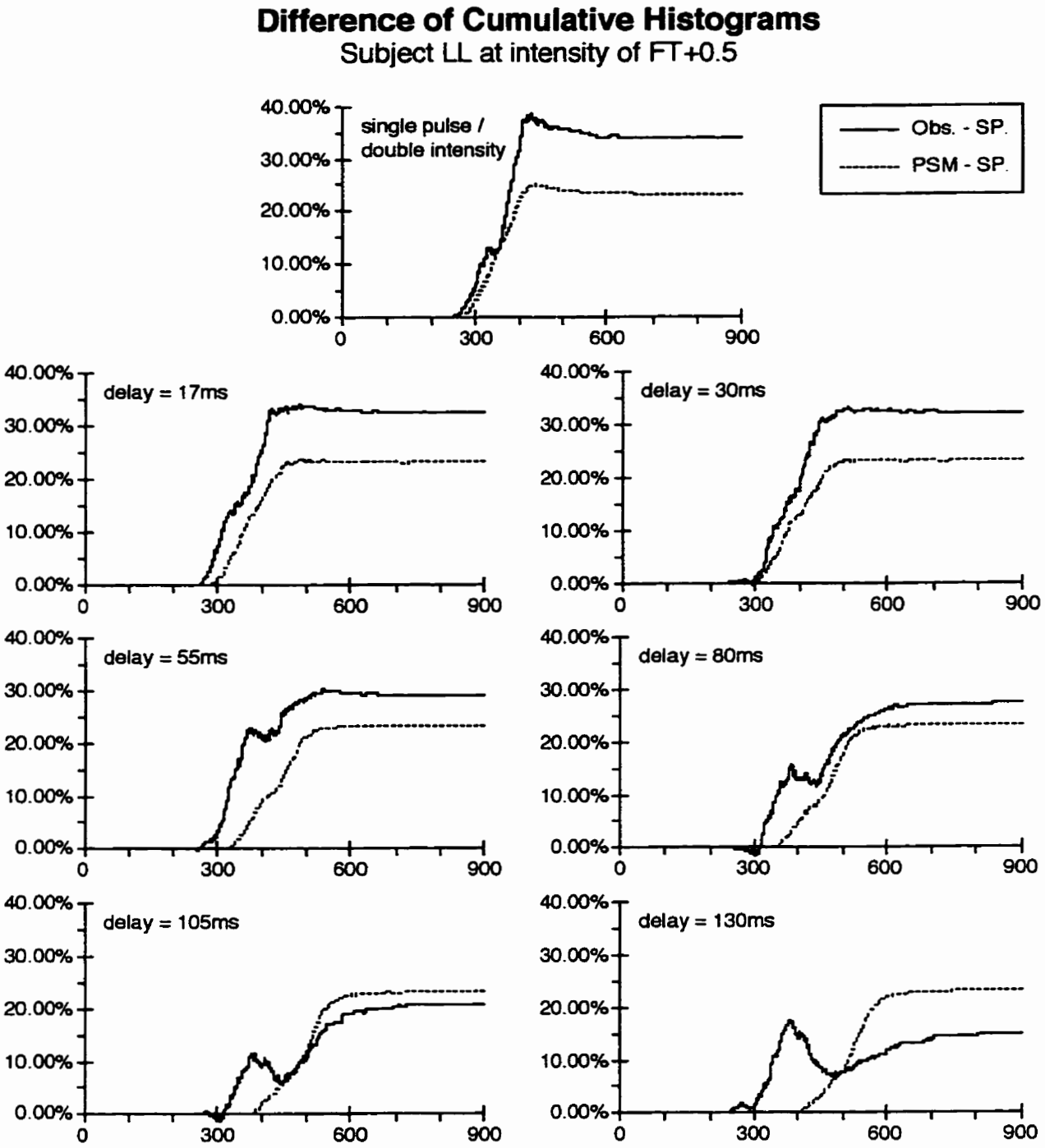

Figure 3.16: The effect of presenting a second pulse of light on latency distribution was determining by comparing the observed data (Obs.) with two baselines--the single pulse/unit intensity condition (SP) and the probability summation model (PSM). The extent of the effect when measured against the PSM baseline is shown by the difference of the two curves. Subject LL at an intensity of FT+0.5.

interact to effect performance, a good baseline ought be one that reflect what should happen if there were no interactions.

By applying elementary probability theory, one can derive just such a baseline which, in the psychophysical literature, could be called the "probability summation" (PSM) baseline. By assuming that the saccadic system treated a 2-pulse stimulus as two 1-pulse stimuli, and that each 1-pulse stimulus was processed independently by the saccadic system, one arrives at the following expected latency distribution:

$$P(\ell < t) = P_{sp}(\ell < t) + P_{sp}(\ell < t - \Delta p) - P_{sp}(\ell < t) \cdot P_{sp}(\ell < t - \Delta p) \quad \ldots\ldots\ldots\ldots\ldots\ldots (3.2)$$

where

$P(\ell < t)$ = the probability of a saccade occurring with latency, ℓ, less that t,
Δp = delay of the second pulse,
$P_{sp}(\ell < t)$ = probability of a saccade occurring with latency, ℓ, less than t when the stimulus is a single pulse at unit intensity (SP).

The function of $P_{sp}(\ell < t)$ was approximated with the empirical single-pulse/unit intensity cumulative histogram curve.

The baseline assumption, that a 2-pulse stimulus would be processed as two independent 1-pulse stimuli may be biologically implausible[2]; however, that should not be the criterion by which the goodness of the baseline is judged; instead, whether a certain baseline is accepted or not ought to be judged by its usefulness in determining how much interaction there exists between the two flashes in the stimulus, and by this criterion, the acceptability of the probability summation model is undisputable.

The comparison was done by overlaying a graph of the difference between the expected distribution from the probability summation model and the observed SP data over one that showed the difference between the observed latency distribution for each stimulus condition and that for the SP condition, since the relative height of the two graphs shows the difference between the observed latencies and the expected latencies.

At the bright intensity of FT+3, the distribution of observed latencies for the subject RC matched those expected from the probability summation model reasonably well when the stimulus

[2] The model is biologically implausible because it would require that the system be able to anticipate that the stimulus will have two units of energy, and that it should process each unit of energy in a separate channel (assuming that a second channel exists). While it is true that there is a great deal of parallelism in the retina, it is not apparent that they will be activated, since retinal drift is small (~10 arc min), and therefore it is unlikely that the second flash in the stimulus will fall on an adjacent channel.

condition was a single-pulse/double intensity flash (Figure 3.10, delay = 0ms). The match for the next two conditions, a delay of 17ms and of 30ms, has worsened slightly, still fairly good. For longer delays, the curve of difference obtained by subtracting the probability summation curve (dotted lines in Figure 3.10) from the observed curves was primarily positive. This meant that, presenting a second pulse of light after a delay of after 55ms or more after the first pulse was facilitatory in the sense that it produced more saccades with shorter latencies than would be expected under a probability summation model, even though the total frequency of response was not improved. The other two subjects showed similar results (Figure 3.12, 3.14 and 3.15)[3] .

These observations were contrary to what one would expect given a "waiting time" model. Since the premise of a waiting time model was that a saccade would be generated (after a constant time lag) when some internal process exceeded a threshold, facilitation should be more likely to happen at short delays, because for a second flash to be able to effect a shortening of the latency, it had to be presented before the threshold has been crossed. Hence, one could argue that the maximum effect should occur when the delay was brief, especially with bright targets when the time to threshold-crossing would be brief. One possible reason for the presence of little or no facilitation when the delay was brief (ie. 17ms or nonexistent) may be that the system was becoming saturated and the additional energy in the second pulse was not used efficiently.

The data collected from the dimmer intensities were less interesting. For all subjects, the observed curves led the probability summation model curves for all tested stimulus conditions and therefore, meant that a second flash, no matter where it was positioned, always resulted in saccades with shorter latencies.

In addition to providing an expected latency distribution, the probability summation model also gives an expected value for the total frequency of saccadic response given a certain delay. For the brighter intensities, the value provided by the model, which is the final value of the cumulative histogram, matched the observed frequency of saccadic response reasonably well (Figure 3.17). For the subject PH, the two values were practically identical; for the other two subjects, the predicted values were marginally better than those observed. At the dimmer intensity, the predictive power of the model was weaker. For the subject PH, the model's values at all delays were consistently better than the observed values; the difference was about 12%, with the largest

[3] The differences between subject LL's data with the other two subjects could be traced to his lower total frequency of response of about 95% versus a value of about 99% in the other two.

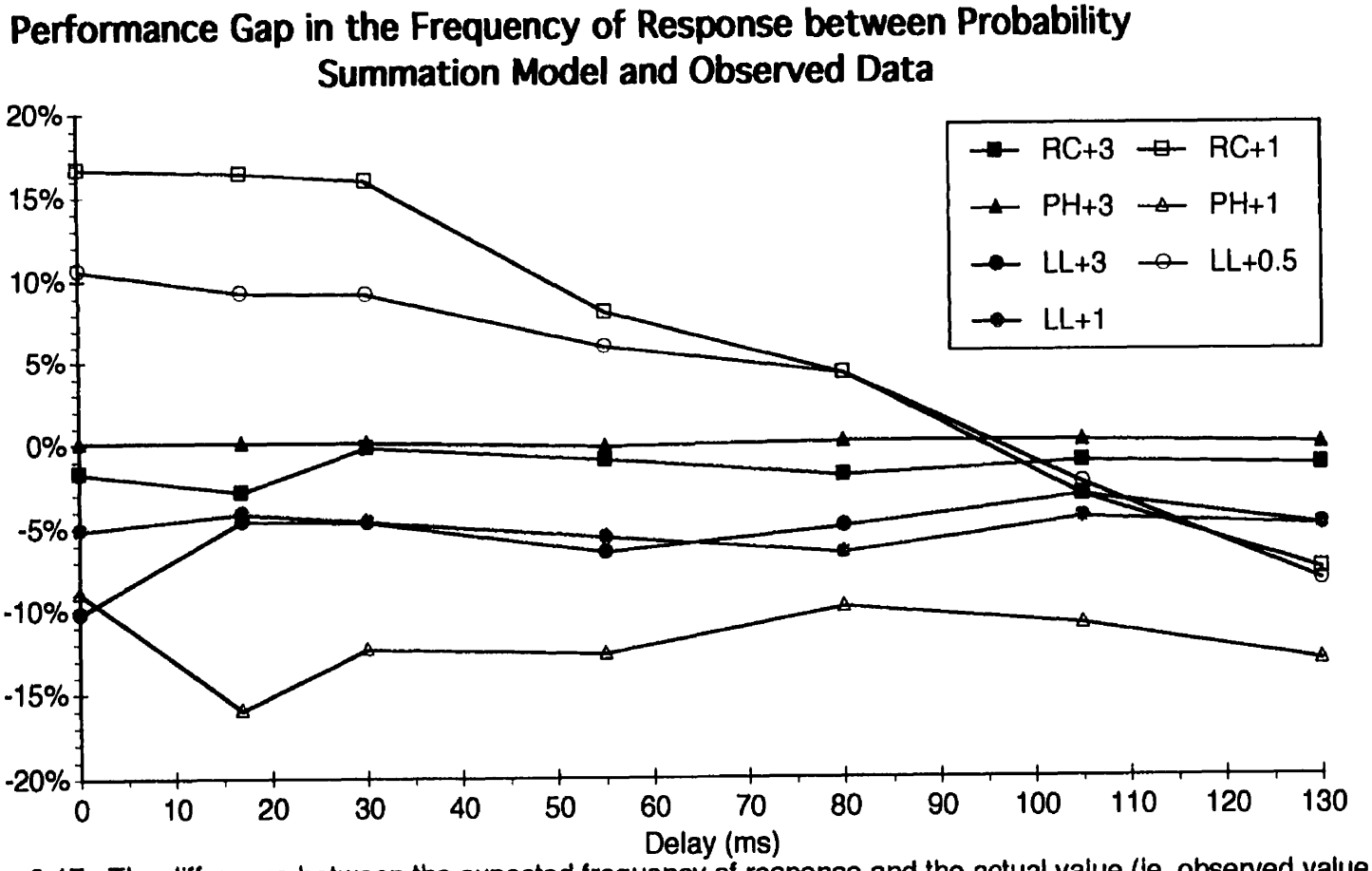

Figure 3.17: The difference between the expected frequency of response and the actual value (ie. observed value - probability summation prediction). At the brighter intensities, the two values were reasonably close together, but at the dim intensities, the model predicted higher frequencies than were observed when the delays were long for two of the subjects. (The model's predictions were higher than the observed frequency for the third subject.)

difference of 16% occurring when the delay was 17ms. For the other two subjects (RC at FT+1 and LL at FT+0.5), the model's predictions were better than observed values only when the delay of the second pulse exceeded 105ms. For them, the difference decreased from around 15% to -7% and from 10% to -8% respectively. This suggested that the impulse response function at the dim intensities contains a late inhibitory phase (or an inhibitory prelude). The residual effects of the first pulse of light that occurred after a long delay were weakly inhibitory on the second pulse of light and caused the detection rate to be lower than if the double-flash stimulus was processed as two independent flashes, even as the latencies of the responses were being shortened.

This divergence in performance has been observed before (Grossberg, 1970). In his experiment, manual reaction time in response to single and double flashes of light was measured, and it was observed that when the time interval between the two flashes was shorter than 50ms, increasing the interval increased the reaction time to a value about equal to that obtained for a solitary flash, while having no effect on total response frequency, which was around 100%. However, when the interval between the flashes exceeded 50ms, the frequency of response decreased monotonically, while latency either remained flat, or increased to a peak only to fall and return to a level observed with a solitary flash.

The fact that switching measuring criterion from frequency of response to reaction time would have an impact on how much effect a second pulse has on performance is not surprising. For example, it has been shown in an experiment that the application of different measuring criterion on the same set of data led to different estimates of the critical duration; moreover, it was also observed that as the criterion became more stringent, the estimate of the critical duration shortened (Bruder & Kietzman, 1973). However, what has been observed is not necessarily an artefact of switching between two criterion of different stringencies: since frequency of response, when compared against reaction time, is the looser criterion, a falling frequency of response should imply a longer latency. Instead, the effect of the late inhibitory phase at low intensity is very clearly reducing the latency of the faster saccades on the one hand, while suppressing the slower saccades on the other.

3.4 Direction Error Saccades

The direction error saccades that were observed during the experiments were tabulated and the results were in general agreement with the literature. For simple foveating tasks, direction error saccades were rare and generally had short latencies; these were usually thought to be of an anticipatory nature and discarded from any analyses. However, direction error saccades with normal or long latencies do exist (Doma & Hallett, 1988a, b). It has been noted that direction error saccades occur more frequently when targets were dim or when target contrast was low (van Asten et al, 1988), and it has been suggested that Troxler fading (Clarke & Belcher, 1962; Doma & Hallett, 1988b) may be the cause for them because "searching saccades" were needed to re-establish the target image. If that was indeed the case, then the number of such saccades has been underreported, because half of these searching saccades would have gone unreported, being hidden by the fact that they would be in the same direction as the target by chance.

The process for identifying direction error saccades was tricky for dim targets. When the target intensity was dim, there was a chance that the subject would not see the flash, and his proper response under than situation was to hold his gaze steady. However, the attention of the subject may drift (since he has been sitting in a dark room and has been performing a monotonous task for some time), and his eye (or his head) may move occasionally as a result. Hence, to filter out such eye movements, it was decided that only saccades with an amplitude in excess of 1° in the wrong direction would be tabulated as direction error saccades. This meant that the number of direction error saccades would be further undercounted. While it would be impossible to determine the number rejected by this screen, one could obtain estimates by using different screens. For example, if the amplitude criterion was dropped to 0.5°, depending on the subject, the number of direction error saccades may not change. On the other extreme, though, the number roughly doubled for another subject when the same 0.5° cutoff was used.

The number of direction error saccades that were observed during the course of the experiment were few (See Table 3.2). As can be seen from the table, the frequency at which direction error saccades occur depended on the subject and on the target intensity being low. Subject LL made very few direction error saccades, even at the dimmest intensity, while the other two subject showed a significant increase when the target intensity went from FT+3 to FT+1.

	Δp=0	Δp=17	Δp=30	Δp=55	Δp=80	Δp=105	Δp=130	SP
RC+3	0	0	0	1	0	2	1	1
RC+1	7	11	10	13	15	17	13	14
PH+3	0	0	1	0	0	0	0	0
PH+1	10	11	12	7	20	11	17	8
LL+3	0	0	0	0	0	0	0	0
LL+1	0	0	0	0	0	1	0	0
LL+0.5	0	0	0	0	2	6	0	2

Table 3.2: Number of direction error saccades. XX+3 refers to the FT+3 data of subject XX.

While there did not appear to be a pattern between the frequency of direction error and the delay of the second pulse, there appeared to be a preferred side. At the FT+1 intensity, all but one of the 118 direction error saccades made by PH were to the left, while the ratio of left to right direction error saccades for RC was about 5:2. Since the majority of saccades made by the two were to the targets on the right half of the field of view, it may be that the ratio of left searching saccades to right searching saccades has been overstated as some right searching saccades might have been misinterpreted as valid responses to targets presented on the right. However, for subject LL, who made a total of 10 direction error saccades at the dim intensity, there was no directional bias, as there were as many left-bounded saccades as right-bounded ones.

The numbers presented here were in rough agreement with other values from similar experiments. Under light-adapted conditions (background intensity of 21.6 cd/m^2), van Asten et al. (1988) observed a rate of direction error saccades in excess of 20% for low contrast targets of short duration at ±16.2° eccentricities. In Kalesnkyas' doctoral dissertation (1994), it was reported that at an intensity of FT, 172 direction error saccades were observed in 516 trials (~33%) for small eccentricities, while for larger eccentricities (2.25° to 6°), the rate was 7 in 209 (~3%). For brighter targets at larger eccentricities, he observed a maximum error rate of around 3%. In Barnes' doctoral thesis (1995), few direction error saccades were evoked at any of the target durations that were tested (2ms to 256ms) at intensities at or above FT+2, but at intensities below FT+1, a decrease in duration led to an increase in the rate of directional error saccades. When the rates of direction error saccades, defined as the number of direction error saccades divided by the number of trials, were plotted against the energy of the target, it was observed that the rate either increased to a plateau for subthreshold targets, or they peaked just below threshold before falling

again for the lowest energies. So, one might conclude that there were no simple relationships between direction error frequency and target energy. However, if one defined direction error frequency as the number of direction error saccades divided by the total number of responses in order to take account of the fact that dim targets elicit less saccades of any kind, then the frequency at which direction errors saccades were made was observed to increase more smoothly with decreasing target energy.

The rates of direction error saccades reported were variable and rates in excess of 20% were observed. For the energy level used in this experiment, she reported maximum rates of 3% and 6% for 10 FTxsec (corresponding to two 5ms pulses at an intensity of FT+3) and 0.1 FTxsec (corresponding to two 5ms pulses at an intensity of FT+1) respectively.

The data gathered here is in general agreement with the view that the rate of direction error saccades tend to increase as target intensity is decreased.

3.5 Saccadic Amplitudes

Before the amplitude data is presented, it should first be said that the eye-tracking apparatus, EMMA, used in the experiment was not the most suitable apparatus for gathering amplitude data. First and foremost, if measuring saccadic amplitude precisely was crucial to the experiment, a more linear eye tracker with a resolution finer than EMMA's resolution of 3 min arc would have been more appropriate. Another barrier was that EMMA's optical head was positioned in such a way as to optimize only the horizontal signal. Even though EMMA was capable of tracking the vertical position of the eye as well, the range over which this was possible was small, and therefore, attempting an X-Y trace of the eye would limit excessively the range of targets positions that could be used. Finally, the fact that there was no feedback to the subject on the accuracy of his saccades further compromised the utility of the experiment to provide amplitude information. Nevertheless, in the name of completeness, it was decided that the amplitude data ought to be included along with the measurements.

The effect of energy, intensity and target duration on saccadic amplitude was mixed. In some reports (Erlandson & Fleming, 1974; Reuter-Lorenz et al, 1991; Barnes, 1995), it was observed that when target energy was low because of either low intensities or short flash

durations, saccades were likely to undershoot the target. On the other hand though, studies (G.R. Barnes & Gresty, 1973; Hallett, 1978; Doma & Hallett 1988b) which showed that saccadic amplitude was affected neither by low target intensities nor short target durations, also exist. Finally, there was also a study (Pernier et al, 1969) which suggested that subjects may be divided in two groups, where one group was composed of subjects who produced saccades with normal latencies and correct amplitudes, and another group had subjects whose saccades occasionally have longer latencies and were hypometric by 25-33% when the flash duration was brief. However, the results of that study should treated with caution because the stimuli used did not adjust for pupil size and other related optical factors.

A number of these studies used only two target positions of equal eccentricity in their experimental procedure, a fact which may raise some concern whether the subject was responding to the target stimulus or was making saccades to a learned eccentricity (ie. Hallett & Doma, 1988b). However, this concern should be somewhat allayed when one considers that using only one eccentricity does not preclude an intensity effect on saccadic amplitude (Reuter-Lorenz et al, 1991).

Like an earlier study (Barnes, 1995), the results were highly dependent on the subject; but unlike that study where amplitude anomalies were for dim targets, it was observed that for the subjects RC and LL, saccades had a tendency to overshoot the targets in the right hemisphere more, regardless of the position of the second pulse. On the other hand, subject PH showed a tendency for hypometric saccades to the right hemisphere at the FT+3 intensity, while at the FT+1 intensity, all his saccades were hypometric. (see Table 3.3, Table 3.4, and Table 3.5. The values in the tables had been normalized to the target amplitude to ease the comparison of saccadic accuracy to different target positions.) Observable differences between left-bound saccades and right-bound saccades are not unknown. The adducting eye (ie. moving in the temporal-to-nasal direction, and in this experiment's case, moving to the right) has been observed to have a tendency to drift after a saccade, usually in the onward direction. The abducting eye (ie. nasal-to-temporal direction), on the other hand, has been observed to have a tendency for dynamic overshoots--a small "saccade" following the main saccade with no delay, but in the opposite direction (Kapoula et al., 1986b).

Finally, saccadic amplitudes to the innermost diodes to the outermost diodes were

Intensity: FT+3

target amplitude	Δp=0 average	Δp=0 pop. size	Δp=17 average	Δp=17 pop. size	Δp=30 average	Δp=30 pop. size	Δp=55 average	Δp=55 pop. size	Δp=80 average	Δp=80 pop. size	Δp=105 average	Δp=105 pop. size	Δp=130 average	Δp=130 pop. size	SP average	SP pop. size
-5.5	1.22	26	1.09	19	1.13	30	1.24	34	1.24	37	1.25	31	1.36	36	1.25	27
-5.0	1.16	23	1.14	24	1.17	31	1.34	35	1.22	29	1.23	31	1.29	41	1.31	35
-4.5	1.22	23	1.18	12	1.28	37	1.19	36	1.29	18	1.23	33	1.35	44	1.24	42
-4.0	1.21	23	1.22	23	1.27	28	1.25	29	1.25	37	1.21	31	1.26	41	1.39	35
-3.5	1.26	18	1.31	21	1.17	32	1.24	33	1.24	27	1.40	30	1.34	34	1.29	38
-3.0	1.19	26	1.28	29	1.28	30	1.24	30	1.35	30	1.18	31	1.37	35	1.39	31
-2.5	1.29	27	1.20	18	1.32	37	1.45	26	1.35	31	1.48	39	1.28	32	1.42	22
2.5	0.87	12	0.82	16	1.13	26	1.04	25	0.99	24	1.10	28	1.10	24	1.06	26
3.0	0.93	18	0.99	15	0.94	31	0.95	26	0.96	31	0.97	22	1.17	22	1.13	36
3.5	0.83	18	0.92	23	1.02	26	0.83	24	0.96	33	1.04	29	1.18	25	1.14	33
4.0	0.93	14	0.83	20	1.11	32	0.98	23	1.06	24	0.98	25	1.12	37	1.07	38
4.5	1.02	18	0.91	17	1.06	22	0.94	26	1.16	27	0.98	31	1.15	38	1.29	37
5.0	0.98	19	0.98	15	1.02	29	0.97	32	0.92	25	1.10	27	1.25	30	1.04	32
5.5	0.88	19	0.93	19	1.02	31	1.10	22	1.00	27	1.18	22	1.10	40	1.10	34

Intensity: FT+1

target amplitude	Δp=0 average	Δp=0 pop. size	Δp=17 average	Δp=17 pop. size	Δp=30 average	Δp=30 pop. size	Δp=55 average	Δp=55 pop. size	Δp=80 average	Δp=80 pop. size	Δp=105 average	Δp=105 pop. size	Δp=130 average	Δp=130 pop. size	SP average	SP pop. size
-5.5	1.16	46	1.19	32	1.17	35	1.13	30	1.20	32	1.18	23	1.17	19	1.00	11
-5.0	1.21	51	1.18	43	1.20	49	1.19	27	1.08	34	1.24	34	1.15	33	1.06	21
-4.5	1.21	40	1.16	34	1.18	38	1.19	37	1.09	36	1.16	28	1.16	24	1.19	12
-4.0	1.13	35	1.17	33	1.14	43	1.15	24	1.18	27	1.08	14	1.08	14	1.08	4
-3.5	1.20	35	1.13	44	1.14	28	1.19	20	1.15	25	1.13	15	1.11	9	1.16	8
-3.0	1.33	22	1.17	28	1.26	26	1.20	14	1.01	15	1.16	18	1.24	6	1.20	5
-2.5	1.36	18	1.25	8	1.34	23	1.22	14	1.19	7	1.68	1	1.11	4	1.36	3
2.5	1.09	9	1.04	10	0.81	3	1.03	2	X	0	X	0	1.00	1	0.76	1
3.0	0.83	12	0.84	15	0.92	17	0.97	10	0.90	10	0.98	3	1.00	2	1.03	4
3.5	X	0	X	0	X	0	X	0	X	0	X	0	X	0	X	0
4.0	0.71	1	X	0	X	0	X	0	X	0	0.63	1	X	0	0.77	1
4.5	X	0	X	0	X	0	X	0	X	0	X	0	X	0	0.65	1
5.0	X	0	X	0	X	0	X	0	X	0	X	0	X	0	0.64	1
5.5	X	0	X	0	X	0	X	0	X	0	X	0	0.83	1	X	0

Table 3.3: Saccadic amplitude normalized to target amplitude for the subject RC.

Intensity: FT+3

	Δp=0		Δp=17		Δp=30		Δp=55		Δp=80		Δp=105		Δp=130		SP	
target amplitude	average	pop. size	average	pop. size	average	pop. size	average	pop. size	average	pop. size	average	pop. size	average	pop. size	average	pop. size
-5.5	0.77	35	0.82	39	0.80	49	0.81	43	0.79	40	0.86	51	0.82	47	0.81	34
-5.0	0.69	32	0.74	31	0.73	39	0.72	34	0.76	31	0.74	47	0.73	35	0.71	33
-4.5	0.73	39	0.72	40	0.75	30	0.73	45	0.72	30	0.70	44	0.74	50	0.70	38
-4.0	0.68	36	0.69	45	0.72	29	0.71	37	0.73	33	0.69	46	0.70	45	0.68	42
-3.5	0.68	42	0.70	30	0.71	38	0.71	26	0.70	42	0.71	46	0.74	37	0.68	42
-3.0	0.72	34	0.69	37	0.75	33	0.75	42	0.69	37	0.70	30	0.72	50	0.70	41
-2.5	0.70	34	0.69	28	0.75	45	0.75	34	0.69	39	0.69	45	0.73	38	0.72	32
2.5	1.16	38	1.09	53	1.17	39	1.11	53	1.08	66	1.08	44	1.06	47	1.06	44
3.0	1.02	52	1.02	53	1.06	59	1.09	51	1.04	58	1.10	45	1.02	41	1.01	38
3.5	0.99	47	0.94	45	0.93	48	0.98	38	0.98	54	0.99	50	1.02	59	0.96	56
4.0	0.96	49	1.02	50	0.98	52	0.96	50	1.01	52	1.06	44	0.99	38	0.95	44
4.5	1.00	36	0.95	41	1.00	50	1.01	38	1.03	61	1.03	53	1.07	43	0.97	32
5.0	1.07	50	0.99	30	0.99	52	1.01	44	1.02	51	1.02	51	1.08	37	1.04	42
5.5	1.06	43	1.02	37	1.11	30	1.03	37	1.08	36	1.12	41	1.09	31	0.93	30

Intensity: FT+1

	Δp=0		Δp=17		Δp=30		Δp=55		Δp=80		Δp=105		Δp=130		SP	
target amplitude	average	pop. size	average	pop. size	average	pop. size	average	pop. size	average	pop. size	average	pop. size	average	pop. size	average	pop. size
-5.5	0.57	42	0.59	32	0.57	46	0.59	55	0.62	48	0.61	48	0.62	49	0.57	37
-5.0	0.56	59	0.57	57	0.54	40	0.56	34	0.60	51	0.53	52	0.56	49	0.57	41
-4.5	0.51	50	0.51	41	0.51	37	0.53	49	0.55	58	0.54	56	0.52	40	0.55	41
-4.0	0.51	41	0.55	28	0.51	48	0.49	55	0.47	44	0.45	47	0.49	52	0.47	39
-3.5	0.48	47	0.49	50	0.52	48	0.46	38	0.48	56	0.48	33	0.43	42	0.49	54
-3.0	0.47	56	0.48	36	0.55	44	0.46	59	0.46	38	0.47	36	0.42	46	0.51	30
-2.5	0.45	44	0.47	39	0.46	49	0.53	40	0.46	39	0.47	37	0.46	32	0.51	34
2.5	0.55	40	0.61	39	0.63	44	0.57	42	0.58	41	0.58	53	0.64	44	0.61	29
3.0	0.67	40	0.59	43	0.67	38	0.62	43	0.60	54	0.66	39	0.66	41	0.57	40
3.5	0.58	8	0.66	2	0.55	2	0.64	2	0.25	1	1.15	3	0.59	4	0.79	2
4.0	0.62	7	0.64	2	0.66	2	0.29	1	0.70	2	0.47	2	X	0	0.33	3
4.5	0.58	9	0.52	1	0.67	2	0.73	2	0.65	1	0.41	3	X	0	0.42	2
5.0	0.85	8	0.50	3	0.38	4	X	0	X	0	0.65	3	0.58	2	0.43	1
5.5	0.71	7	0.53	1	0.52	4	X	0	X	0	0.29	2	0.46	2	0.36	1

Table 3.4: Saccadic amplitude normalized to target amplitude for the subject PH.

Intensity: FT+3

	Δp=0		Δp=17		Δp=30		Δp=55		Δp=80		Δp=105		Δp=130		SP	
target amplitude	average	pop. size	average	pop. size	average	pop. size	average	pop. size	average	pop. size	average	pop. size	average	pop. size	average	pop. size
-5.5	1.58	25	1.41	34	1.50	22	1.45	18	1.31	34	1.35	22	1.38	21	1.51	35
-5.0	1.48	24	1.51	28	1.31	26	1.49	26	1.48	31	1.38	31	1.50	34	1.46	18
-4.5	1.38	30	1.55	32	1.43	30	1.37	28	1.47	23	1.47	24	1.46	31	1.37	31
-4.0	1.57	28	1.56	28	1.43	27	1.39	25	1.39	35	1.60	25	1.59	31	1.37	26
-3.5	1.44	44	1.56	31	1.50	30	1.45	32	1.46	27	1.46	23	1.44	36	1.54	26
-3.0	1.53	34	1.37	42	1.39	33	1.42	27	1.59	27	1.59	23	1.63	31	1.32	25
-2.5	1.30	42	1.51	33	1.42	35	1.62	25	1.57	34	1.57	23	1.57	31	1.50	33
2.5	1.08	33	1.11	45	1.15	40	1.21	26	1.20	32	1.18	30	1.14	27	1.21	28
3.0	0.99	27	1.14	37	1.15	39	1.26	28	1.23	35	1.11	29	1.23	26	1.11	31
3.5	1.20	27	1.06	30	1.12	43	1.25	31	1.16	35	1.14	47	1.12	30	1.10	23
4.0	1.09	24	1.11	34	1.17	39	1.23	30	1.09	45	1.05	22	1.15	36	1.02	33
4.5	1.15	33	1.15	33	1.09	30	1.12	39	1.27	31	1.08	39	1.19	36	1.04	27
5.0	1.09	35	1.12	29	1.13	25	1.21	34	1.09	31	1.19	39	1.12	39	1.09	39
5.5	1.10	25	1.04	32	1.21	33	1.23	38	1.09	41	1.06	42	1.20	30	1.11	24

Intensity: FT+1

	Δp=0		Δp=17		Δp=30		Δp=55		Δp=80		Δp=105		Δp=130		SP	
target amplitude	average	pop. size	average	pop. size	average	pop. size	average	pop. size	average	pop. size	average	pop. size	average	pop. size	average	pop. size
-5.5	1.52	33	1.33	27	1.48	38	1.45	24	1.47	35	1.52	31	1.52	31	1.41	29
-5.0	1.54	24	1.54	31	1.40	22	1.46	31	1.36	32	1.56	41	1.49	36	1.56	35
-4.5	1.37	33	1.46	34	1.42	35	1.46	26	1.44	24	1.53	44	1.56	31	1.40	26
-4.0	1.50	36	1.48	35	1.52	28	1.45	22	1.66	46	1.55	31	1.66	35	1.40	28
-3.5	1.50	27	1.49	37	1.51	34	1.46	36	1.51	29	1.49	37	1.46	40	1.57	23
-3.0	1.38	40	1.51	31	1.56	31	1.56	22	1.60	37	1.48	29	1.63	44	1.51	32
-2.5	1.43	42	1.49	27	1.52	27	1.39	36	1.54	37	1.48	29	1.55	24	1.43	34
2.5	1.11	27	1.22	41	1.38	29	1.28	34	1.28	34	1.27	27	1.38	30	1.09	29
3.0	1.19	39	1.27	34	1.30	29	1.36	34	1.28	34	1.26	26	1.26	40	1.26	26
3.5	1.22	36	1.29	32	1.23	48	1.23	35	1.26	33	1.39	26	1.16	25	1.18	29
4.0	1.14	29	1.16	34	1.09	31	1.27	36	1.19	22	1.20	42	1.38	30	1.27	42
4.5	1.22	38	1.13	35	1.14	31	1.32	31	1.20	38	1.23	26	1.33	29	1.12	39
5.0	1.22	30	1.26	27	1.16	36	1.19	35	1.15	37	1.21	39	1.31	28	1.13	36
5.5	1.14	43	1.24	38	1.18	34	1.11	24	1.12	37	1.32	36	1.20	31	1.23	24

Intensity: FT+0.5

	Δp=0		Δp=17		Δp=30		Δp=55		Δp=80		Δp=105		Δp=130		SP	
target amplitude	average	pop. size	average	pop. size	average	pop. size	average	pop. size	average	pop. size	average	pop. size	average	pop. size	average	pop. size
-5.5	1.49	35	1.33	46	1.35	50	1.32	42	1.35	49	1.36	37	1.31	59	1.34	41
-5.0	1.32	44	1.37	42	1.24	51	1.28	52	1.31	49	1.33	52	1.39	56	1.32	48
-4.5	1.37	48	1.41	38	1.38	49	1.37	54	1.36	41	1.42	60	1.32	60	1.37	43
-4.0	1.40	37	1.46	42	1.30	50	1.43	58	1.48	42	1.35	58	1.33	53	1.35	28
-3.5	1.38	46	1.52	45	1.31	41	1.38	48	1.35	45	1.30	47	1.40	62	1.28	47
-3.0	1.30	36	1.21	36	1.33	54	1.45	44	1.35	53	1.47	43	1.22	45	1.29	48
-2.5	1.39	37	1.52	42	1.51	50	1.36	35	1.36	25	1.36	29	1.33	21	1.04	19
2.5	0.95	34	0.92	34	0.90	48	0.90	41	1.04	29	1.05	25	0.96	25	1.00	22
3.0	0.92	42	0.91	44	0.86	47	0.92	55	0.95	44	0.91	39	1.03	46	0.91	29
3.5	0.92	42	0.93	35	0.87	56	0.90	42	0.99	47	0.96	54	1.01	41	0.85	35
4.0	0.90	39	0.93	53	0.95	55	0.88	57	0.96	42	0.93	34	1.01	49	0.92	41
4.5	0.92	48	0.91	38	0.93	49	0.92	52	0.97	46	0.95	47	0.93	36	0.97	32
5.0	0.89	36	0.97	39	0.90	48	0.96	52	0.87	55	0.92	42	0.92	36	0.87	42
5.5	0.90	51	0.94	36	0.90	53	0.93	47	0.85	38	0.96	44	0.90	45	0.89	24

Table 3.5: Saccadic amplitude normalized to target amplitude for the subject LL.

compared to determine if the data supported a range effect (Kapoula, 1985). The effect, where subjects would make hypermetric saccades to targets of lesser eccentricity and hypometric saccades to targets of greater eccentricity for a given stimulus set, was reported to be dynamic in that the gain of the saccades would be adjusted to suit the set of target eccentricities used.

Support for a range effect in the present data was marginal and the majority of target conditions did not exhibit the effect. For the dimmer intensities, the same comment could be made, but the strength of the claim was weakened by the paucity of response and the absence of saccades to certain targets in the left.

3.6 Response to Red Targets

When examining data such as those presented here from a photoreceptor model perspective, an important question to ask is how did the rod and cones photoreceptors contribute to the process? One way to examine it was to take advantage of the photoreceptors' different spectral sensitivities and observe how colour would affect the response. (Bleaching probably would have been a better approach, but the resulting experiment would have been too time-consuming because a bleach, being effective only for a short while, would have to be repeated many times in order to amass the amount of data needed.) In Barnes' thesis (1995), the consequences of using red targets in place of yellow green targets were minimal: Bloch's law for the frequency of saccadic response was preserved; latency plotted as a function of target energy yielded the same two-region graph where in one region, latency was a function of energy and in the other, a function of intensity; frequency of direction error increased as target energy was decreased. In additional to those findings, it was also observed that there were little differences between latencies to red or yellow-green targets at high intensities such as FT+3; however, while latencies to red target at low intensities (ie. FT+1) and long durations were matched for yellow-green and red targets, those to red targets of short durations at the same intensities were longer. The conclusions drawn from these observations was that at the high intensities, the responses to both colours were mediated by cones, while at the low intensities, responses were mediated by cones for targets of long durations and by rods for targets of short durations.

The present experiment was repeated with red LEDs (peak wavelength of 635nm) with one

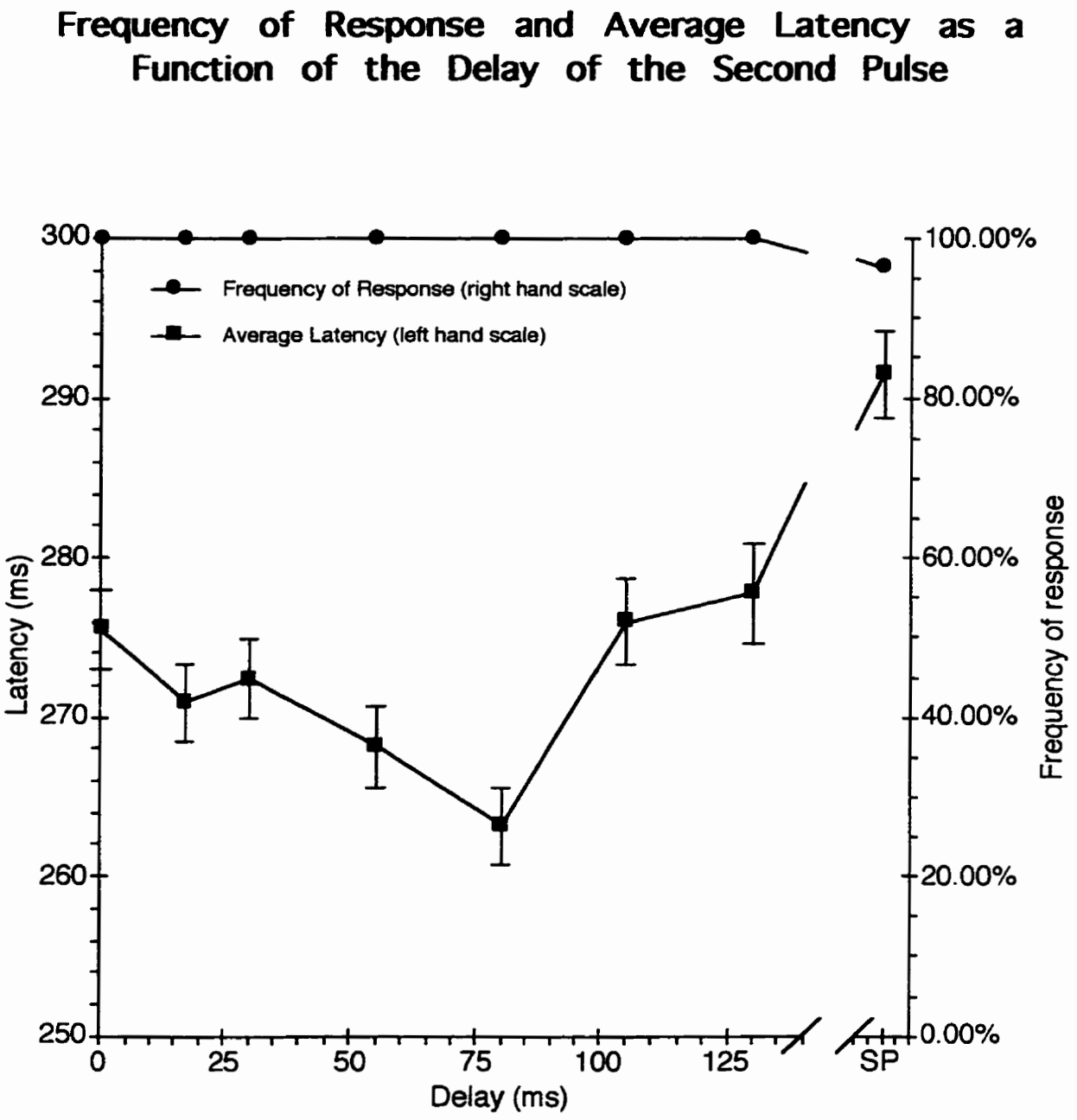

Figure 3.18: Frequency of response and average latency as a function of the delay of the second pulse. The above graph shows the frequency of response and average latency that results when stimuli were red LEDs (peak wavelength of 635nm) flashed at an intensity of FT+3.

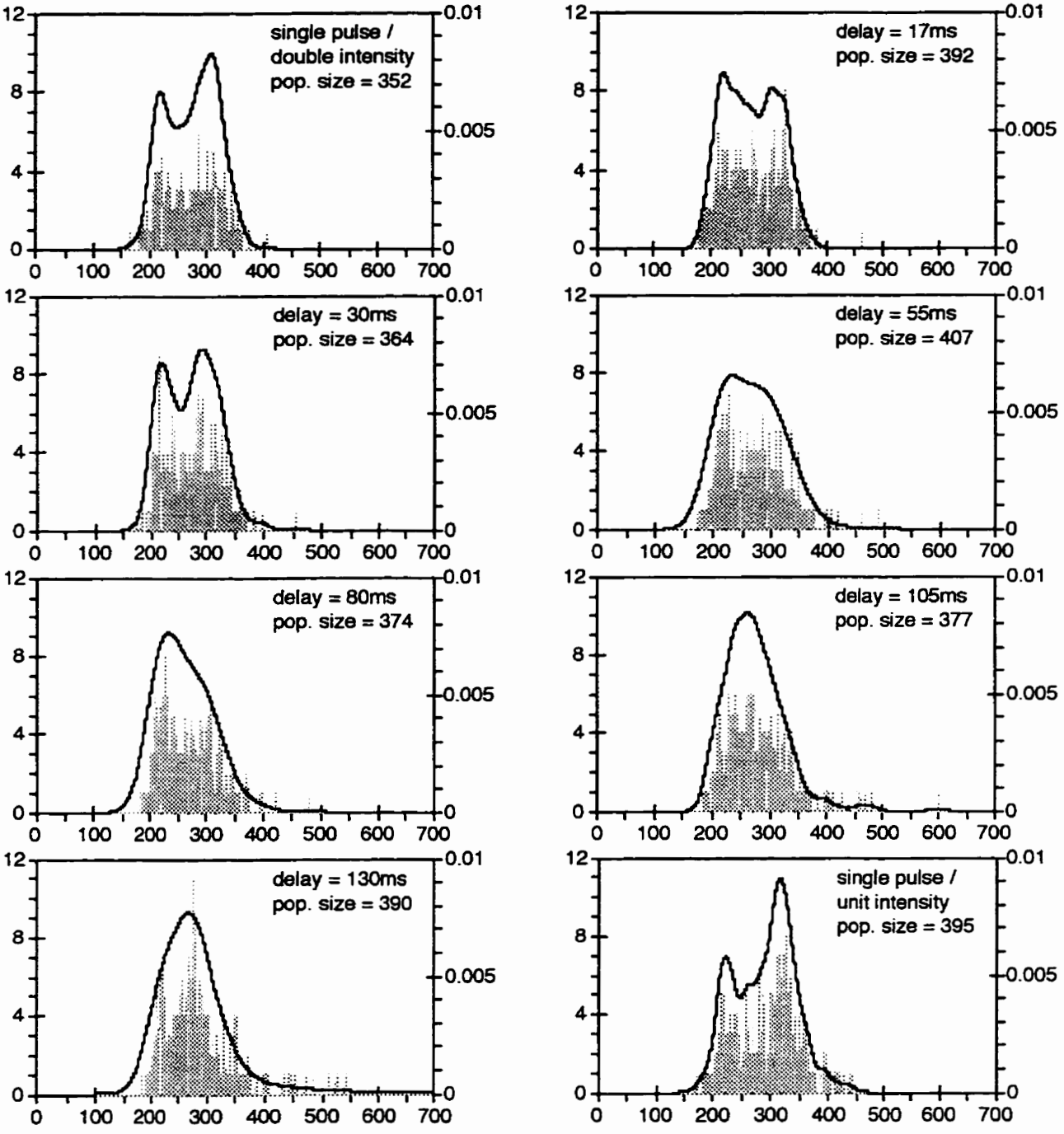

Figure 3.19: Latency histogram and their kernel density estimates. The kernel density estimates were obtained by convolving the histogram with a Gaussian using the values, taken from Table 3.6, which have an ASL-value of at least 0.1. The scale for the histogram is on the left; the one for the density estimate, the right. The data shown here is of subject LL at an intensity of FT+3 using red LEDs as stimulus.

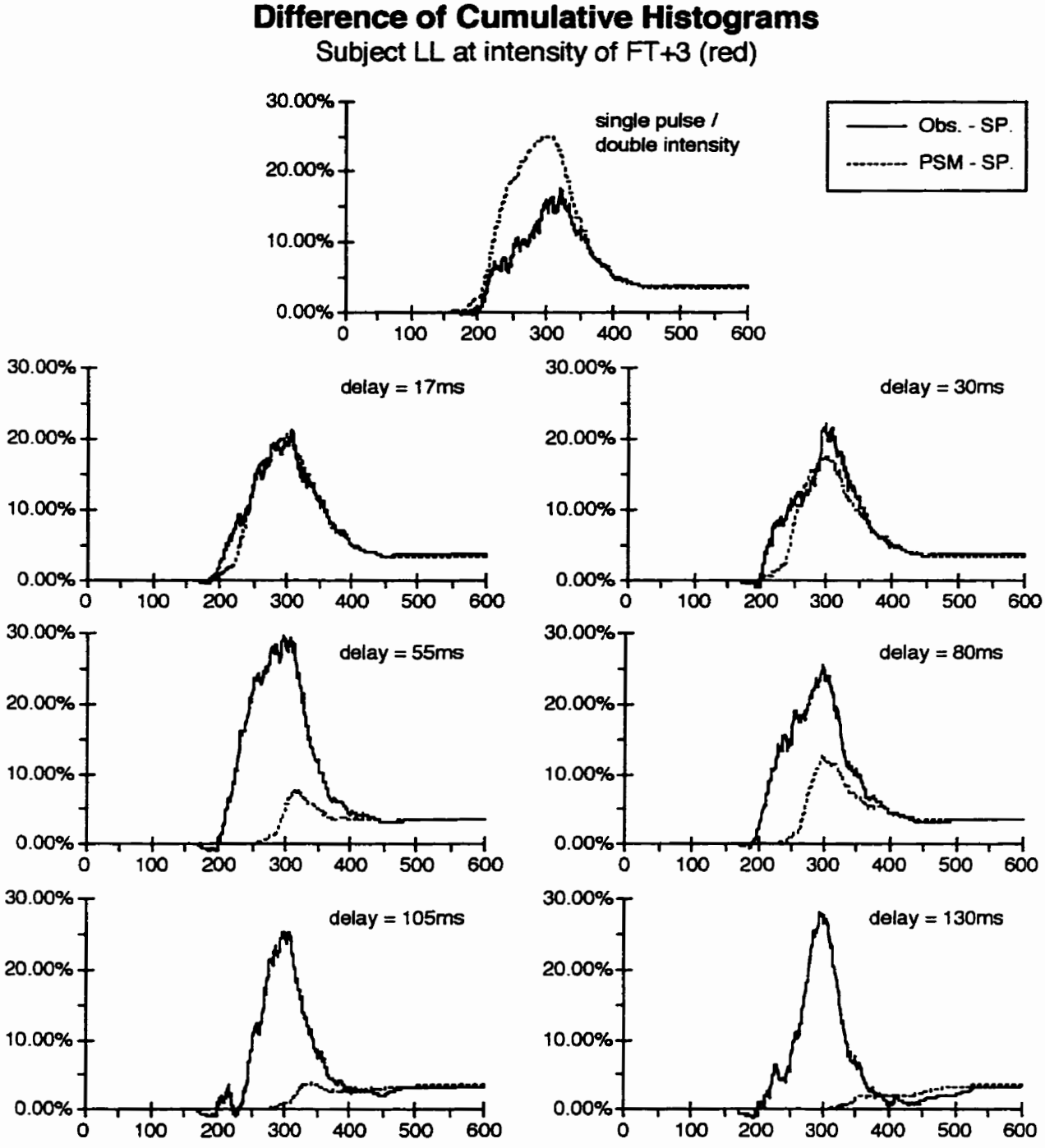

Figure 3.20: The effect of presenting a second pulse of light on latency distribution was determining by comparing the observed data (Obs.) with two baselines--the single pulse/unit intensity condition (SP) and the probability summation model (PSM). The extent of the effect when measured against the PSM baseline is shown by the difference of the two curves. Subject LL at an intensity of FT+3 with red LEDs.

subject (LL). The results obtained for the target intensity of FT+3 were qualitatively similar to those obtained with yellow-green LEDs. The frequency of response was 100% except for the single pulse/unit intensity stimulus which drew a response 96% of the time. Average latency for all stimulus conditions with two unit of energy was around 270ms while the average latency of a single pulse/unit intensity stimulus was 291ms (Figure 3.18). The majority of the latency histograms had either one or two modes if the ASL cutoff was taken at 10% (see Table 3.6 and Figure 3.19). In the bimodal distributions, the two peaks are located around 220ms and 300ms; for unimodal distributions, the main peak is around 240ms, and some show a shoulder around 300ms. Like the bootstrap results for yellow-green targets, the presence of the shoulder, whose location coincide with the location of the second mode in the bimodal distributions, may mean that the latency distribution is composed of two population of saccades. Finally, the comments that applied to the yellow-green difference of cumulative histograms curves were also applicable to the red data (Figure 3.20). At the dimmer intensity of FT+1, the red targets were only detected only at a very low rate (ie. less than 5%). The lack of response to the briefly flashed red targets at the FT+1 intensity was confirmed when the experiment was repeated with another subject (RC).

The last observation indicated that the only rod photoreceptors were contributing to the saccadic process at the yellow-green FT+1 intensity. However, the situation at the FT+3 intensity was not as clear. Because the results of the red targets were very similar to those of the yellow-green, it may be that both photoreceptors systems were involved; alternately, it may be that only the cone photoreceptor was at work. In view of Barnes' work, the second explanation seemed more likely, but unless a further experiment capable of isolating the contributions of either the rod or the cones is undertaken, one cannot safely reject one possibility over the other.

Subject LL:
Intensity = FT+3 (red)

modes	Δp=0	Δp=17	Δp=30	Δp=55	Δp=80	Δp=105	Δp=130	SP
1	0.02 (23)	0.00 (24)	0.05 (25)	0.21 (25)	0.13 (25)	0.07 (42)	0.05 (52)	0.01 (22)
2	0.26 (12)	0.74 (9)	0.03 (20)	0.01 (22)	0.25 (14)	0.06 (26)	0.27 (25)	0.82 (9)
3	0.13 (10)	0.26 (8)	0.16 (12)	0.13 (14)	0.29 (11)	0.29 (13)	0.33 (17)	0.57 (9)

Table 3.6: The results of the bootstrap for the red data. The ASL-value of the first 3 modalities are shown with its window width, hk, rounded to the nearest millisecond, in parenthesis.

Discussion

As the data presented in the observation section has shown, the interpretation of the second pulse's effect depends on the choice of the baseline. For example, if the single pulse/unit intensity (SP) cumulative histogram was used, then the data showed that a second pulse was always facilitatory; however, if the probability summation model (PSM) baseline was used, then the second pulse was facilitatory only for the longer delays at the bright intensity. In addition to those two, another obvious baseline that could have been used was the single pulse/double intensity (DP) cumulative histogram. This path of examination was never taken because it seemed unlikely to be useful. The SP and DP condition could be thought of as the two conditions that define the upper and lower limits of what could be expected of a two-pulse stimulus, and since the use of the DP cumulative histogram would not have avoided the problem of probability summation introduced by the fact that the stimulus had two flashes, the use of the DP condition as a baseline would not appear to be something that would lead to anything new.

The probability summation baseline was introduced as a means of reflecting the fact that because saccades are elicited probabilistically, the saccadic system should have, theoretically speaking, two chances to respond to a stimulus composed of two flashes. However, the fact that a two-flash stimulus is unlikely to be processed as two independent single flashes (ie. consider the single pulse/double intensity configuration) might be cited as an argument against adopting such a baseline. However, such an objection is beside the point because the purpose of a baseline is to be a yardstick that embodies the experimenter's expectations on what the data should look like, so that the actual data can be set against it to determine how one's expectation diverges from reality. Therefore, it can be argued that biological plausibility is not a prerequisite for an good baseline.

In addition to this, consider the situation in which the stimulus is composed of two flashes with such a long delay between them that interaction is not possible. For such a stimulus, the shortcoming of the single-pulse/unit intensity cumulative histogram baseline is illustrated because if the subject missed the first pulse in the pair and had to respond to the second pulse, the portion of the responses directly attributable to the second pulse would be interpreted as the result of the facilitatory interaction between the two pulses, if the SP cumulative histogram were used as the baseline. Viewed from this angle, using the PSM as a baseline would then follow logically since

this theoretical stimulus and those used in the experiment can be seen as something drawn from the same spectrum of possible 2-pulse stimulus configurations.

Another possibility for a baseline is to use the impulse response functions of the photoreceptors obtained from measurement (ie. Baylor et al, 1984; Schnapf et al, 1990; Kraft et al, 1993) as the linear filters in a leaky integrator model. This approach has its limits since there are more to the neural processes that lead to a saccade than just the transduction of photons into neuronal impulses, but it may prove instructional by illuminating some of the properties of the processes that go on between the photoreceptor and the actual saccade.

As was pointed out in the introduction, any latency function would be a rather insensitive measure of the rising phase of the impulse response function. Therefore, while using the data amassed here to derive the impulse function is ruled out, it still could be shifted for clues on the nature of the impulse response function. First, the data, especially the difference of cumulative histograms in Appendix B (ie. Figure B.1 versus B.2), showed evidence that support the stance that the impulse response function changes with intensity (Kelly, 1971a, b; Stock & Falk, 1987). Second, the data also suggested that at the dim intensity, the impulse response function is positive over the range of delays tested, and that it has a late inhibitory aftermath. The idea that there exists a late inhibitory aftermath at the dim intensity may be surprising, but it is not novel. A number of the impulse response papers, that were listed in the introduction and examined the effect of luminance, have impulse response function that also have a late (and small) inhibitory aftermath (Kelly, 1971a, b; Stock & Falk, 1987). Finally, at the bright intensities, the impulse response function is likely positive between 55ms and 130ms; before 55ms, the current data does not indicate whether it is positive or negative, but its amplitude is likely to be small.

A popular model that is used to emulate the temporal summation properties of the visual system--such as the "waiting-time" leaky integrator model mentioned several times in this thesis--is to treat the system as a linear filter with a threshold. However, such an approach is flawed because it is deterministic and hence devices must be added if such a model is to reflect the variability in the response. One way to accomplish this is to add noise to the filter's output, or in other words, to view the output as some value indicating the likelihood that the threshold is being crossed at that particular point in time. The leaky integrator model was introduced as a photoreceptor model because it was simple and its parts could be easily related to neurophysiological processes-the

leaky integration corresponded to the neural activity occurring at the retinal level, and the fixed constant delay, the higher neuronal processes. However, while intuitive, certain elements in the data pointed to the inadequacies of such a view of the saccadic system. The range of delays ran from 17ms to 130ms, and therefore, the second pulse in a stimulus with a delay from the short end of the range should arrive at the eye at a time when the neuronal activities caused by the first pulse of light were still at the retinal level. On the other hand, the second pulse from a stimulus with a delay taken from the long end of the range would arrive at the eye at a time when neuronal activities caused by the first pulse would have expanded to the cortical level. Hence, if one were to try to interpret the data using a purely photoreceptor model, one might expect to see a break in the results to reflect the necessity of invoking a second mechanism to deal with stimulus configurations with a long delay. However, because the difference of cumulative histograms (Figure 3.10-3.16) showed that a gradual progression of results as the delay was increased from 17ms to 130ms, and hence argued against the presence of two mechanisms, it would therefore appear unlikely that a photoreceptor model would be able to account for all the observations.

Appendix

Appendix A: Estimates of the critical duration for subjects LL and RC

The interchangeability of stimulus duration and intensity has been known for a long time. Bloch's law, as this relationship is known, states that the effects of decreasing the stimulus duration may be compensated for by increasing the stimulus intensity, as long as the duration do not exceed some critical duration, Δt_c, or as long as the intensity do not fall below some threshold intensity, I_c. The law is a special case of the more general class of models using linear filters; in this case, the convolving function integrates the stimulus intensity over some time period.

Estimates of Δt_c varies as definitions of it vary due to the fact that departure from Bloch's law is gradually. Nevertheless, in spite of this, Δt_c could still be a useful measure of the temporal properties of the visual system; for example, it offers some guidance on whether one should expect the response to a 2-pulse stimulus with a delay of 30ms to be the same as that of a single pulse/ double intensity stimulus.

Estimates of the critical duration, Δt_c, for the subjects LL and RC were obtained by measuring their saccadic reaction time to solitary pulses of light of various durations. The subjects were first given 1 to 2 drops of a 0.5% solution of mydriacyl in their left eye, and was told to sit in a dark room for about 20 minutes to allow their eyes to dark adapt. Once the dark adaptation period was over, they were presented with a red fixation point in the centre of their field of view and was instructed to fixate it. After a random period of between 1.5s to 2.5s, the fixation point was extinguished and was replaced by a yellow-green target in his periphery. The duration of the target was variable and chosen randomly; fourteen values were possible and they ranged from 2ms to 120ms. The instruction to the subject was to make a saccade to the target as quickly as possible and fixate. After the subject has responded to the stimulus or when one second has elapsed after the offset of the stimulus, the stimulus was relit to provide feedback to the subject. A tone was also generated to cue the subject that a stimulus was presented, and a higher tone was generated as feedback to let the subject know that the computer was tracking the saccadic response. The reason why the tone was included in the experimental procedure was that it has been observed that the inclusion of a tone in such experiments reduced the standard deviation of the latency data (Hallett & Adams, 1980; Kalesnykas, 1994). Eye movement was tracked with EMMA.

Data were gathered at the FT+3 and FT+1 intensity from the subject LL, and at FT+3 from

the subject RC.

The critical duration was estimated by fitting the average latency for each target duration to the function

$$y = k_0 + k_1 \cdot \exp(-k_2 x) \quad \text{(A.1)}$$

where

y = primary saccadic latency (ms)
x = target duration (ms).

The 3 free parameters of the model, k_0, k_1 and k_2, were estimated with a statistical program called Axum using a gradient-descent type algorithm to minimize the least squared error. The results of the computation are tabulated in Table A.1.

Subject	k0	k1	k2
RC @ FT+3	235.51	43.36	0.05
LL @ FT+3	229.39	35.63	0.28
LL @ FT+1	299.08	419.96	0.37
PH @ FT+2	229.15	62.64	0.26
PH @ FT+1	279.42	157.41	0.08
CB @ FT+3	268.09	23.88	0.11
CB @ FT+1	322.19	149.69	0.09

Table A.1: Values for the constants k_0, k_1 and k_2 in Equation A.1. All values are in milliseconds. The values for PH and CB were taken from the appendix of Barnes' doctoral thesis (1995) and are included for comparison purposes.

	Values of ε			
Subject	3 SEM	1 SEM	2ms	1ms
RC @ FT+3	17	40	61	75
LL @ FT+3	4	7	10	13
LL @ FT+1	9	12	14	16
PH @ FT+2	7	11	N/A	N/A
PH @ FT+1	36	51	N/A	N/A
CB @ FT+3	15	25	N/A	N/A
CB @ FT+1	45	33	N/A	N/A

Table A.2: Various estimates of the critical duration, Δt_c, based on various values of ε. All values are in milliseconds. The values for PH and CB were from Barnes' doctoral thesis (1995) and are included here for comparison purposes.

The critical duration was then estimated by calculating the duration at which the equation A.1 exceeded the plateau value of k_0 by a certain amount, ε. Several values of ε--3 times the standard error of the mean (SEM), standard error of the mean, 2ms, and 1ms--were used to see how robust the estimates were; the results are shown in Table A.2.

The data presented here were gathered and analysed by Vivek Patel.

Appendix B:Saccadic latencies to 2-pulse stimuli with long delays

In addition to the eight stimulus configurations that were used in the main experiment, a small pilot study was undertaken to see the effect, if any, of a second pulse of light when the delay was significantly longer than 130ms. This was prompted by the observation of interactions for the 130ms-delayed 2-pulse stimulus and a curiosity of the extent over which 2-pulse of light will interact to facilitate or delay the saccadic response.

The pilot study was identical to the main experiment in all respects, with the exception of the set of stimulus configurations that were used. Five stimulus configurations were used: a single flash, a double flash with a delay of 130ms, a double flash with a delay of 255ms, a double flash with a delay of 505ms and a single flash, but with twice the intensity. The single flash-double intensity stimulus and the 130ms-delayed double flash stimulus were included in the set of possible stimulus configurations as a means of assessing if the data were compatible with those in the main experiment. Only one subject from the main experiment, LL, participated in the study. Because this pilot study was completed before the realization that there was a problem with intensity calibration with this subject, the data presented here is dogged by the same problems as those in the main experiment: instead of being a representative of a dim intensity stimulus, the FT+1 log data of LL resembled those of the FT+3 log data, and one needs to turn to the FT+0.5 log data for results of targets of dim intensities.

After filtering the data for bad data points using the same screens as those used in the main experiments, about 200 data points remained for each stimulus configurations. These were then converted into cumulative histograms so that the effects of the second pulse could be assessed in the same manner as the main study.

The results are illustrated in Figures B.1, B.2, and B.3. At the bright intensities (ie. FT+3 log and FT+1 log; Figure B.1 and B.2 respectively) and the dim intensity (ie. FT+0.5 log; Figure B.3), the first two graphs of each intensity series, which depicts the results for the single pulse at double intensity and the double pulse with a 130ms delay, showed results that were qualitatively similar to those in the main study, and thus gave some assurances that the other data in this pilot study could be viewed as an extension to the main study.

The interpretation for all the graphs presented here should begin at the 505ms-delay configuration. Logic would argue that if most saccades occur within 500ms of stimulus onset,

then the difference between the 505ms-delay data and the SP condition should be negligible, and that any deviation from the zero should be measurement error inherent in these plots of the about 200 data points. Using these curves as an estimate of the size of the uncertainty in these plots, one can see that the difference between the observed data and the SP condition for the longer delays were only marginally greater, which meant that the data argued against the effect of a second pulse extending over long delays.

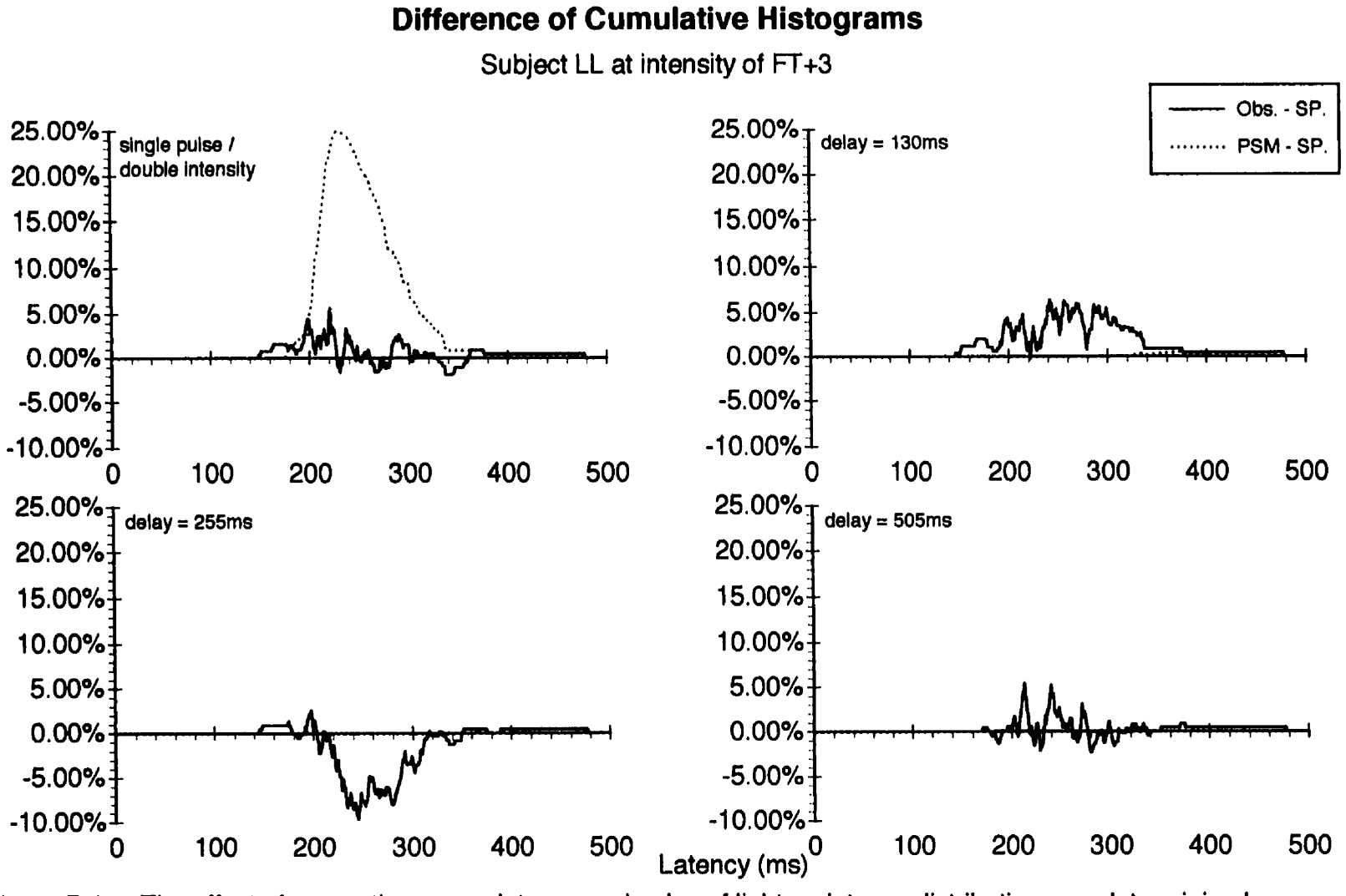

Figure B.1: The effect of presenting a very late second pulse of light on latency distribution was determining by comparing the observed data (Obs.) with two baselines--the single pulse/unit intensity condition (SP) and the probability summation model (PSM). The extent of the effect when measured against the PSM baseline is shown by the difference of the two curves. For very long delays, the PSM-SP curve is not apparent because its value is very close to zero. Subject LL at an intensity of FT+3.

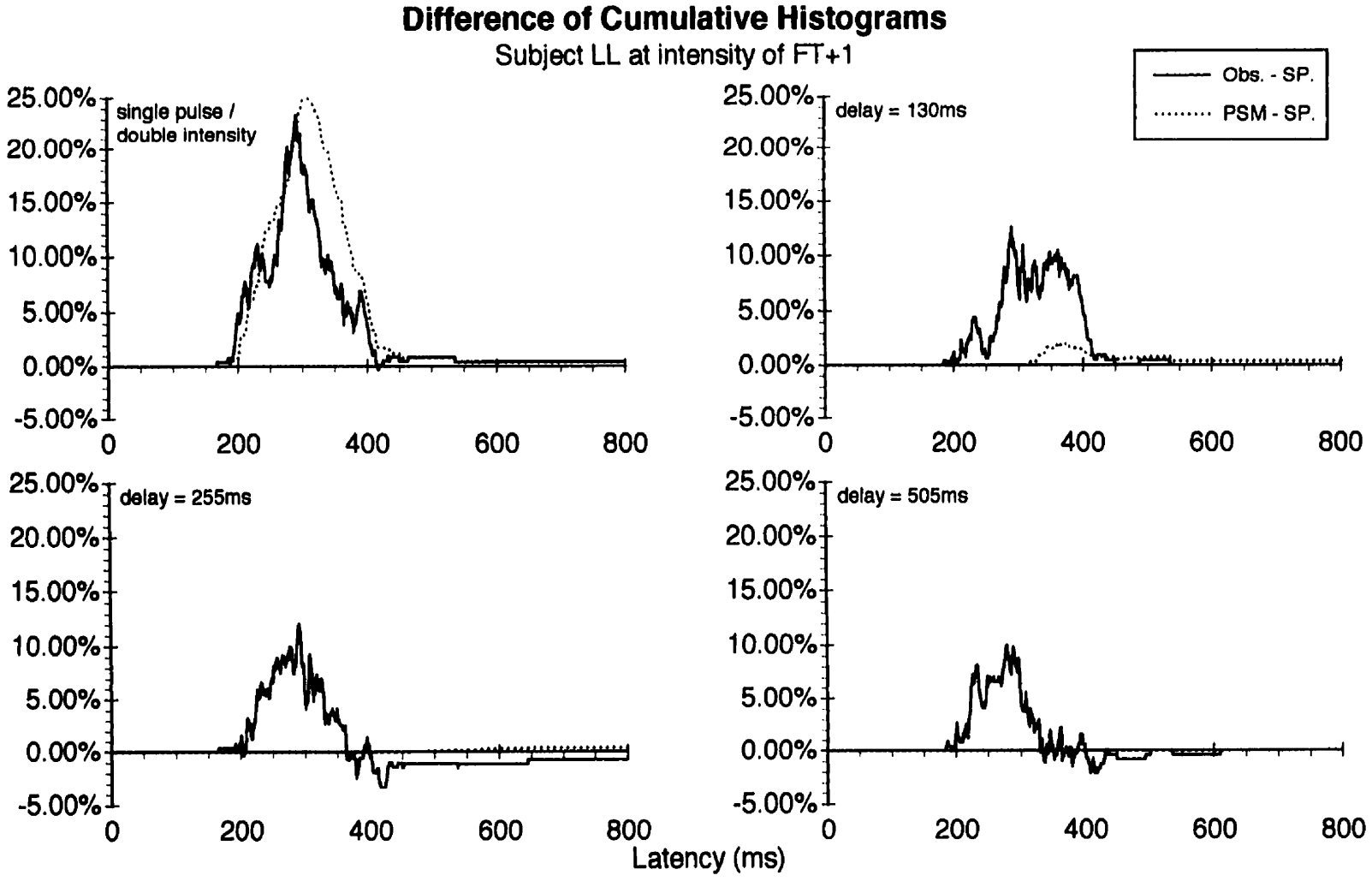

Figure B.2: The effect of presenting a very late second pulse of light on latency distribution was determining by comparing the observed data (Obs.) with two baselines--the single pulse/unit intensity condition (SP) and the probability summation model (PSM). The extent of the effect when measured against the PSM baseline is shown by the difference of the two curves. For very long delays, the PSM-SP curve is not apparent because its value is very close to zero. Subject LL at an intensity of FT+1.

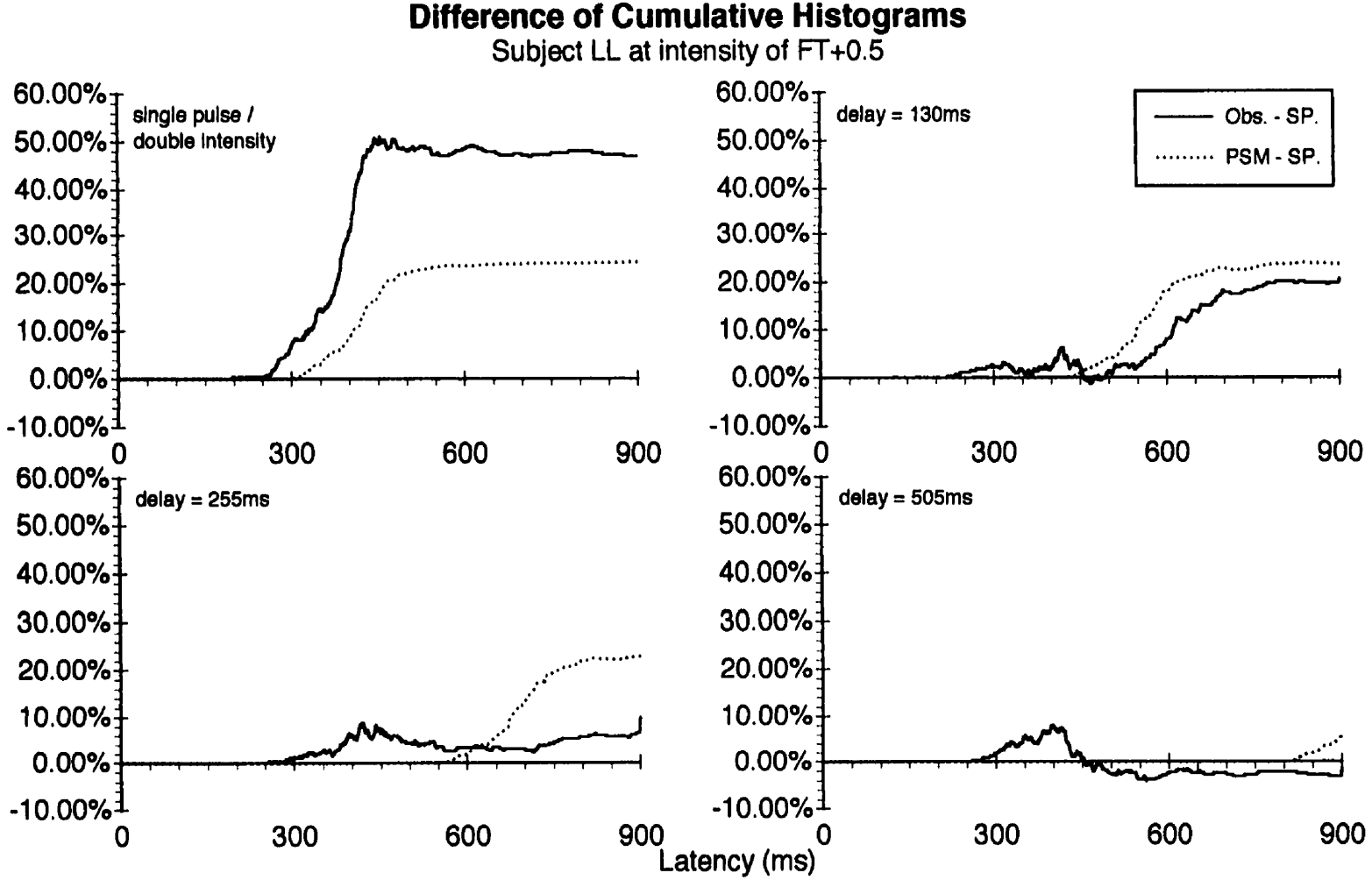

Figure B.3: The effect of presenting a very late second pulse of light on latency distribution was determining by comparing the observed data (Obs.) with two baselines--the single pulse/unit intensity condition (SP) and the probability summation model (PSM). The extent of the effect when measured against the PSM baseline is shown by the difference of the two curves. For very long delays, the PSM-SP curve may not be apparent because its value is very close to zero. Subject LL at an intensity of FT+0.5.

References

Abrams R.A. & Jonides J. (1988). Programming Saccadic Eye Movements. Journal of Experimental Psychology: Human Perception and Performance 14(3):428-443.

Barnes C.S. (1995). Human eye saccades to targets of low energy. PhD Thesis, University of Toronto.

Barnes G.R. & Gresty M.A. (1973). Characteristics of eye movements to targets of short duration. Aerospace Medicine 44(11): 1236-1240.

Baylor D.A., Nunn B.J. & Schnapf J.L. (1984). The photocurrent, noise, and spectral sensitivity of rods of the monkey *Macaca Fascicularis*. Journal of Physiology 357:575-607.

Boch R., Fischer B. & Ramsperger E. (1984). Express-saccades of the monkey: Reaction times versus intensity, size, duration, and eccentricity of their targets. Experimental Brain Research 55:223-231.

Boynton R.M. (1972). Discrimination of homogeneous double pulses of light. Handbook of Sensory Physiology VII-4:202-232.

Bruder G.E. & Kietzman M.L. (1973). Visual temporal integration for threshold, signal detectability, and reaction time measures. Perception & Psychophysics 13(2):293-300.

Burbeck S., & Luce R.D. (1982). Evidence from auditory simple reaction times for both change and level detectors. Perception & Psychophysics 32(2):117-133.

Cameron E.L. & Albano J.E. (1994). Saccadic latency varies with target predictability. Investigative Ophthalmology and Visual Science 35(4):1550.

Carpenter R.H.S. (1977). Saccades. In *Movements of the eyes*. Pion Limited, London.

Clarke F.J.J & Belcher S.J. (1962). On the localization of Troxler's effect in the visual pathway. Vision Research 2:53-68.

Doma H. & Hallett P.E. (1988a). Rod-cone dependence of saccadic eye-movement latency in a foveating task. Vision Research 28: 899-913.

Doma H. & Hallett P.E. (1988b). Dependence of saccadic eye-movements on stimulus luminance, and an effect of task. Vision Research 28:915-928.

Efron B. & Tibshirani R.J. (1993). *An introduction to the bootstrap*. New York: Chapman & Hall.

Eizenman M., Frecker R.C. & Hallett P.E. (1984). Precise non-contacting measurement using the corneal reflex. Vision Research 24:167-174.

Erlandson R.F. & Fleming D.G. (1974). Uncertainty sets associated with saccadic eye movements--Basis of satisfaction control. Vision Research 14:481-486.

Fischer B. & Boch R. (1983). Saccadic eye movements after extremely short reaction times in the monkey. Brain Research 260:21-26.

Fischer B. & Ramsperger E. (1984). Human express saccades: extremely short reaction times of goal-directed eye movements. Experimental Brain Research 57:191-195.

Fischer B. & Weber H. (1993). Express saccades and visual attention. Behavioral and Brain Sciences 16:553-610.

Fischer B., Weber H., Biscaldi M., Aiple F., Otto P. & Stuhr, V. (1993). Separate populations of visually guided saccades in humans: reaction times and amplitudes. Experimental Brain Research 92: 528-41.

Fuortes M.G.F. & Hodgkin A.L. (1964). Changes in time scale and sensitivity in the ommatidia of Limulus. Journal of Physiology 172:239-263.

Geisler W.S. & Davila K.D. (1985). Ideal discriminators in spatial vision: two-point stimuli. Journal of the Optical Society of America A 2(9):1483-1497

Georgeson M.A. (1987). Temporal properties of spatial contrast vision. Vision Research 27(5):765-780.

Glickstein M. (1972). Brain mechanisms in reaction time. Brain Research 40: 33-37.

Grossberg M. (1968). The latency of response in relation to Bloch's law at threshold. Perception and Psychophysics 4:229-232.

Grossberg M. (1970). Frequency and latencies in detecting two-flash stimuli. Perception & Psychophysics 7(6):377-380.

Hallett P.E. (1978). Primary and secondary saccades to goals defined by instructions. Vision Research 18:1279-1296.

Hallett P.E. (1986). Eye movements. Chapter 10 in Boff K.R., Kaufman L., & Thomas J.P. (Eds) *Handbook of perception and human performance*. John Wiley and Sons, Toronto.

Hallett P.E. (1993). Complexity and modes as factors underlying saccadic latencies. Behavioural and Brain Sciences 16(3):578-579.

Hallett P.E & Adams B.D. (1980). The predictability of saccadic latency in a novel voluntary oculomotor task. Vision Research 20:329:339.

Hofmann M.I., Barnes C.S. & Hallett P.E. (1990). Detection of briefly flashed sine-gratings in dark-adapted vision. Vision Research 30(10):1453-1466.

Hammett S.T., Snowden R.J., & Smith A.T. (1993). Perceived Contrast as a Function of Adaptation Duration. Vision Research 34(1):31-40.

Hecht S., Schlaer S. & Pirenne M.H. (1942). Energy, quanta, and vision. Journal of General Physiology 25:819-840.

Hess R.F. & Snowden R.J. (1992). Temporal properties of human visual filters: number, shapes and spatial covariation. Vision Research 32(1):47-59.

Hood D.C., Ilves T., Maurer E., Wandell B., & Buckingham E. (1978). Human cone saturation as a function of ambient intensity: a test of models of shifts in the dynamic range. Vision Research 18: 983-993.

Izenman A.J., & Sommer C.J. (1988). Philatelic mixtures and multimodal densities. Journal of the American Statististical Association 83: 941-953.

Kahneman D. & Norman J. (1964). The time-intensity relation in visual perception as a function of observer's task. Journal of Experimental Psychology 68(3):215-220.

Kalesnykas R.P. (1994). Sensorimotor aspects of human saccadic eye-movement latency as a function of stimulus eccentricity, stimulus condition and attention. PhD Thesis, University of Toronto.

Kalesnykas R.P. & Hallett P.E. (1987). The differentiation of visually guided and anticipatory saccades in gap and overlap paradigms. Experimental Brain Research 68:115-121.

Kalesnykas R.P. & Hallett P.E. (1994). Retinal eccentricity and the latency of eye saccades. Vision Research 34:517:531.

Kapoula Z. (1985). Evidence for a range effect in the saccadic system. Vision Research 25(8):1155-1157.

Kapoula Z., & Robinson, D.A. (1986a). Saccadic undershoot is not inevitable: saccades can be accurate. Vision Research 26(5): 735-743.

Kapoula Z., Robinson, D.A., & Hain T.C. (1986b). Motion of the eye immediately after a saccade. Experimental Brain Research 61:386-394.

Kelly D.H. (1971a). Theory of flicker and transient response, I. Uniform Fields. Journal of the Optical Society of America 61(4):537-546.

Kelly D.H. (1971b). Theory of flicker and transient responses, II. Counterphase Gratings. Journal of the Optical Society of America 61(5):632-640.

Kirschfeld K., Feiler R. & Wolf-Oberhollenzer F. (1996). Cortical oscillations and the origin of express saccades. Proceedings of the Royal Society of London B 263:459-468.

Kraft T.W., Schneeweis D.M., & Schnapf J.L. (1993). Visual transduction in human rod phtoreceptors. Journal of Physiology 464:747-765.

Kortum P.T. & Geisler W.S. (1995). Adaptation mechanisms in spatial vision—II. Flash thresholds and background adaptation.Vision Research 35(11):1595-1609.

Libet B., Gleason C.A., Writh E.W. & Pearl D.K. (1983). Time of conscious intention to act in relation to onset of cerebral activity (readiness-potential). Brain 106:623-642.

Marriott F.H.C. (1963). The foveal absolute visual threshold for short flashes and small fields. Journal of Physiology 169:416-423.

Manahilov V. (1995). Spatiotemporal visual response to suprathreshold stimuli. Vision Research 35(2):227-237.

Mansfield R.J.W. (1973). Latency functions in human vision. Vision Research 13:2219-2234.

Pernier J., Jeannerod, M., Gerin P. (1969). Elaboration et decision des saccades: adaption a la trace du stimulus. Vision Research 9:1149-1165.

Quick, R.F. (1974). A vector-magnitude model of contrast detection. Kybernetik 16:65-7.

Rashbass R.C. (1970). The visibility of transient changes of luminace. Journal of Physiology 210:165-186.

Reuter-Lorenz P.A., Hughes H.C. & Fendrich R. (1991). The reduction of saccadic latency by prior offset of the fixation point: An analysis of the gap effect. Perception and Psychophysics 49:167-175.

Robson J.G. (1966). Spatial and temporal contrast-sensitivity functions of the visual system. Journal of the Optical Society of America 56:1141-1142.

Roufs J.A.J. & Blommaert F.J.J. (1981). Temporal impulse and step responses of the human eye obtained psychophysically by means of a drift-correcting perturbation technique. Vision Research 21:1203-1221.

Saslow M.G. (1967). Effects of components of displacement-step stimuli upon latency for saccadic eye movement. Journal of the Optical Society of America 57(8):1024-1029.

Schnapf J.L., Nunn B.J., Meister M. & Baylor D.A. (1990). Visual transduction in cones of the monkey *Macaca Fascicularis*. Journal of Physiology 427:681-713.

Silverman B.W. (1981). Using kernal density estimates to investigate multimodality. Journal of the Royal Statistical Society B43:97-99.

Snowden R.J. & Hess R.F. (1992). Temporal frequency filters in the human peripheral visual field. Vision Research 32(1):61-72.

Stork D.G. & Falk D.S. (1987). Temporal impulse responses from flicker sensitivities. Journal of the Optical Society of America A 4(6):1130-1135.

Tyler C.W. (1992). Psychophysical derivation of the impulse response through generation of ultrabrief responses: complex inverse estimation without minimum-phase assumptions. Journal of the Optical Society of America A 9(7):1025-1040.

van Asten W.N.J.C., Gielen C.C.A.M. and de Winkel M.E.M. (1988). The effect of isoluminant and isochromatic stimuli on latency and amplitude of saccades. Vision Research 28:827-840.

Vaughan H.G., Costa L.D. & Gilden L. (1966). The functional relation of visual evoked response and reaction time to stimulus intensity. Vision Research 6:645-656.

Victor J.D. (1989). Temporal impulse responses from flicker sensitivities: causality, linearity, and amplitude data do not determine phase. Journal of the Optical Society of America A 6(9):1302-1303.

Watson A.B. & Nachmias J. (1977). Patterns of temporal interaction in the detection of gratings.

Vision Research 17:893:902.

Watson A.B. (1979). Probability summation over time. Vision Research 19:515-22.

Watson A.B. (1982). Derivation of the impulse response: comments on the method of Roufs and Blommaert. Vision Research 22:1335-1337.

Watson A.B. (1986). Temporal sensitivity. Chapter 6 in Boff K.R., Kaufman L., & Thomas J.P. (Eds) *Handbook of perception and human performance*. John Wiley and Sons, Toronto.

Wenban-Smith M.G., & Findlay J.M. (1991). Express saccades: is there a separate population in humans? Experimental Brain Research 87: 218-222.

Wheeless L.L.Jr, Boynton R.M. & Cohen G.H. (1966). Eye-movement responses to step and pulse-step stimuli. Journal of the Optical Society of America 56(7):956-960.

Wheeless L.L. Jr, Cohen G.H. & Boynton R.M. (1967). Luminance as a parameter of the eye-movement control system. Journal of the Optical Society of America 57:394-400.

Zacks J.L. (1970). Temporal summation phenomena at threshold: their relation to visual mechanisms. Science 170:197-199.

IMAGE EVALUATION
TEST TARGET (QA-3)

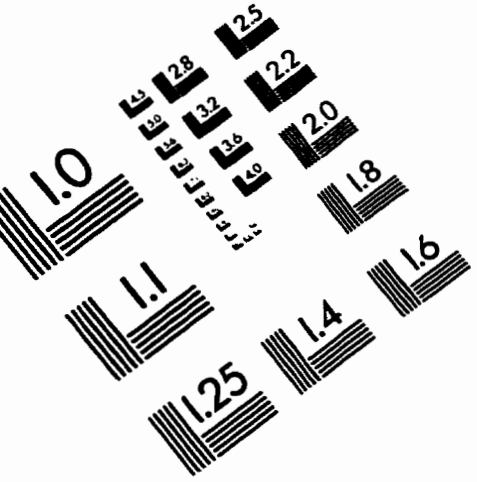

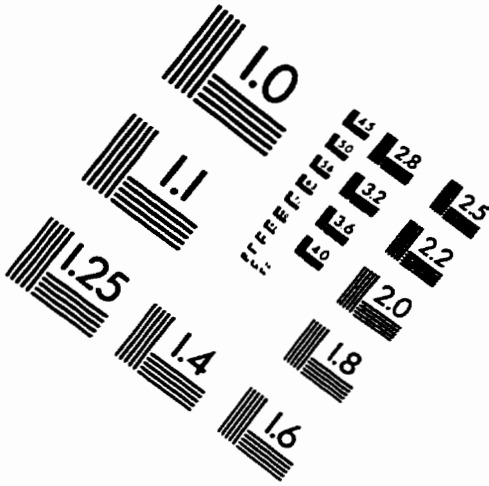

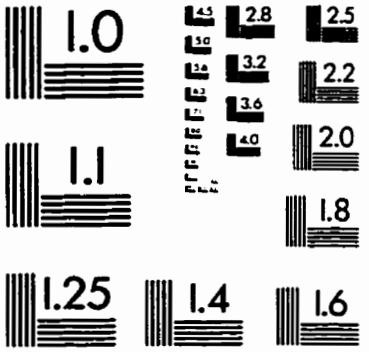

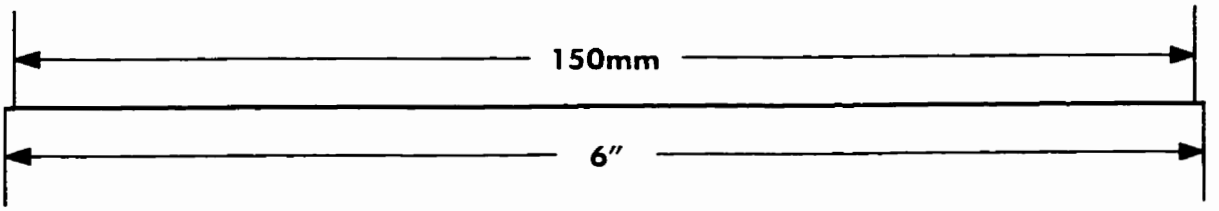

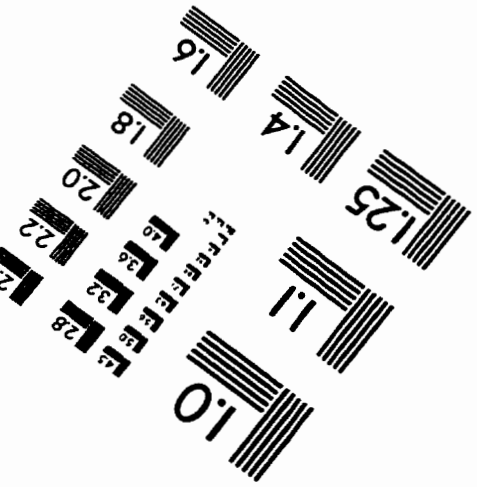

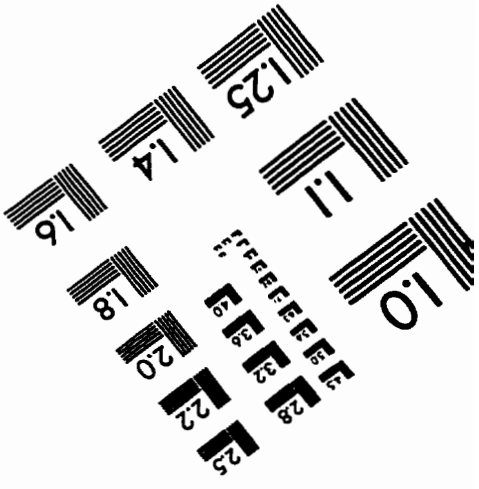

APPLIED IMAGE, Inc
1653 East Main Street
Rochester, NY 14609 USA
Phone: 716/482-0300
Fax: 716/288-5989